Relay Diversity Techniques for OFDM and MC-CDMA

Abdul Razak, Nur Idora Binti

Awarding institution:
King's College London

Title: Relay Diversity Techniques for OFDM and MC-CDMA

Author: Nur Idora Abdul Razak

Relay Diversity Techniques for OFDM and MC-CDMA

Nur I. Abdul Razak

Centre for Telecommunications Research

King's College London

A thesis submitted for the degree of

Doctor of Philosophy

January 2012

I would like to dedicate this thesis to my loving parents ...

Acknowledgements

My heartfelt gratitude goes to Dr. Fatin Said and Prof. A. Hamid Aghvami for giving me the opportunity to do my PhD. research in a friendly environment of Centre for Telecommunications Research (CTR). Their valuable instructions, suggestions, technical advises and supervision have enormous contribution in this dissertation. I also would like to thank the Malaysian Ministry of Higher Education and Universiti Teknologi MARA, Malaysia for the financial support throughout the study period.

I would also like to thank all my friends at CTR especially Aimal, Tuan, Vahid and many others who provided the excellent environment over the period of four years. Outside CTR, I would like to thank Noor Shuhaida and Raudhah for all the emotional support, friendship, entertainment, and caring they provided.

I am grateful to have an understanding husband, Wan Husaini Wan Deraman who is always having his attention on me although we're thousands miles apart. Also special thanks to my sisters, brother and the extended family for their love and support.

Last but not least, I wish to thank my parents, Abdul Razak Ujang and Normala Sha'ari for the great love, guidance and prayers which they provided throughout their lives. To them I dedicate this thesis.

Abstract

The future of mobile and personal communications requires a system that can support a large number of users and has the ability to provide high-speed services. Meeting this demand is challenging since wireless communications are subject to these four major constraints: complex fading channels, a scarce usable radio spectrum, and limitations on the power and size of the mobile terminals. Space-time codes, such as the Alamouti/space-time block coding (STBC) and cyclic delay diversity (CDD) can provide diversity and coding gains in multiple-input multiple-output (MIMO) systems over fading channels.

However in an ad-hoc network, nodes are often constrained in hardware complexity and size, which makes MIMO systems impractical for certain applications. Cooperative relay diversity schemes have been introduced in an effort to overcome these limitations. Cooperative techniques allow a collection of communication nodes to cooperate with to relay signals amongst each other, effectively creating a virtual antenna array, which combat multipath fading in wireless channels.

This thesis investigates relay diversity techniques in cooperative communications, namely the distributed space-time block coding (DSTBC) and relay cyclic delay diversity (RCDD) for OFDM and MC-CDMA systems. The performance analysis of the wireless relay networks under different protocols and fading channels are investigated. We derived the formulas for the symbol error rate (SER) of the investigated schemes in fading channels.

Finally, a novel hybrid relay diversity (HRD) is presented for OFDM-based system. This new relay structure addresses the issue of achieving a full spatial and multipath diversity by developing a hybrid for

CDD and STBC. Simulation on the system performance of HRD shows the superiority of the technique compared to standalone DSTBC and RCDD.

Contents

List of Figures

Nomenclature

Functions

$\delta(\cdot)$	Kronecker delta function
$\Gamma(\cdot)$	Euler Gamma function
$E\{x\}$	Expectation of x
$p_x(x)$	PDF of x
$sgn(\cdot)$	Signum function

Acronyms

AD	Analog-to-digital
ADSL	Asymmetric Digital Subscriber Line
AF	Amplify-and-forward
AWGN	Additive White Gaussian Noise
BER	Bit Error Rate
CDD	Cyclic Delay Diversity
CDF	Cumulative Distribution Function
CDMA	Code Division Multiple Access
CIR	Channel Impulse Response

CLT	Central Limit Theorem
CP	Cyclic Prefix
CSI	Channel State Information
CT	Cooperative Transmission
DAB	Digital Audio Broadcasting
D/A	Digital-to-analog
DD	Delay Diversity
DF	Decode-and-forward
DFT	Discrete Fourier Transform
DS-CDMA	Direct Sequence CDMA
DS	Direct Sequence
DSTBC	Distributed Space-time Block Coding
DSTC	Distributed Space-time Code
DT	Direct Transmission
DVB-H	Digital Video Broadcasting-Handheld
DVB-T	Digital Video Broadcasting-Terrestrial
EGC	Equal Gain Combining
FDMA	Frequency Division Multiple Access
FDM	Frequency Division Multiplexing
FEC	Forward Error Correction
FFT	Fast Fourier Transform
HRD	Hybrid Relay Diversity

ICI	Interchannel Interference
IDFT	Inverse Discrete Fourier Transform
IFFT	Inverse Fast Fourier Transform
ISI	Intersymbol Interference
WLAN	Wireless Local Area Network
LoS	Line-of-sight
MAI	Multiple Access Interference
MC-CDMA	Multi-carrier Code Division Multiple Access
MC	Multicarrier
MF	Matched Filter
MGF	Moment Generating Function
MIMO	Multiple-input Multiple-output
MMSE	Minimumm Mean Square Error
M-PSK	M-ary Phase Shift Keying
M-QAM	M-ary Quadrature Amplitude Modulation
MRC	Maximum Ratio Combining
MT-CDMA	Multitone CDMA
NLoS	Non Line-of-sight
OFDM	Orthogonal Frequency Division Multiplexing
OFDM	Orthogonal Frequency Division Multiplexing
ORC	Orthogonal Restoring Combining
PAPR	Peak-to-Average Power Ratio

PDF	Probability Density Function
PDP	Power Delay Profile
PEP	Pairwise Error Probability
QoS	Quality of Service
QoS	Quality-of-services
RCDD	Relay Cyclic Delay Diversity
RMS	Root Mean Square
RV	Random Variables
SC-FDE	Single Carrier with Frequency Domain Equalization
SER	Symbol Error Rate
SINR	Signal to Noise and Interference Ratio
SISO	Single-input Single-output
SNR	Signal-to-Noise Ratio
SNR	Signal-to-noise Ratio
STBC	Space-time Block Code
STC	Space-time Code
STTC	Space-time Trellis Code
TDMA	Time Division Multiple Access
VDSL	Very-high-bit rate Digital Subscriber Line
WiMAX	Worldwide Interoperability for Microwave Access
WSSUS	Wide Sense Stationary Uncorrelated Scattering
WSS	Wide Sense Stationary

ZF	Zero Forcing

Symbols

f_c	Carrier frequency
I_0	Zeroth-order modified Bessel function
B	Bandwidth
B_c	Coherence bandwidth
dB	Decibel
f_D	Doppler frequency
E_S	Symbol energy
$f_{D_{\max}}$	Maximum Doppler frequency
G_{fq}	Frequency diversity gain
G_t	Time diversity gain
I_N	$N \times N$ identity matrix
k	Subcarrier index
L_{cp}	Length of cyclic prefix
N	Number of subcarriers
α	Amplitude of channel tap
L	Length of multipath channel taps
T_c	Coherence time
T_g	Guard interval
T_S	OFDM symbol duration

Chapter 1

Overview

1.1 Introduction

Demand for mobile wireless communications is growing at a rapid pace in terms of the number of potential users and the speed of data. Meeting this demand is challenging as wireless communication channels are subject to a phenomenon known as multipath fading.

Multipath fading refers to the drastic changes in signal amplitude and phase as a result of small changes in spatial separation between the transmitter and the receiver. It occurs due to reflection, scattering and diffraction of the transmitted signal at natural or man-made obstacles. A multitude of waves arrive from many different directions with varying delays, amplitudes and phases, caused by the mobility of the transmitter and/or receiver. At the receiver, the superposition of this signals results in amplitude and phase variation of the composite signal which cause the multipath fading.

The effect of fading can be exploited by increasing the diversity of the transmission. Diversity gains can be obtained when the information signal is passed through multiple independent realizations of the channel. Spatial diversity gain can be achieved by employing multiple antennas at the transmitter and/or receiver. This technique is known as multiple-input multiple-output (MIMO). By having multiple antennas, signal is transmitted through different independent channels that increase the likelihood of one signal experiencing good channel

condition. However, it is often impractical to have a large number of antennas on mobile devices due to size, power, cost and complexity constraints.

To cater the demands of spectral and power efficiency as well as increase reliability without having multiple antenna on devices, idle users in the network can cooperate to form a virtual MIMO system. This is known as cooperative communications. Cooperation provides a method of achieving spatial diversity without the need for multiple antennas at the mobile device. Cooperation also offers higher throughput than direct transmission among users [78].

Cooperation between nodes is certainly beneficial in the communication between mobile users and base stations. It can offer longer battery life and higher throughput that enables high data rate multimedia applications. Besides cellular, cooperative communications can also be implemented for ad-hoc and sensor networks [31, 66]. For example, power conservation is important in sensor networks thus cooperation between sensor nodes can be used to reduce the likelihood of decoding error. Therefore, the nodes are able to operate at low power and still achieve the required data and error rates.

In the following, the basic concept of cooperative communications will be described in details with the introduction on relay network and relay protocols. Next, a brief overview on the context a brief overview on the context of cooperative communications and wireless relay network will be given. The key concept of power allocation method in wireless relay network, relay diversity schemes and performance analysis will be presented. Finally, the main contributions of the thesis will be outlined and the organization of the thesis will be given at the end of this chapter.

1.2 Basic Concept of Cooperative Communications

Cooperative communications [49, 78, 79] exploit the spatial diversity in multiuser systems by allowing users with different channel qualities to cooperate and relay each other's signal to the intended destination. Each signal is transmitted through multiple independent paths, thus the probability that the signal fail to be received

at the destination is reduced. Through cooperation, each user may have only one antenna but still achieve the diversity gain of a MIMO system, thus it is also known as virtual MIMO system. Figure 1.1 shows the (a) MIMO system and (b) cooperative network or virtual MIMO system.

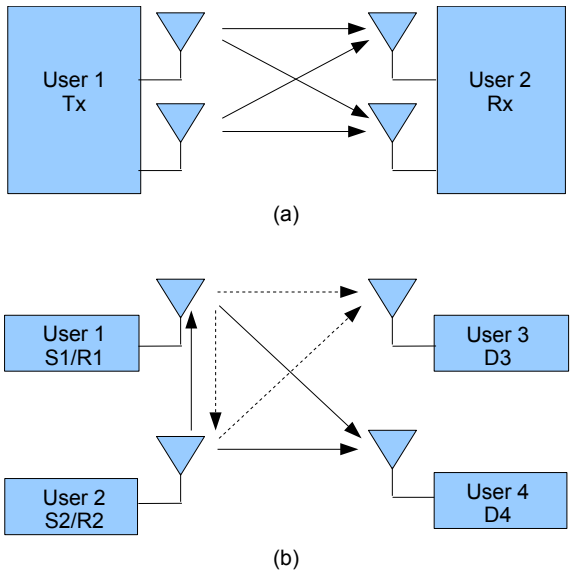

Figure 1.1: (a) MIMO system and (b) cooperative network or vitual MIMO system

Cooperative transmission scheme is different from the conventional point-to-point system in which the user cooperation use multiple users' resources to transmit the signal from a single source and proper combination of signals is required at the destination [98]. When two users transmit their signals to the destination over independent fading channels, the channels are said to have deep fade when the signal-to-noise ratio (SNR) falls under the pre-determined threshold. If the two users cooperate by relying each other's signals and the channel between the users (inter-user channel) is reliable, the communication outage only occurs when both users experience deep fade simultaneously. Hence, user cooperation mitigates multipath fading by providing the destination with redundant signal from the relay and the receiver to average the individual channel effects. Studies on various relaying schemes and discussion on diversity gain of cooperative networks can be found in [30, 48].

1.2.1 Relay network

The most fundamental concept of a cooperative communication in the relay network, which was first introduced in [15, 92]. A simple relay network consists of a source node, a destination node and a relay node that assists the communications between the source and destination nodes, as shown on Figure 1.2. Although the concept of relaying has been investigated since more than 30 years ago, there are still many open problems for the relay channel. For example, in general, the capacity of the relay channel is still unknown even for the case of Gaussian channel. As a result, most of the research efforts have focused on finding efficient protocols that lead to lower bound on the capacity [49].

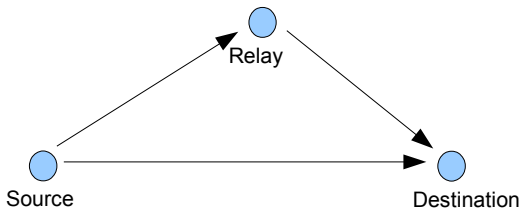

Figure 1.2: Simple relay network consists of a source node, a destination node and a relay node

Traditionally, relays have been used to extend the coverage of wireless communication systems. However, there are many other applications of relay communications have emerged recently. For example, relaying is used to assist the communication between the source and destination using some cooperation protocols. The diversity of the communication system can be improved by controlling medium access between source and relay nodes, and appropriately choose the modulation and coding schemes. In multiuser systems, the idle users can act as relays and share their resources to assist each other in signal transmission, creating a cooperative network.

1.2.2 Relay Protocols

This section outline several relay protocols and demonstrate their robustness on fairly general channel conditions. The two main relaying protocols are amplify-and-forward (AF) and decode-and-forward (DF). In AF, the relay node amplifies

the received signal before transmit to the destination node, while in DF, the relay node decodes the received signal, re-encode and then forward the signal to the destination node. Other cooperation strategies with different relaying protocols have been studied in [48]. Repetition and space-time algorithm has been proposed in [49] to achieve diversity gain, where the mutual information and outage probability are analyzed. In repetition-based cooperation, relay nodes retransmit the signal in a time division multiple access (TDMA) manner, while in space-time cooperation, relay simultaneously retransmit the signal using a suitable space-time code. Distributed space-time codes (DSTC) have been proposed to improve the bandwidth efficiency of cooperative transmissions [63, 77, 91, 94].

1.2.2.1 Amplify-and-forward

Amplify-and-forward is a simple cooperative signaling method. The relay node receives a noisy version of the original transmitted signal from the source node. As the name implies, the relay node amplifies the received noisy signal and retransmit to the destination node. At the destination node, the signals received from the source and relay nodes are combined and detection process is done. Although noise is amplified through relaying, the destination node receives two independent degraded versions of the signal and will make decision for information detection. The method has been proposed in [48, 50] where for two-user case, AF achieves diversity order of two, which is the best possible outcome at high SNR. It is assumed that the destination node knows the inter-user channel coefficient to do optimal decoding. Therefore, some mechanism of exchanging or estimating the channel information must be implemented. Another possible challenge is that sampling, amplifying and retransmitting analog values are technologically non-trivial. Nevertheless AF is a simple relaying protocol and has been very useful in further understanding cooperative communication systems.

1.2.2.2 Decode-and-forward

The concept of decode-and-forward protocol is similar to traditional relay. In DF, relay node attempts to decode the received signal and re-encode before forward the coded signal to the destination node. The relay nodes may be pre-assigned by

the destination or through some techniques. Several techniques on relay selection have been studied in the literature such as in [10, 56]. It is possible that the relay node is not able to detect the information successfully, in which case cooperation can be detrimental. The destination node needs to know the error characteristics of the inter-user channel. To avoid error propagation, a hybrid DF method is proposed in [50] where the relay node only participate in cooperation when the fading channel instantaneous SNR is high. Another method is proposed in [90] where cooperation protocol is decided based on SNR threshold at relay node. If the channel has high SNR, DF will be chosen as the protocol, else the relay will choose AF.

1.3 Power Allocation Method

This section presents power allocation methods under different network topologies, cooperation methods and channel state information (CSI) assumptions. Two main topologies have been considered: dual-hop topology and general multihop topology. If the source node does not know the CSI, the diversity gain is achieved by allowing all user nodes to have a fair share of each other's resources. On the other hand, if CSI is known, significant improvement in terms of error probability, outage probability and capacity can be obtained by applying optimal power allocation among cooperating user nodes.

1.3.1 Two-hop relay network

Consider a two-hop wireless relay network as shown in Figure 1.3 that consists of a source node, S, a destination node, D and R relay nodes, denoted by $RN_r, r = 1, ..., R$. Let h_{Sr} and h_{rD} be the complex channel coefficients from S to RN_r and from RN_r to D respectively. In this case, power allocation becomes interesting due to the increased degree of freedom due to multiple relay nodes. Relaying is done in two phases: in the first phase, S broadcasts its message signal and in the second phase, relay nodes $RN_r, r = 1, ..., R$ transmit the processed version of the received signal to D. The transmit power of S and RN_r are denoted as P_1 and $P_{2,r}$, respectively. The total power budget is obtained from the summation of

relay powers, i.e. $\sum_{r=1}^{R} P_{2,r} = P_2$. The optimal power allocation schemes depends on the quality of service (QoS) measures such as the outage probability, capacity, SNR and SER. The objective is to find the optimum P_1 and $P_{2,r}$ to maximize the QoS performance at the destination subject to total power constraint. The reverse optimization can also be considered in which total power is minimized given set of constraint on the QoS, for example the SER and outage probability.

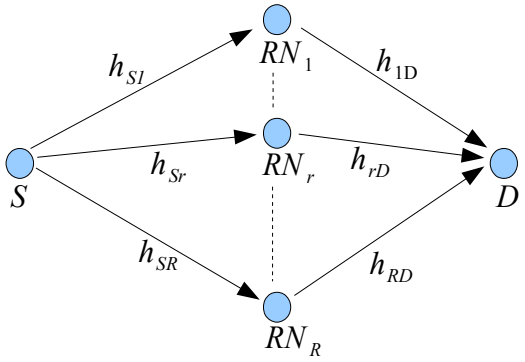

Figure 1.3: Wireless relay network consisting of a source S, a destination D, and R relay nodes RN.

The relay network in Figure 1.3 can be viewed as a virtual antenna array that transmits noisy versions of the original information signal from the source node. If CSI is known at relay nodes, precoding techniques can be used to compensate the channel gain and phase rotation to achieve better detection performance. For orthogonal relaying channel (repetitions-based cooperation), D receives R copies of the source information signal from relay nodes with no interuser interference. With the knowledge of the exact channel coefficients, the R information signals can be combined coherently at D to increase the received SNR.

For AF relaying protocol, the capacity for two-hop relay network is given as [61]

$$C_{AF} = \frac{1}{2}\log\left(1 + \sum_{r=1}^{R} \frac{P_S P_r |h_{Sr}|^2 |h_{rD}|^2}{P_S |h_{Sr}|^2 + P_r |h_{rD}|^2 + 1}\right) \tag{1.1}$$

and the capacity-maximizing power allocation strategy results in the water-filling solution $P_r = \frac{|h_{Sr}|^2}{\sqrt{\gamma_r}}\left(\frac{1}{\sqrt{\eta}} - \frac{1}{\sqrt{\gamma_i}}\right)^+$ where $(x)^+ = \max(x, 0)$ and $\gamma_r = \frac{|h_{Sr}|^2 |h_{rd}|^2}{P_1 |h_{Sr}|^2 + 1}$ [61]. The Lagrange multiplier η is chosen to meet total power constraint of the relay node. The relay node RN_r is allowed to transmit if and only if $\gamma_r > \eta$.

Power allocation for the DF relay protocol with orthogonal relay channels was derived in [49] to maximize the capacity. Assume a set of relay nodes **RN** correctly decode the signal received from the source node. These relay nodes then forward the signal to the destination node, similar to multiple antennas on a single user terminal. In low SNR regime, the optimum power allocation is to choose the relay node in **RN** with the best channel condition and allocate the power to that particular relay node [62]. This shows that the selective relaying scheme is optimal for DF relaying protocol with orthogonal relay channel.

For the case of non-orthogonal relay channel where relay nodes simultaneously transmit to the destination node, beamforming technique can be used. The optimal beamforming factor for AF has been derived in [23] to optimize the received signal when full CSI is available at relay nodes. If the phase information is not available to the relay nodes, all power should be allocated to one relay [11, 58, 103]. It is shown in [11] that selective relaying is optimal in minimizing the outage probability for the DF space-time encoded scheme under total power constraint. A selective relaying strategy has been derived in [58] for AF space-time encoded scheme, which is optimal in minimizing the SER.

The power allocation strategies described above may not contribute to longer network lifetime as the objective functions do not take residual battery energy of each relay node into account. The relay selection strategies in [14, 32] are used to extend network lifeline and power allocation scheme that consider residual battery energy at relays is proposed in [55]. The latter scheme can extend the network lifetime considerably compared to the power allocation that depends only on the channel conditions.

In practice, it is normally hard to obtain the instantaneous CSI for all channel links of the system. Therefore, power allocation strategies with less stringent assumptions on CSI have been proposed. For example, a power allocation strategy for DF space-time encoded scheme was derived in [53] by assuming that the relay node r, RN_r knows only the instantaneous channel gain of the first hop $|h_{Sr}|$ and the average channel gain of the second hop, $E|h_{rD}|^2$. A near optimal solution that minimizes the outage probability is derived by selecting a set of relay nodes and allocating them with an equal share of power.

With the same amount of channel information, the optimal power allocation

strategy for the AF protocol was derived in [101]. Furthermore, when only statistics of channels are available at the relays, power allocation strategies for the AF space-time-encoded scheme are proposed in [58]. The signal received at relay node r, RN_r is scaled by a real factor A_r to keep the average power of RN_r as $P_{2,r}$. There are two different choices of the factor A_r, as given below

$$A_r = \sqrt{\frac{P_{2,r}}{|h_{Sr}|^2 P_1 + N_o}} \tag{1.2}$$

$$A_r = \sqrt{\frac{P_{2,r}}{\sigma^2_{h_{Sr}} P_1 + N_o}} \tag{1.3}$$

where $\sigma^2_{h_{Sr}}$ is the variance of the source to relay node r channel and N_o is the noise variance. The second choice of A_r is recommended since it is not a random value while keeps the power constraint from the long term point of view. Besides h_{Sr} in (1.2) could only be replaced by its estimate $\hat{h}_{Sr}$ which may not keep the average relay power exactly as $P_{2,r}$. In this thesis, A_r in (1.3) will be adopted. Nevertheless, the provided studies could be easily extended for A_r in (1.2).

1.3.2 Multihop relay network

The wireless relay network can be extended to multihop scenario where several relay nodes are connected in series. The idea will be similar as the two-hop case. One possible hopping strategy could be that by concatenating multiples of the three-node or the two-hop networks each level of relay nodes retrieves the source information by processing the signals from the two closest previous levels of relays. Instead of restricting to the two-hop cooperation, signals from N hops away can be combined to enhance the detection at the destination.

In conventional multi-hop systems, the received signals that contain insufficient energy for reliable detection are discarded, e.g., signals from distant transmitters. On the contrary, with cooperation, the receiver may combine signals transmitted via different relays, regardless of the signal strength, to enhance the detection performance or to reduce the energy consumption. In [13] the concept of multihop diversity is introduced where the benefits of spatial diversity are

achieved from the concurrent reception of signals that have been transmitted by multiple previous terminals along the single primary route. This scheme exploits the broadcast nature of wireless networks where the communications channel is shared among multiple terminals.

On the other hand, the routing problem in the cooperative radio transmission model over static channels is studied in [47], where it is allowed that multiple nodes along a path coordinate together to transmit a message to the next hop as long as the combined signal at the receiver satisfies a given SNR threshold value. The gain in energy efficiency and the respective power allocation strategies have been also studied in [31, 34, 60]. In [60], a new cooperative routing protocol is introduced using the Alamouti space-time code for the purpose of energy savings, given a required outage probability at the destination. Two efficient power allocation schemes are derived, which depend only on the statistics of the channels.

It has been proven in [51] that the minimum energy cooperative path routing problem, i.e., to find the minimum-energy route using cooperative radio transmission, is NP-complete. This is due to the fact that the optimal path could be a combination of cooperative transmissions and point-to-point transmissions. Therefore, two types of building blocks can be considered: direct transmission (DT) and cooperative transmission (CT) building blocks. In Figure 1.4 the DT block is represented by the link (RN_1, RN_2), where RN_1 is the sender and RN_1 is the receiver. In addition, the CT block is represented by the links (RN_3, RN_5), (RN_3, RN_4), and (RN_4, RN_5), where relay node RN_3 is the sender, relay node RN_4 is a relay, and relay node RN_5 is the receiver. The route can be considered as a cascade of any number of these two building blocks, and the total power of the route is the summation of the transmission powers along the route. Thus, the minimum energy cooperative path routing problem can be solved by applying any distributed shortest-path routing algorithm such as the distributed Bellman-Ford algorithm [34].

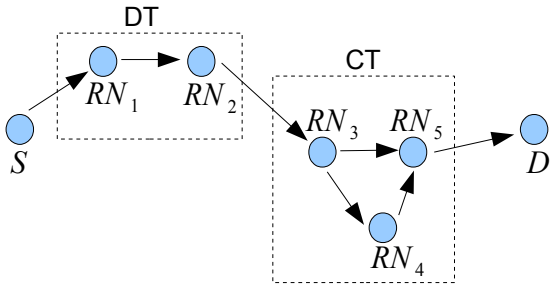

Figure 1.4: Multihop relay network: Cooperative Transmission (CT) and Direct Transmission (DT) modes as building blocks for any route

1.4 Relay Diversity Schemes

The main problem with the repetition-based multinode DF protocol [75] and AF protocol [74], as it is discussed in previous section, is the loss in data rate as the number of relay nodes increases. This is due to the multi-phases nature of repetition-based cooperation. The use of orthogonal subchannels for the relay node transmissions, either through TDMA or FDMA, results in a high loss of the system spectral efficiency. Therefore, relay diversity schemes are introduced where relay nodes are allowed to transmit simultaneously over the same channel.

1.4.1 Distributed Space-Time Coding

In wireless communication systems, the spatial diversity can be achieved by multiple independent paths between multiple antennas at the transmitter and the receiver, possibly in conjunction with space-time codes (STCs).

Space-time trellis code (STTC) has been proposed in [88] as an STC that combines signal processing at the receiver with coding techniques appropriate to multiple transmit antennas. STTC designed for two, three and four transmit antennas perform extremely well in slow-fading environment which is typical for indoor transmission and has a very close outage capacity to multiple-antenna system in [89] and [42]. However, when the number of transmit antenna is fixed, the decoding complexity of STTC, measured by the number of trellis states in the decoder, increases exponentially with the transmission rate. In addressing

this problem, Alamouti proposed a remarkable scheme for transmission using two transmit antennas in [2]. Alamouti code [2] has less complexity but there is performance loss compared to STTC. Despite the performance penalty, Alamouti code is still appealing in terms of simplicity and performance that motivates the search for similar schemes for more than two transmit antennas. Alamouti code is created based on the theory of orthogonal design which has been studied by Radon in [70]. Tarokh in [86] has extended the orthogonal code to be used for transmission using more than two transmit antennas, namely space-time block code (STBC).

Recently, the idea of space time coding has been applied in wireless relay networks in the name of distributed space time coding (DSTC) to extract similar benefit as in point to point MIMO systems. Several works have considered the application of the existing space-time codes in a distributed fashion for the wireless relay network (e.g., see [5, 6, 82]). Most of these works have considered a two-hop relay network where a direct link between the source and destination nodes does not exist, as shown in Figure 1.3. In [59], the direct link between the source and destination nodes is also incorporated in the DSTC. Mainly there are two types of distributed space time coding techniques discussed in the literature: (1) DF-based DSTC [49], where in a subset (chosen based on some criteria) of the relay nodes decode the symbols from the source and transmit a row/column of a STBC and (2) AF-based DSTC [40], where all the relay nodes perform linear processing on the received symbols according to a DSTBC and transmit the resulting symbols to the destination. The AF-based DSTC is of special interest because the operations at the relay nodes are greatly simplified and moreover there is no need for every relay node to inform the destination once every quasi-static duration whether it will be participating in the DSTC process as is the casein DF-based DSTC [49]. The design of practical DSTCs leading to reliable communication in wireless relay networks has been considered in [40, 59, 72].

In [39], a cooperative strategy was proposed, which achieves a diversity factor of R in an R-relay wireless network, using the so-called DSTC. In this strategy, a two-phase protocol is used. In phase one, the transmitter sends the information signal to the relays and in phase two, the relays send information to the receiver. The signal sent by every relay in the second phase is designed as a linear func-

tion of its received signals and their complex conjugate. It was shown that the relays can generate a linear STC at the receiver, as in a multiple antenna system, although they only cooperate distributively. The technique was also shown to achieve optimal diversity at high SNRs [39]. The design of practical DSTCs that lead to reliable communication in wireless relay networks has also been recently considered [40, 59, 72].

Although AF-based DSTC does not need instantaneous channel information at the relays, it requires full (transmitter-to-relays and relays-to-receiver)channel information at the receiver, implying that training symbols need to be sent from both the transmitter and relays. For example, in [40], the destination was assumed to have perfect knowledge of all the channel fading gains from the source to the relays and those from the relays to the destination. To overcome the need for channel knowledge, distributed differential space time coding was studied in [41, 67, 73], which is essentially an extension of differential unitary STC for point to point MIMO systems to the relay network case. In [71], an AF DSTC involving a combination of training, channel estimation and detection in conjunction with existing coherent distributed STBCs is proposed for non-coherent communication in AF relay networks.

Distributed space-time coding was generalized to networks with multiple-antenna nodes in [38], and the design of practical DSTCs with multiple antennas terminals has also been recently considered in [54, 57, 67]. In [54, 57], the orthogonal and quasi-orthogonal space-time design is used for AF-based wireless relay networks with multiple-antenna nodes.

1.4.2 Distributed Delay Diversity

As an alternative to DSTC, an artificial diversity, which mimics the effects of spatial diversity, can be introduced in wireless communication systems by the use of artificial delays. The idea is to transmit the same information modulated symbols from separate antennas with different time delays, thereby causing multipath replicas even when the channel is flat. With the help of an equalizer the receiver can extract these paths and achieve a delay diversity (DD) gain [97]. For communication systems that employ the inverse fast Fourier transform (IFFT)

and fast Fourier transform (FFT) operators such as OFDM and single carrier with frequency domain equalization (SC-FDE), DD can be achieved through the use of a cyclic delay. Cyclic delay diversity (CDD) has been used in combination with OFDM in [12, 96] and has been used with SC-FDE systems with no additional complexity at the receiver in [83]. In this context, cyclic delay increases the selectivity of the fading channel which in the presence of channel coding can increase the diversity gain of the system. The use of CDD distributively (i.e. located at different users) to exploit macro-diversity has been presented in [33]. This scheme is also known as relay cyclic delay diversity (RCDD). The drawback of this scheme is that the wireless infrastructure must rely on radio network controller to deliver in a timely fashion the data to multiple transmitters. Obviously, the control and data signaling in the backhaul will be very high. To avoid this complexity, distributed relay nodes should be used instead. In analogy to CDD and in order to provide frequency selectivity and spatial diversity in a cooperative relaying wireless communication system, a set of distributed users is treated as a single entity composed of multiple antennas where at each relay node transmit antenna, a cyclic shift is applied to the OFDM symbol and will be forwarded between to the destination node.

According to the proposed methods of artificial frequency selectivity, spatial diversity is provided in a cooperative relaying wireless communication system. The artificial frequency selectivity is exploited in conjunction with forward error correction coding (FEC) to provide a coding diversity gain. It is interesting to mention that the destination node does not need any information about the number of relay nodes. The destination node receives the multiple access signals and decodes the data that may be combined with the signal directly received from the source node. The combined signal as experienced by the destination node will in a sense be similar to the signal from a transmitter with multiple antennas, utilizing CDD, but with the added benefits with regards to gain and coverage associated with cooperative relaying.

1.5 Main Contributions of the Thesis

The thesis provides analytical studies of DSTBC and RCDD for two-hop multiple relay OFDM and MC-CDMA systems. The analysis are conducted for spatially uncorrelated relay configurations with coherent modulation. Pathloss and shadowing are assumed to be perfectly counteracted by perfect power control and only the multipath fading has been considered. The contributions of the thesis are highlighted below:

1.5.1 Distributed space-time block coding (DSTBC)

A practical DSTBC for wireless relay network is designed using AF scheme, where each relay transmits a scaled version of the linear combination of the received symbol and their complex conjugate. The focus is on the STC cooperation using generalized orthogonal STBC, which are systematically constructed, orthogonally decodable, full-rate and full-diversity. The scheme is valid for any number of relays with linear orthogonal decoding in the destination, which make it feasible to employ large number of potential relay to improve the diversity order. The DSTBC is generalized in AF mode when the source-destination link does not exist in both phases of the transmission. The PEP is derived to evaluate the diversity gain of the DSTBC system. Another contribution is the derivation of the approximate average SER for AF Alamouti with linearly-precoded OFDM over frequency selective Rayleigh fading channel. The results can be easily extended to any full-diversity, full-rate DSTBC such as the orthogonal code in [86]. The analytical results are confirmed by simulations, indicating the accuracy of the analysis and the fact that DSTBC can be designed based on orthogonal codes.

1.5.2 Relay cyclic delay diversity (RCDD)

A low-complexity RCDD is designed for AF relaying where each relay transmits a scaled and cyclically-delayed version of the received signal. The focus is on the construction of delay matrix for RCDD so that the end-to-end relay channel becomes consecutive in their delay lags. The scheme is valid for any number of relay nodes and it is simple to implement. The PEP is derived to evaluate

the diversity gain of the RCDD system. The analytical results are confirmed by simulations, indicating the accuracy of the analysis and the fact that RCDD can be a contender for DSTBC in wireless relay network.

1.5.3 DSTBC and RCDD MC-CDMA

DSTBC and RCDD are designed for multiuser MC-CDMA system. Distributed framework for cooperative MC-CDMA is presented where the multiple access signals are transmitted through relay nodes and then forwarded to the destination. The main contribution is the derivation of the closed-form expression of average SER for DSTBC and RCDD.

1.5.4 Hybrid Relay Diversity

A novel relay diversity scheme known as HRD is designed for AF relaying. HRD combines the advantages of DSTBC and RCDD thus creating a simple yet superior technique in cooperative communication. The performance vs. complexity trade-off of HRD is determined by the order trade-off of DSTBC and RCDD. Simulations of HRD over frequency selective Rayleigh fading channel with different configurations show the superior performance of HRD compared to DSTBC and RCDD.

1.6 Organization of the Thesis

This thesis consists of seven chapters. In Chapter 2, the fundamentals of wireless communications are briefly reviewed. Then Rayleigh, Rician and Nakagami-m multipath fading models are characterized for frequency flat case and further extended for selective environments. Later in the chapter, the basic principles and data detection techniques of OFDM and MC-CDMA systems are reviewed. The signal structures of these systems are explained by using their simplified models. For MC-CDMA, different single user detection techniques are formulated which are used in Chapter 5.

Chapter 3 starts by revisiting the design and performance criterion of DSTBC OFDM. Diversity gain of the system is derived and simulations have been done to

prove the theoretical gain. Then the performance of distributed Alamouti system is investigated in frequency selective channel environment.

In Chapter 4, relay CDD is presented for OFDM relay system using amplify and forward protocol. First, the transformation of spatial diversity into frequency is shown by using PD which is frequency domain equivalent of cyclic delay. Then performance of RCDD in term of diversity gain and error rate is investigated under several scenarios.

Chapter 5 presents a new framework of distributed MC-CDMA system where the first relaying hop is a multiple access scenario and the second hop is a downlink transmission. The error rate performance for RCDD and distributed orthogonal block codes have been investigated in this system with decode-and-forward protocol. Similar to Chapter 4 and 3, both schemes are generalized for arbitrary number of relay nodes.

Chapter 6 presents a novel hybrid relay diversity (HRD) which is a combination of CDD and orthogonal block codes employed at relay nodes. Equipped with CDD, a fraction of the total number of relay nodes is used to extract the frequency (multipath) diversity, while the remaining relay nodes employing ST block codes provide maximum spatial diversity. The hybrid architecture makes full use of frequency domain spreading and channel coding, thereby providing excellent spatial and frequency diversity which is otherwise impossible to realize with standalone CDD or block codes. The simulation of performance of the system is presented in relay OFDM with amplify and forward protocol.

Finally, the concluding remarks are given in Chapter 7. Future research direction is outlined.

Chapter 2

Fundamentals

2.1 Introduction

Orthogonal frequency-division multiplexing (OFDM) has been the interest of researchers in the recent years due to its ability to prevent intersymbol interference (ISI) in broadband wireless channels. It is a digital modulation scheme which is based upon the principle of frequency-division multiplexing (FDM). The modulated and coded high-rate bit stream is split into several parallel low-rate bit streams which will be transmitted over one subchannel. The subcarrier frequencies are chosen so that the modulated data streams are orthogonal to each other and therefore the interchannel interference (ICI) which is the crosstalk between the subchannels can be eliminated. OFDM symbols are separated by a guard interval which is the copy of the last bits of the symbol with a length longer than the maximum channel delay spread to prevent ISI. Therefore, channel equalization is simplified by using many slowly modulated narrowband signals instead of one rapidly modulated wideband signal.

OFDM has been employed by several latest technology for wideband digital communications system. Among numerous applications, few are asymmetric digital subscriber line (ADSL) and very high bit rate digital subscriber line (VDSL) broadband access which employ the existing telephone network copper wires. Then, IEEE 802.11a/g which are the standards for wireless local area network (WLANs) plus the digital audio broadcasting (DAB) systems like EUREKA 147,

digital radio Mondiale, high definition radio, terrestrial and mobile digital video broadcasting systems (DVB-T, DVB-H). In recent years, the certification of IEEE 802.16 standards i.e. fixed and mobile worldwide interoperability for microwave access (WiMAX) systems will introduce OFDM into the cellular wireless networks [35, 65].

Despite all the benefits of OFDM, there are still challenges to design a very high speed wireless links that offers acceptable quality-of-services (QoS) in both line-of-sight (LoS) and non-LOS (NLoS) environments. The work of Nyquist and Shannon [80] on fundamental limits of digital communication systems by formulating the channel capacity, has inspired many researchers to design a system that the maximum amount of error-free information that can be transmitted over the channel in a given time and bandwidth. Assuming perfect channel conditions, a standard single-input single-output (SISO) wireless link can achieve data rates of above 10^9 bits/sec by using a nominal spectral efficiency of 4-5 bits/sec/Hz over a 250 MHz. However it is almost impossible to have a SISO system with such high spectral efficiency due to cost, transmit power and spectrum regulatory constraints. The transmit power and received signal-to-noise ratio (SNR) is restricted due to biohazard considerations. Typical values for mobile or close proximity devices are set to be as low as 1 Watt indoor and about ten times higher in outdoor tower-mounted base stations. Also, the cost in manufacturing of highly linear receivers limits peak SNR ranges. Current regulatory standards for spectrum allocation limits bandwidth availability and very costly, especially for the frequency band below 6 GHz which are most suitable for NLoS networks. Large chunks of bandwidth are easier to obtain in higher frequency band ranges (above 40 GHz) but at frequency higher than 6-7 GHz, the effect of shadowing caused by obstruction in the propagation environments increases making NLoS wireless link unreliable and most of the time useless. Therefore, spectrally efficient wireless links are neither feasible in conventional SISO system due to peak and average SNR limitations nor can they be realized by utilizing bigger bandwidth chunks in higher frequency bands as it results in severe reduction in ranges.

MIMO architecture presents a technological breakthrough that will meet the ever increasing demands of wireless networks by providing an increased in spectral efficiency through spatial multiplexing gain and improved link reliability with

diversity gain from the multiple antenna structure. These gain can be achieved without additional transmit power or receive SNR. However, such systems posed transceiver complexity which becomes more complicated in broadband systems. Although OFDM-based air-interfaces can provide solution to the issue of broadband channel, increasing the number of antennas at user terminals especially mobile devices is often impractical due to size and hardware complexity. This limitations motivate the current research trend in cooperative communications as presented in Chapter 1.

This chapter presents the fundamental knowledge to further appreciate the work in this thesis. A review on system performance measures is given, highlighting the derivation of average SNR, outage probability and diversity gain. Next, a detail description of mobile wireless channel is given as well as the channel modeling. With the appropriate channel model, the performance analysis of wireless relay network is derived. Finally, OFDM and MC-CDMA structure and detection is presented.

2.2 System Performance Measures

2.2.1 Average SNR

The most common and well understood performance measure characteristic of a digital communication system is SNR. In simple mathematical terms, if γ denotes the instantaneous SNR, which is a random variable at the receiver output that includes the effect of fading, then

$$\bar{\gamma} = \int_0^\infty \gamma p_\gamma(\gamma) d\gamma \tag{2.1}$$

is the average SNR, where $p_\gamma(\gamma)$ denotes the probability density function (PDF) of γ.

2.2.2 Outage Probability

Another standard performance criterion characteristic of diversity systems operating over fading channels is the so-called outage probability - denoted by P_{out}.

The outage probability defined as the probability that the instantaneous error probability exceeds a specified value or equivalently the probability that the output SNR, γ, falls below a certain specified threshold, γ_{th}. Mathematically speaking, we have

$$P_{\text{out}} = \int_0^{\gamma_{\text{th}}} p_\gamma(\gamma) d\gamma \tag{2.2}$$

which is the cumulative distribution function (CDF) of γ, evaluated at $\gamma = \gamma_{\text{th}}$.

2.2.3 Diversity Gain

Providing additional independent copies of the same information via independent shadowing and fading channels yields diversity gains. These gains stem from the fact that with the amount of additional copies increasing, the probability of all of them being illegible decreases. The provision of such copies can be achieved, for example, by having a relay provide a copy in addition to the information received already via the direct link; or by having several relays provide copies in parallel. Diversity gains improve the performance of the system, such as the probability of error P_e or outage P_{out}. Either probability depends on the rate R in a similar fashion and is known to be related to the diversity gain at asymptotically high SNRs as [20]

$$P_{\text{out}}(R) = \frac{\text{const}(R)}{\text{SNR}^d} \tag{2.3}$$

where d is the diversity gain or diversity order, and $\text{const}(R)$ is some constant depending on R. It effectively equals the number of copies of the same information; for instance, having one relay and a direct link providing two independent copies of the same information, yields $d = 2$. At the same level of performance metric, for example, requiring an outage probability of 1%, increasing the diversity order allows a saving in transmit power; for instance, with $d = 2$ about 3 dB transmission power can be saved in a flat Rayleigh fading channel.

2.3 Mobile Wireless Channel

In wireless communications, the communication medium between terminals is called a mobile radio channel. Radio wave propagation through this wireless

channels is a complicated phenomenon characterized by various effects, such as noise, interference and fading. Noise is the most common form of distortion in communication system which originates from the operating temperatures of the ohmic elements in the receivers, thereby limiting its sensitivity. The degradation in cellular networks can also result form intra, inter, adjacent and co-channel interferences which vary with frequency reuse patterns and duplexing modes. Multiple access interference (MAI) exists in multiple access network, where multiple users share the network resources of time, frequency, code or the combination of them, to increase the number of users supported by the network. Multipath propagation of a signal caused fading in mobile radio channel. Multipath fading can be divided into two broad categories: large-scale fading and small-scale fading [76].

Large-scale fading is represented by the average signal power attenuation due to motion over large areas and is affected by prominent terrain contours such as hills, forests and man-made structures. The statistics of large-scale fading provide a way of computing an estimation of the average signal strength loss as a function of distance. This is described in terms of pathloss and shadowing. Pathloss can be defined as the decay of the mean signal power with distance from the transmitter. It includes all possible elements associated with interactions between the propagating wave and any object between the transmit and receive antennas. In free space, the mean signal power decreases with the square of the distance from the transmitter. In wireless channels, where often no direct LoS path exists between the transmitter and receiver, the signal power decreases with a power higher than two and is typically in order of three to five [76].

Shadowing is caused by the obstruction of the transmitted waves, for example by hills, building, walls and trees. This results in some paths with increased loss while others less obstructed reaching the receiver with increased signal strength. This varying signal strength exhibit a log-normal behavior and generally modeled by log-normal distribution [76].

Provided that the other fading (small-scale fading) components are removed by correct averaging, the effects of mean pathloss and shadowing can be noted by plotting the average signal level for different points in a propagation medium against distance, which fits into a line [69]. The slope of the line depends on

the frequency used for transmission, antenna height and propagation environment. The associated standard deviation of the large scale fading depends on the medium and has been observed to vary between 5 to 12 dB [76]. When designing communication systems, a power margin is set aside to compensate for these types of fading.

Small-scale fading is commonly known as multipath fading which refers to the drastic changes in signal amplitude and phase as a result of small changes in spatial separation between the receiver and the transmitter. It occurs due to reflection, scattering and diffraction of the transmitted electromagnetic wave at natural or man-made objects. A multitude of waves arrive from many different directions with varying delays, amplitudes and phases, caused by the mobility of either the receiver, the moving objects or both, in the wireless channel. At the receiver, the superposition of these waves results in amplitude and phase variations of the composite received wave resulting in time-variant multipath propagation. The varying signal strength due to small-scale fading is highly sensitive even to small displacement in the order of the wavelength and may result in a totally different wave superposition.

The attenuation of received signal strength caused by large-scale fading (shadowing and pathloss) can be counteracted completely by power control/margins and are not considered further in this thesis. Also, the thesis considers only a single cell scenario with MAI.

Next, an overview of the wireless channel is discussed with respect to the small-scale multipath fading characteristics.

2.3.1 Time-variant Multipath Propagation

The small-scale fading manifests itself in two mechanisms of time variance and signal time-spreading. A statistical description of multipath channel based on Bello's model [8] has been used here to explain these mechanisms, since a deterministic description appears impossible in practice. Bello proposed the concept of wide sense stationary uncorrelated scattering (WSSUS) which treats signal variation arriving with different delays as uncorrelated and assumes that such a channel is effectively WSS in both time and frequency domains. In the case of

a mobile wireless channels, this model contains four functions; two describe the signal time-spreading (one in the time and the other in the frequency domain), and two describe the time-variance of the channel due to motion (also covering both time and frequency domains). Next, these functions and the way they are connected with each other are briefly reviewed.

The mobile wireless channel is described by the time-variant channel impulse response $h(\tau, t)$, which represents the response of the channel at time t due to an impulse applied at $t - \tau$. The Fourier transform of $h(\tau, t)$ is the time-variant channel transfer function $H(f)$. The assumption of WSS represents a channel whose fading statistics remain constant over short period of time or small spatial distances. This makes the mean value of the channel random process independent of time and its auto correlation depending only on the time differences. In multipath propagation environments, the channel impulse response is composed of a large number of scattered impulses received over L different paths and can be expressed as [69]

$$h(\tau, t) = \sum_{l=0}^{L-1} \alpha_l e^{j(2\pi f_{D,l} t + \theta_l)} \delta(t - \tau_l) \tag{2.4}$$

where $\delta(\cdot)$ is the Kronecker delta function with α_l, $f_{D,l}$, θ_l and τ_l are the amplitude, Doppler frequency, phase and the propagation delay of the lth path, respectively. The Doppler frequency $f_{D,l} = \frac{v_c f_c}{c} \cos \theta_l$ depends on the velocity v_c of the receiver, the speed of light c, the carrier frequency f_c and the angle of incidence θ_l of the lth path.

The correlation function of the channel impulse response is sufficient to characterize the time-variant behavior or the fading rapidity of wireless channels. Defining the autocorrelation function as [76]

$$R(\tau_i, \tau_j, \Delta t) = \frac{1}{2} E\left\{h(\tau_i, t) h^*(\tau_j, t + \Delta t)\right\} \tag{2.5}$$

where Δt denotes the observation time difference. Under the presumption of WSSUS, random processes $h(\tau_i, t)$ and $h(\tau_j, t)$ are uncorrelated for $\tau_i \neq \tau_j$ (scattering at two different paths is uncorrelated in most radio transmissions), the

autocorrelation function of (2.5) simplifies to

$$R\left(\tau_i, \tau_j, \Delta t\right) = \phi(\tau_i, \Delta t)\delta(\tau_i - \tau_j) \tag{2.6}$$

where $\phi(\tau, \Delta t)$ represents the delay cross-power spectral density [8], and the wireless channel characterized by (2.6) is referred to as WSSUS channel. The Fourier transform of $\phi(\tau, \Delta t)$ in Δt yields the scattering function which provides a measure of average power output of the channel as function of delay τ and the Doppler frequency f_D. The scattering function can be expressed as

$$\bar{S}(\tau, f_D) = \int_{-\infty}^{\infty} \phi(\tau, \Delta t) e^{-j2\pi f_D \Delta t} d(\Delta t) \tag{2.7}$$

By integrating (2.7) over the Doppler frequency f_D, the power delay density spectrum is obtained which is identical to the delay cross-power spectral density $R(\tau_i)$ at $\Delta t = 0$. This power power delay density spectrum gives the average power of the channel output as a function of delay τ and can be viewed as a scattering function averaged over all Doppler shifts. By further assuming that L paths have the normalized autocorrelation function, but different average powers and denoting the average power of lth path as P_l, then 2.5 can be written as

$$P_l = \frac{1}{2} E\left\{h(\tau_l, t) h^*(\tau_l, t)\right\} \tag{2.8}$$

where $P_l, l = 0, 1, ..., L-1$ represents the power delay profile (PDP) of the channel which is characterized by excess delay, mean delay and most importantly root mean square (RMS) delay spread. The delay of any path relative to first arriving path is called excess delay, while total excess delay is also called the maximum delay spread $\tau_{\max}$, represents the difference between the delay of the first and the last path. If the duration of the transmitted symbol is significantly larger than $\tau_{\max}$, the channel produces the minimum of ISI. This effect is efficiently exploited in OFDM where the duration per transmitted symbol increases with the number of subcarriers and hence, the amount of ISI is reduced. The most common and simplest approach to quantify the time spreading of multipath channel is by using the PDP characteristic parameters in time domain, in particular the mean delay

and RMS delay spread. The PDP is described in the delay dimension to yield L individual paths or taps of power $P_0, ..., P_{L-1}$. Mean delay which is the delay corresponding to the center of gravity of the profile is given by

$$\tau_m = \frac{1}{P_T} \sum_{l=0}^{L-1} P_l \tau_l \tag{2.9}$$

where the total power in the channel is $P_T = \sum_{l=0}^{L-1} P_l$.

RMS delay spread is the second moment or spread of the paths. It takes into account the relative powers of the paths as well as their delays, thereby making it a better indicator of system performance and is defined by [76]

$$\tau_{\text{rms}} = \sqrt{\frac{1}{P_T} \sum_{l=0}^{L-1} P_l \tau_l^2 - \tau_m^2} \tag{2.10}$$

The coherence bandwidth B_c of a wireless channel measures the frequency range over which the fading process is correlated; i.e. the bandwidth over which the correlation function of two samples of the channel response taken at the same time but at different frequencies falls below a suitable value. It is inversely proportional to the delay spread τ_{rms} and defined as the bandwidth over which frequency correlation function is above $\frac{1}{2}$ and can be approximated by $B_c \approx \frac{1}{5\tau_{\text{rms}}}$. More specifically for a correlation level ρ_c, it can be expressed as [76]

$$B_c \geq \frac{1}{2\pi\tau_{\text{rms}}} \cos^{-1} \rho_c \tag{2.11}$$

Frequency selectivity, which is an important characteristics of wireless channel is determined by the coherence bandwidth. If all the spectral components of the transmitted signal are affected in a similar manner, the fading is said to be frequency non-selective or equivalently, frequency flat. This is the case for narrowband systems in which the transmitted signal bandwidth B is much smaller than the channel's coherence bandwidth B_c. On the other hand, if the spectral components of the transmitted signal are affected by different amplitude gains and phase shifts, the fading is said to be frequency selective. This applies to broadband systems in which the transmitted signal bandwidth B is larger than

the coherence bandwidth B_c. The coherence bandwidth also helps in evaluating the performance of spreading and frequency interleaving techniques that are used to exploit the inherent frequency diversity G_{fq} of the wireless channel. In the case of OFDM based system, frequency diversity is exploited if the separation of the subcarriers transmitting the same information exceeds the coherence bandwidth. The maximum achievable frequency diversity is approximated by the ratio between the signal bandwidth and coherence bandwidth as $G_{fq} \approx \frac{B}{B_c}$ and consequently, depends on the delay spread τ_{rms} of the channel [21].

The maximum Doppler frequency $f_{D_{\max}}$ quantifies the frequency-dispersive properties of multipath channel. For OFDM, if the sub-channel spacing is significantly larger than the maximum Doppler frequency $f_{D_{\max}}$, the channel produces a negligible amount of ICI. An equally important wireless channels' parameter is the channel coherence time T_c . This is the duration over which the channel characteristics can be considered as time invariant. T_c is inversely proportional to the $f_{D_{\max}}$ and can be defined as the time over which the time correlation function is above $\frac{1}{2}$ and can be approximated as [76]

$$T_c \approx \frac{9}{16\pi f_{D_{\max}}} \tag{2.12}$$

The channel is said to be time selective, if the duration of the transmitted symbol is larger than the coherence time T_c. Conversely, if it is smaller than T_c, the channel is time-selective or flat. Time selective and non-selective channels are also referred as fast and slow (quasi-static) fading channels, respectively. The coherence time of the channel is important for evaluating the performance of FEC, channel coding and interleaving techniques that try to exploit the inherent time diversity G_t of the mobile radio channel. Normally, block fading models are used for such analysis. Unlike quasi-static fading, block fading channels assume that a frame may span multiple independent fading blocks where in each block the fading remains invariant. Time diversity is exploited when the separation between successive time slots carrying the same information exceeds the coherence time T_c and is approximated by the ratio between the frame duration which consists

of a number of time slots and the coherence time T_c given by

$$G_t \approx \frac{T_{\text{frame}}}{T_c} \tag{2.13}$$

which consequently depends on the maximum Doppler frequency $f_{D_{\max}}$ of the channel.

2.4 Modeling of Multipath Channels

Statistical characterization of wireless fading channels has remain a very important research area and considerable efforts have been devoted for the accurate modeling of such propagation environments. The results of these intense efforts provide a range of relatively simple and accurate statistical models for wireless channels which depends on the particular propagation environment and the underlying communication scenario. In this section, a review of Rayleigh, Rician and Nakagami-m fading models is presented. First, these models are explained for frequency flat fading channels and then extended for broadband frequency selective scenario. Finally, considering the OFDM-based system, the frequency domain modeling of subject channels is also presented.

2.4.1 Frequency Flat Fading Channels

The signal transmitted through the wireless channel is subjected to envelope and phase distortions. Among these two distortions, the latter results in severe performance degradation of coherent modulated system, unless measures are taken to compensate for them at the receiver. Conversely, non-coherent modulation does not require phase information at the receiver and the performance remains independent of phase variations for such systems. Most often, the system analysis are conducted with ideal coherence modulation which assumes perfect corrected phase variations and only the fading envelope statistics are taken into account at the receiver. The same assumption has been invoke in this thesis.

In frequency narrowband environments, the received signal is subjected to two random processes. First, it is modulated by the fading path amplitude and then

further corrupted by additive white Gaussian noise (AWGN). The path amplitude α, defined in (2.5) is a random variable (RV) with mean square and probability density function (PDF) denoted by $\Omega = E\{\alpha^2\}$ and $p_\alpha(\alpha)$, respectively. AWGN is typically assumed to be statistically independent of α and characterized by one-sided power spectral density N_0 (Watts/Hz). The instantaneous and average SNR can be defined as $\gamma = \alpha^2 \frac{E_s}{N_0}$ and $\bar{\gamma} = \Omega \frac{E_s}{N_0}$, respectively, where E_s is the energy per symbol. Following [81], the PDF of γ can be calculated by introducing a change of variables in the fading PDF $p_\alpha(\alpha)$ of α, expressed as

$$p_\gamma(\gamma) = \frac{p_\alpha(\sqrt{\Omega\gamma/\bar{\gamma}})}{2\sqrt{\gamma\bar{\gamma}/\Omega}} \tag{2.14}$$

with the associated moment generating function (MGF) is given by

$$\mathcal{M}_\gamma(\mu) = \int_0^\infty p_\gamma(\gamma) e^{\mu\gamma} d\gamma \tag{2.15}$$

Next,the PDFs and MGFs of Rayleigh, Rician and Nakagami-m channel model are revisited.

Rayleigh Model

Rayleigh distribution is frequently used to model multipath fading in NLoS environments with the fading channel amplitude α distributed according to [64]

$$p_\alpha(\alpha) = \frac{2\alpha}{\Omega} \exp\left(-\frac{\alpha^2}{\Omega}\right), \ \alpha \geq 0 \tag{2.16}$$

Using (2.14), the instantaneous SNR γ of a Rayleigh channel is exponentially distributed and can be expressed as

$$p_\gamma(\gamma) = \frac{1}{\bar{\gamma}} \exp\left(-\frac{\gamma}{\bar{\gamma}}\right), \ \gamma \geq 0 \tag{2.17}$$

and the respective MGF is given by [81]

$$\mathcal{M}_\gamma(\mu) = (1 - \mu\bar{\gamma})^{-1} \tag{2.18}$$

Rician Model

Rician model is also known as Nakagami-n. It is usually employed to characterize a propagation environment where there exists a strong LoS path with many random indirect weaker components. In this case, the channel fading amplitudes α is distributed according to [64]

$$p_\alpha(\alpha) = \frac{2(1+n^2)e^{-n^2}\alpha}{\Omega} \exp\left[-\frac{(1+n^2)\alpha^2}{\Omega}\right] I_0\left(2n\alpha\sqrt{\frac{1+n^2}{\Omega}}\right), \ \alpha \geq 0 \quad (2.19)$$

where I_0 is the zeroth-order modified Bessel function of the first kind and n is the Nakagami-n fading parameter ranging from 0 to ∞, which is also related to the Rician K factor by $K = n^2$. The parameter K represents the ratio of the power received in the LoS path to the total power received vis indirect scattered paths. Using (2.14), the instantaneous SNR γ of a Rician channel is non-central chi-square distributed and given by

$$p_\gamma(\gamma) = \frac{(1+n^2)e^{-n^2}}{\bar{\gamma}} \exp\left[-\frac{(1+n^2)\gamma}{\bar{\gamma}}\right] I_0\left(2n\sqrt{\frac{1+n^2\gamma}{\bar{\gamma}}}\right), \ \gamma \geq 0 \quad (2.20)$$

with the corresponding MGF expressed as

$$\mathcal{M}_\gamma(\mu) = \frac{1+n^2}{(1+n^2)-\mu\bar{\gamma}} \exp\left[\frac{n^2\mu\bar{\gamma}}{(1+n^2)-\mu\bar{\gamma}}\right] \quad (2.21)$$

$$F_n = \frac{1+2n^2}{(1+n^2)^2}, \ n \geq 2 \quad (2.22)$$

Nakagami-m Model

This fading model introduced by Nakagami in [64] has received considerable attention due to its great versatility in terms of flexibility and accuracy in providing a better match to various empirically obtained measurement data than Rayleigh or Rician distributions. It is often gives the best fit to land, indoor-mobile multipath propagation as well as scintillating ionospheric radio links [81]. The Nakagami-m

PDF is in essence a central chi-square distribution given by [64]

$$p_\alpha(\alpha) = \frac{2}{\Gamma(m)} \left(\frac{m}{\Omega}\right)^m \alpha^{2m-1} \exp\left(-\frac{m}{\Omega}\alpha^2\right), \ \alpha \geq 0 \tag{2.23}$$

where $\Gamma(\cdot)$ is the Euler Gamma function and m is the Nakagami-m fading parameter ranging from 0 to ∞. Using (2.14), the instantaneous SNR γ of a Nakagami-m channel is gamma distributed and given by

$$p_\gamma(\gamma) = \frac{1}{\Gamma(m)} \left(\frac{m}{\bar{\gamma}}\right)^m \gamma^{m-1} \exp\left(-\frac{m\gamma}{\bar{\gamma}}\right), \ \gamma \geq 0 \tag{2.24}$$

with the corresponding MGF is expressed as

$$\mathcal{M}_\gamma(\mu) = \left(1 - \frac{\mu\bar{\gamma}}{m}\right)^{-m} \tag{2.25}$$

The fading figure and m parameter are related by

$$m = \frac{1}{F_m} = \frac{\Omega^2}{E\left\{(\alpha^2 - \Omega)^2\right\}}, \ m \geq \frac{1}{2} \tag{2.26}$$

In Figure 2.1, the Nakagami-m PDF is plotted for various values of m parameter with $\Omega = 1$. This distribution, with the flexibility of m parameter, span the widest range of fading figure from 0 to 2. As special cases, it includes the one-sided Gaussian and Rayleigh distribution for $m = \frac{1}{2}$ and $m = 1$ respectively. For the limit as $m \to +\infty$, the Nakagami-m fading channel converges to a non-fading AWGN channel. Furthermore, when $m > 1$, equating (2.22) and (2.26), the Nakagami-m distribution gives a one-to-one mapping between the m parameter and the n parameter (equivalently, the Rician K factor), making it possible to closely approximate the Rician distribution. The mapping can be expressed as

$$m \approx \frac{(1+n^2)^2}{1+2n^2}, \quad n \geq 0, \quad n \approx \sqrt{\frac{\sqrt{m^2-m}}{m-\sqrt{m^2-m}}}, \ m \geq 1 \tag{2.27}$$

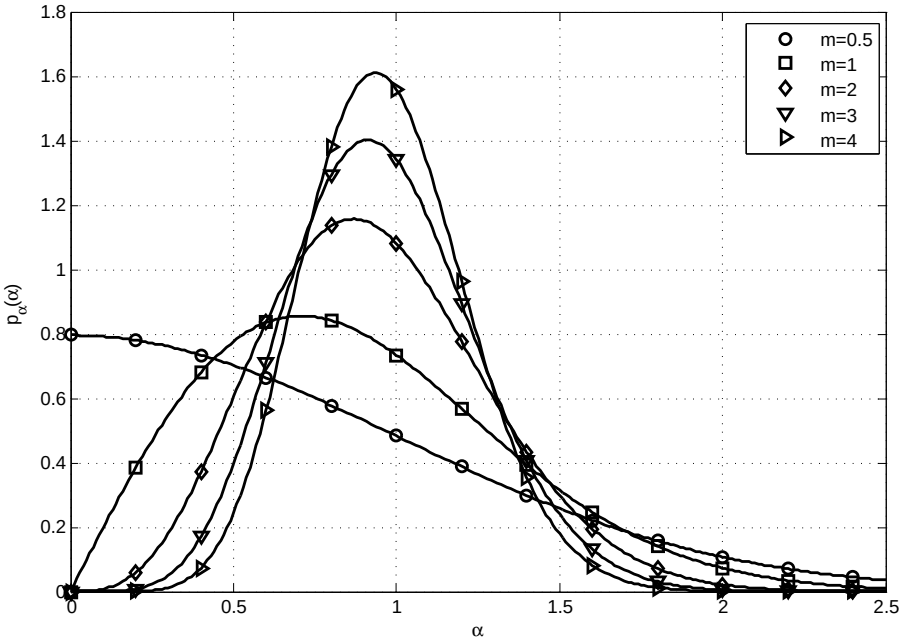

Figure 2.1: Nakagami-m PDF with various values of fading parameter m

2.4.2 Frequency Selective Fading Channel

In broadband environment, the spectrum of the signals is affected by the channel transfer function as they propagate through the frequency selective channel. Selective fading can be modeled by the complex valued low-pass equivalent impulse response of (2.4). Assuming the slow fading channel in which L multipaths remain constant over a period of time, thus making the path amplitude α_l, phase θ_l and delays τ_l for $l = 0, ..., L-1$ constant over a symbol interval. Thanks to WSSUS and considering the fact that in realistic environment, the different paths of a given impulse response are originated by different scatterers exhibiting negligible correlations and making it reasonable to model $\{\alpha_l\}_{l=0}^{L-1}$ paths as statistically independent RVs. Therefore it is straightforward to extend the flat fading notations of section 2.4.1 by assuming the the lth resolvable path amplitude α_l is an RV with mean square value $\Omega_l = E\{\alpha_l^2\}$, PDF $p_{\alpha_l}(\alpha_l)$ and can be from the Rayleigh or Nakagami-m PDF. Extending the flat fading analysis, the instantaneous and average SNR per symbol of the lth multipath in the frequency selective scenario can be expressed by $\gamma_l = \alpha_l^2 \frac{E_S}{N_0}$ and $\bar{\gamma}_l = \Omega \frac{E_S}{N_0}$, respectively.

The channel PDP is typically a decreasing function of delay and directly related to $\{\Omega_l\}_{l=0}^{L-1}$. It can assume various forms depending on propagation conditions and whether the model is for indoor or outdoor environments. Generally, it can be represented by $\Omega_l = \Omega_0 e^{l\delta}$, where $\delta \geq 0$ is the rate of average power decay and Ω_0 is the average power of the first multipath (tap).

2.4.3 Frequency-domain Channel Modeling

For the performance analysis of OFDM-based systems, it is necessary to derive the statistics of the multipath channel in the frequency domain. The frequency domain modeling of Nakagami-m has been presented in [43]. In [43], it is shown that the channel frequency response can be well approximated by Nakagami-m random variable with frequency domain fading parameter m_f and mean power Ω_f, which in general are different from their time domain counterparts m and Ω respectively. Although for the special case of Rayleigh ($m = 1$), both time and frequency domain fading remains the same.

Considering the time-domain channel impulse response of (2.4), each path amplitude α_l can be represented by a Nakagami-m RV and the PDF can be expressed by including the path index l to the expression of (2.23). The modified PDF becomes

$$p_{\alpha_l}(\alpha_l) = \frac{2}{\Gamma(m_l)} \left(\frac{m_l}{\Omega_l}\right)^{m_l} \alpha_l^{2m_l-1} \exp\left(-\frac{m_l}{\Omega_l}\alpha_l^2\right), \ \alpha \geq 0 \tag{2.28}$$

In an OFDM-based system, the N-point discrete Fourier transform (DFT) of the channel frequency response at the kth subcarrier can be expressed as

$$H(k) = \frac{1}{\sqrt{N}} \sum_{l=0}^{L-1} \alpha_l e^{-j2\pi kl/N} \tag{2.29}$$

which confirms that the channel frequency responses at each subcarrier are the DFT of the same impulse responses and hence correlated in frequency. Now, based on the original derivation of [64], it can be shown that $\beta(k) = |H(k)|$ also

approximately follows the Nakagami-m distribution with the PDF

$$p_\beta(\beta) = \frac{2}{\Gamma(m_f)} \left(\frac{m_f}{\Omega_f}\right)^{m_f} \beta^{2m_f-1} \exp\left(-\frac{m_f}{\Omega_f}\beta^2\right), \ \beta \geq 0 \tag{2.30}$$

and the frequency domain fading parameter m_f and mean power Ω_f given by

$$m_f = \frac{\left(\sum_{k=0}^{L-1} \Omega_k\right)^2}{\sum_{k=0}^{L-1} \left(\frac{\Omega_k^2}{m_k}\right) + \sum_{k=0}^{L-1} \sum_{l=0,l\neq k}^{L-1} \Omega_k \Omega_l} \tag{2.31}$$

$$\Omega_f = \frac{1}{N} \sum_{k=0}^{L-1} \Omega_k \tag{2.32}$$

Assuming equal fading parameters for all paths ($m_l = m$) and exponential PDP, (2.31) and (2.32) simplify to

$$m_f = \frac{1}{\left(\frac{1}{m} - 1\right)\left(\frac{1-e^{-2L\delta}}{1-e^{-2\delta}}\right)\left(\frac{1-e^{-\delta}}{1-e^{-L\delta}}\right)^2 + 1} \tag{2.33}$$

$$\Omega_f = \frac{1-e^{-L\delta}}{1-e^{-\delta}} \left(\frac{\Omega_0}{N}\right) \tag{2.34}$$

From the above, it can be summarized:

- for constant PDP with $\delta = 0$, the frequency domain fading parameter become $m_f = \left(\frac{Lm}{Lm-m+1}\right)$ and $\Omega_f = \left(\frac{L}{N}\right)\Omega$
- for flat fading with $\delta = \infty$, $m_f = m$ and $\Omega_f = \left(\frac{1}{N}\right)\Omega$
- when $m < 1$, then $m \leq m_f < 1$ and $m > 1$, then $1 \leq m_f < m$
- finally, for Rayleigh fading case $m = m_f = 1$, i.e. Rayleigh fading in time domain always yields Rayleigh fading in the frequency domain.

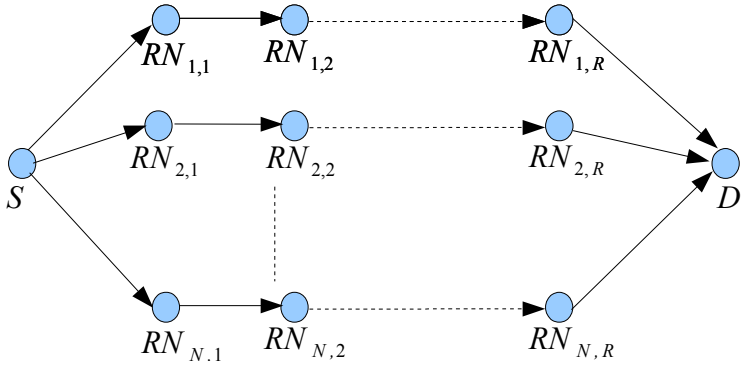

Figure 2.2: Wireless relay network with multihop, multi-branch transmission

2.5 Performance Analysis of Wireless Relay Networks

The performance analysis of multihop wireless communication systems operating in fading channels has been an important field of research in the past few years. Thus, performance analysis of cooperative networks has yielded many interesting results including average SNR, information theoretic metrics like outage probability, and average SER expressions over fading channels.

The analytical expressions for the performance of wireless relay network can also give us insight into the optimal allocation of the resources like power and bandwidth. For AF relay networks, in which the performance metrics at the destination usually depend on channel characteristics of all hops, the performance analysis becomes more challenging, comparing to the collocated MIMO or DF relay systems. Hence, a large portion of this thesis is dedicated to the performance analysis of AF based relay networks.

Also in this thesis, for sufficiently large SNR, the closed-form expressions for the average SER and outage probability are derived under different topologies, cooperation methods, and CSI assumptions. The simplicity of the asymptotic results provides valuable insights into the performance of cooperative networks and suggests means of optimizing them. In addition, the diversity order of the wireless systems can be found via the asymptotic behavior of the average SER or

outage probability. A tractable definition of the diversity or diversity gain is [37]

$$d = -\lim_{SNR\to\infty} \frac{\log(P_e)}{\log(SNR)} \tag{2.35}$$

where instead of the average SER P_e, the outage probability P_{out} can be also used.

The average SER formula allows us to clearly illustrate the advantage that the distributed diversity system has in overcoming the severe penalty in SNR caused by Rayleigh fading. In [5], DSTC based on the Alamouti scheme and AF cooperation protocol was analyzed and an expression for the average SER was derived. Authors in [3] presented an exact average symbol error rate analysis for the repetition- based cooperation, in which relays transmit in orthogonal channels via time division multiple access (TDMA) or frequency division multiple access (FDMA). Using simple bounds on the probability of error, [3] shows that the cooperative network amplifying relays achieves full diversity order. Hasna and Alouini in [27] have presented a useful and semi-analytical framework for the evaluation of the end-to-end outage probability of multihop wireless systems with AF CSI-assisted relays over Nakagami-m fading channels. Moreover, the same authors have studied the dual-hop systems with DF and AF (CSI-assisted or fixed gain) relays over Rayleigh [28] and Nakagami-m [29] fading channels. Recently, Boyer et al. [13], have proposed and characterized four channel models for multihop wireless communication and also have introduced the concept of multihop diversity. Finally, Karagiannidis et al. [45] have studied the performance bounds for multihop wireless communications with blind (fixed gain) relays over Rice, Hoyt, and Nakagami-m fading channels, using the moments-based approach [44]. In [46], efficient performance bounds are presented for the end-to-end SNR of multihop wireless communication systems with CSI-assisted or fixed gain relays operating in non-identical Nakagami-m fading channels. Using expressions for MGF and PDF, closed-form lower bounds are presented in [46] for important end-to-end system performance metrics, such as outage probability and average SER for BPSK, while simple asymptotic expressions are also given for the bounds at high SNRs.

For sufficiently high SNR, [74] derives general average SER expressions, for

AF links with multiple cooperating branches, composed of multiple cooperating hops, as it is shown in Figure 2.2. In [74] the authors derived asymptotic average SER for AF cooperative diversity networks. The resulting expressions derived in [74] using the bounding approach are general for any type of fading distributions provided the PDF of zero instantaneous SNR is not zero, which is not applicable for the Nakagami-m fading distribution. In [36], the error rate and the outage probability of cooperative diversity wireless networks with AF relaying are determined over independent, non-identical, Nakagami-m fading channels.

In [6], a performance analysis of the gain using DF based cooperation among nodes was considered, assuming that the number of relays that are available for cooperation is a Poisson random variable. The authors compared the performance of different DSTBC designed for the MIMO channels under this assumption. In [84], authors considered a DF cooperation protocol, and derived closed-form SER for the DF cooperation systems with M-PSK and M-QAM signals. Since the closed-form SER formulation is complicated, [84] established two SER upper bounds to show the asymptotic performance of the cooperation system, in which one of them is tight at high SNR. Based on the SER performance analysis, the optimum power allocation for the cooperation systems is determined.

2.6 OFDM Data Structure & Detection

Parallel data transmission commonly known as multicarrier (MC) communication provides an effective approach to prevent ISI. The principle of MC modulation as shown in Figure 2.3 is to convert a high rate data stream into N low-rate substreams, where N is the number of subcarriers used for data transmission. Each substream is modulated on its assigned subcarrier $f_k, k = 1, ..., N-1$, which divide the available channel bandwidth into N successive narrow subcarriers that appear frequency flat. The data symbol rate per subcarrier is reduced to a factor proportional to the number of assigned subcarriers and with that the effect of delay spreads and consequently ISI, significantly decreases, thereby reducing the complexity of equalizers. FDM is the the most common realization of MC communication where the subchannels are completely separated in frequency domain and ICI is controlled by ensuring the subchannel spacing greater than the

Nyquist bandwidth [21]. However, this complete frequency separation leads to inefficient use of available spectrum. OFDM provides an effective and profitable bandwidth utilization solution by allowing the spectrum to overlap between adjacent subchannels. It employs rectangular pulse shaping with the subcarrier spacing equal to the reciprocal of the symbol duration per subcarrier, thereby maintaining the orthogonality between them. In wireless environments, one of the main design goals for an OFDM system is that the channel can be considered as time-invariant during one OFDM symbol and the fading per subcarrier can be considered as flat. This condition can only be fulfilled if the OFDM symbol duration is smaller than the coherence time of the channel and the subcarrier spacing smaller then the coherence bandwidth. If these conditions are fulfilled, the realization of low complexity receivers become possible.

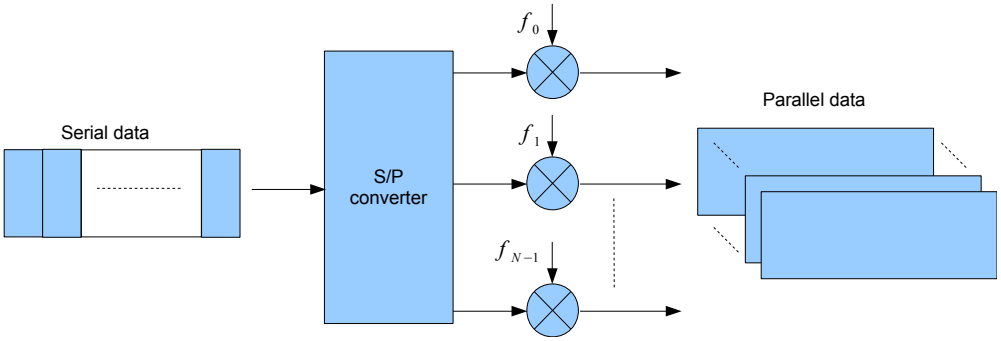

Figure 2.3: Principle of multicarrier modulation

An OFDM modulator takes N serial source symbols to produce a sequence $S(k), k = 0, ..., N$. The source symbols may be obtained after source and channel coding, time-interleaving and appropriate symbol mapping. These source symbols of rate $1/T$ are then placed on N parallel substreams, where T is the individual symbol duration. By doing so, the rate per substream reduces to $1/T_S = 1/NT$, where $T_S = NT$ is the OFDM symbol duration with the respective OFDM symbol rate given by $1/T_S$. Throughout the thesis, frequency domain variables such as the source symbols $S(k), k = 0, ..., N-1$ are written with capital letters. Also, for brevity but without loss of generality, the transmission of a single but arbitrary sequence $S(k)$ is considered in this section, so that no additional time index required. The reason being the isolated assumption of $S(k)$ is valid as ISI and

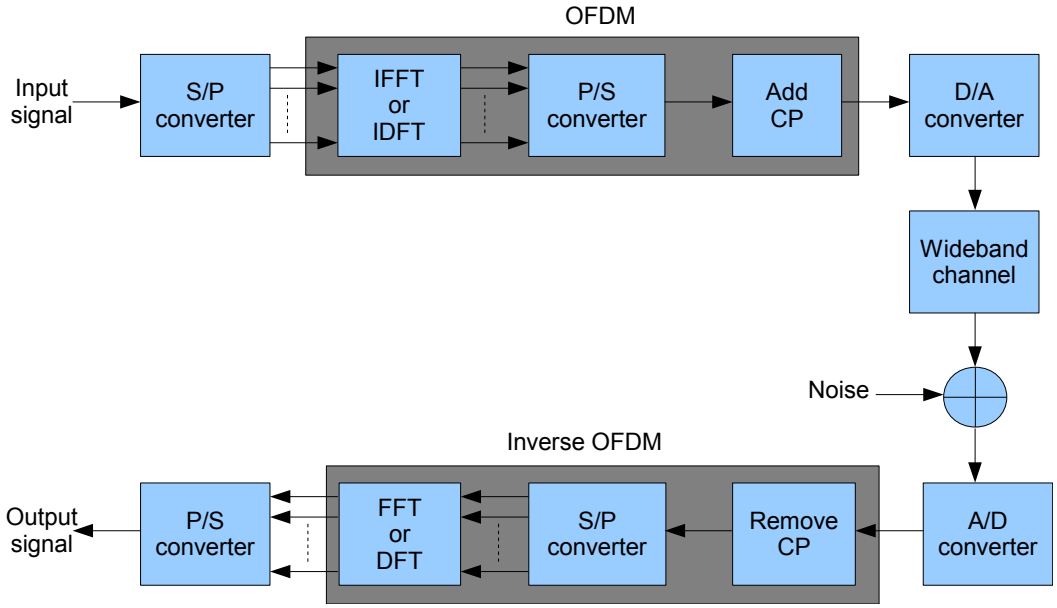

Figure 2.4: OFDM system model

ICI can be avoided with OFDM. These parallel substreams are then modulated on N subcarriers with spacing of $f_s = 1/T_S$, which provides spectral overlap as well as orthogonality between signals.

The complex envelope of an OFDM symbol with rectangular pulse shaping can be expressed as [21]

$$s(t) = \frac{1}{\sqrt{N}} \sum_{k=0}^{N-1} S(k) \text{rect}\left(\frac{t}{T_S} - \frac{k}{2}\right) e^{j2\pi f_k t} \tag{2.36}$$

where $\frac{1}{\sqrt{N}}$ is the energy normalization factor and the subcarrier frequencies at positions

$$f_k = \frac{k}{T_S}, \;\; k = 0, 1, ..., N-1 \tag{2.37}$$

with the center of the frequency spectrum is located at $\frac{N-1}{2T_S}$. The energy density spectrum $|X(f)|^2$ of an OFDM symbol is the sum of the energy density spectra

of N independently modulated subcarriers, given by

$$|X(f)|^2 = \frac{1}{N}\sum_{k=0}^{N-1}\left|S(k)T_S\frac{\sin\left(\pi\left(f-f_k\right)T_S\right)}{\pi\left(f-f_k\right)T_S}\right|^2 \tag{2.38}$$

One of the major breakthroughs that made OFDM highly attractive in the present era is its implementation in discrete domain by using the inverse discrete Fourier transform (IDFT) or more computationally efficient, inverse fast Fourier transform (IFFT) [95]. The block diagram of an OFDM modulator employing IDFT/IFFT and the respective demodulator equipped with DFT/FFT is shown in Figure 2.4. If the complex envelope $s(t)$ of (2.36) is sampled at time $t = \frac{nT_S}{N}$ for $n = 0, ..., N-1$ with sampling rate N/T_S, then the resulting samples can be expressed as

$$s(n) = \frac{1}{\sqrt{N}}\sum_{k=0}^{N-1} S(k)e^{j2\pi kn/N},\ \ n = 0, ..., N-1 \tag{2.39}$$

which shows that the sampled sequence $s(n),\ n = 0, ..., N-1$ is the IDFT/IFFT of the source symbol sequence $S(k),\ k = 0, ..., N-1$. As the number of subcarrier increases, the OFDM symbol duration T_S becomes large compared to the maximum delay spread $\tau_{\max}$ of the channel and with that, the amount of ISI reduces. The complete elimination of ISI and perfect orthogonality (zero ICI) between all signals in the N subcarriers is achieved by introducing a guard interval of duration $T_g \geq \tau_{\max}$ between the adjacent OFDM symbols [69]. The guard interval is actually a cyclic prefix (CP) added to each OFDM symbol and obtained by extending the duration of an OFDM symbol to $T'_S = T_g + T_S$. The discrete length of the CP has to be $L_{cp} \geq \left\lceil \frac{\tau_{\max} N}{T_S} \right\rceil$ samples to prevent ISI.

The sampled sequence $s(n)$ with the addition of CP can be represented by

$$s(n) = \frac{1}{\sqrt{N}}\sum_{k=0}^{N-1} S(k)e^{j2\pi kn/N},\ \ n = -L_g, -L_g+1, ..., N-1 \tag{2.40}$$

and passed through a digital-to-analog (DA) converter whose output ideally should be the signal waveform $s(n)$ given in (2.39) with the extended OFDM symbol duration T'_S. The waveform passes through the wideband channel and then further perturbed by the noise at the receiver. Invoking central limit theo-

rem, this noise which contains the inherent disturbance of transmission system is modeled as AWGN [69]. The received signal is then down-converted with analog-to-digital (AD) converter and after the removal of the first L_{cp} samples that is corrupted by ISI, of each OFDM symbol, the rest of received signals are fed to the OFDM demodulator for DFT/IFFT operation. With complete elimination of ICI and ISI, the received FFT operated signal $Y(k),\ k = 0, ..., N-1$, can be considered separately for each subcarrier and can be represented as [21]

$$Y(k) = H(k)S(k) + Z(k),\ k = 0, ..., N-1 \tag{2.41}$$

where $H(k)$ is the frequency response on the kth subcarrier as in (2.29) and $Z(k)$ represents AWGN with real and imaginary components assumed to be statistically independent Gaussian distributed RVs having zero mean and equal variance of $\sigma^2_{Z(k)} = E\{|Z(k)|^2]\}$ for $k = 0, ..., N-1$. In Figure 2.5, using the expression of (2.41), the OFDM system is shown by an equivalent simplified model as a discrete time-frequency transmission system with a set of N parallel channels with different complex-valued attenuation factors. Based on this simplified model, (2.41) can be represented in the matrix-vector notation as

$$\mathbf{y} = \mathbf{Hs} + \mathbf{z} \tag{2.42}$$

when the transmitted signal $\mathbf{s}$, received signal $\mathbf{y}$ and AWGN column vectors $\mathbf{z}$ are given by $\mathbf{s} = [S(0), ..., S(N-1)]^T$, $\mathbf{y} = [Y(0), ..., Y(N-1)]^T$ and $\mathbf{z} = [Z(0), ..., Z(N-1)]^T$, respectively. Also, the interference free $N \times N$ diagonal channel matrix $\mathbf{H}$ is given by

$$\mathbf{H} = \begin{bmatrix} H(0) & 0 & \dots & 0 \\ 0 & H(1) & \dots & 0 \\ \vdots & \vdots & \ddots & \vdots \\ 0 & 0 & \dots & H(N-1) \end{bmatrix} \tag{2.43}$$

From (2.42), it can be seen that the equalization required in frequency selective channels can simply be achieved by one complex-valued multiplication per subcarrier, which becomes the major motivation for using OFDM in broadband

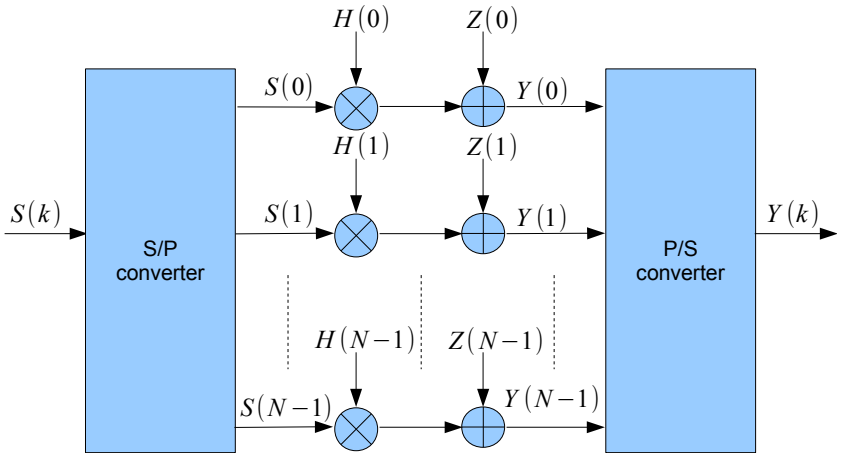

Figure 2.5: Simplified OFDM system model

environments where the realization of bandwidth efficient systems supporting simple receiver structures become possible. However, like any other transmission method, the advantages obtained from employing OFDM are also associated with some drawbacks. Although not in the scope of this thesis, some of the major implementation issues are briefly highlighted below:

- **Peak-to-Average Power Ratio (PAPR):** For wireless applications, efficient power amplification is essential for adequate area coverage and enhanced battery life. Since the OFDM symbols are composed of independently modulated sine waves giving the envelope a Gaussian distribution. This results in high PAPR and puts high demands on linear amplifiers. For the OFDM signal with N subcarriers, PAPR of the transmitted signal has shown to be N [21]. Hence for $N = 256$ only, PAPR becomes as high as 24 dB and when passed through a non-linear power amplifier, the signal may suffer significant spectral spreading and in-band distortion. To tackle PAPR conventional approaches such as using linear amplifiers result in significant power efficiency penalties. PAPR reduction techniques has remained an active and important area of research. Schemes ranging from pre-distortion of transmitted signal with complimentary non-linearity to simple and some very systematics data encoding strategies on OFDM subcarriers were proposed. Also,in the context of combined spread spectrum and OFDM systems, new set of spreading codes have been proposed

to reduce PAPR. An extensive review and possible measure for reducing PAPR can be found in [21, 24].

- **Time and frequency synchronization:** One of the main problems of OFDM is its sensitivity to synchronization errors. Orthogonality among subcarriers may easily be lost in the receiver due to the Doppler effect causing a frequency mismatch between transmitter and receiver local oscillators, therefore resulting in a large bit error rate (BER) degradation. Timing offset can also cause the symbol phase to be rotated which leads to decision errors, however its effect is less severe then that due to the frequency offset. The investigation of synchronization errors is not part of this thesis and the related work can be found in the reference within [24].

2.7 MC-CDMA Signal Structure & Detection

The success of OFDM in broadcast applications motivated many researchers around the world to investigate the suitablity of MC and in particular, OFDM for broadband mobile communications networks and several novel MC-based spread spectrum techniques were proposed [100]. In general, spread spectrum signals are characterized by the multiple repetition of each data symbol which is achieved by mulitplication with a high rate spreading code in either time, frequency or both domains. The time domain spreading typically employs adjacent time slots to transmit the data modulated chips of a spreading code. In contrast, frequency domain spread spectrum system provide greater design flexibility by transmitting the data modulated chips of the spreading sequence on not necessarily neighbouring subcarriers.

Apart from the single carrier direct sequence CDMA (SC DS-CDMA) system which employs time-domain DS spreading, the two main MC-based techniques are MC-CDMA [100] and MC DS-CDMA [18]. The former spread the data only in the frequency domain, while the latter incorporates both time and frequency-domain spreading. Multi-tone CDMA (MT-CDMA), which is a variant of MC DS-CDMA, was also presented in [93]. A detailed overview and comparison of these techniques can be found in the excellent contributions by Hara and Prasad [25] and Yang

and Hanzo [99]. Both MC-CDMA and MC DS-CDMA mitigates the degradation due to severe multipaths with the help of OFDM. Typically, in an MC-CDMA system, flat fading is maintained on each subcarrier which ensures no ISI as well as any impairment of the subcarrier auto-correlation. Hence the number of users supported by the system remains independent of the correlation characteristics of the spreading codes. Conversely, in MC-DS-CDMA, the DS spread subcarriers are subjected to frequency selective fading which makes the total number of users supported by the system not only dependent on the time and frequency domain spreading but also on the auto- and cross-correlation of the codes [99]. Moreover, the frequency selective fading per subcarrier requires multi-finger Rake receivers for MC DS-CDMA system, thereby increasing the complexity and making it less attractive than MC-CDMA. In short, the simple but flexible structure of MC-CDMA system uses spread and coded signals over parallel subcarriers, thereby guaranteeing symbol detection and making full advantage of frequency diversity. All these characteristics makes MC-CDMA one of the most promising multi-access schemes for future cellular networks.

The principle of MC-CDMA for a single user is shown in Figure 2.6, representing the serial concatenation of DS spreading and MC modulation. The high speed data stream is first spread and then OFDM modulated in such a way that the chips of the spread data symbols are transmitted in parallel on different subcarriers. If the number of subcarriers is equal to the spreading code length which in the case in Figure 2.6, MC-CDMA requires the total bandwidth for the transmission of a single data symbol. Each data symbol is copied N substreams before multiplication with one chip of the spreading code per substream. This frequency domain spreading offers additional flexibility by making signal reconstruction simple and less complex at the receiver. The block diagram of a synchronous downlink MC-CDMA system model is shown in Figure 2.7. The same model holds for the uth user in the uplink scenario due to the absence of other users' signals. The number of users supported by the system is $U, u = 1, ..., U$ and restricted by $U \leq G$, where G is the spreading factor (SF). The equiprobable source data stream of the uth user is modulated and mapped as symbol selected from the M-ary phase shift keying (M-PSK) or M-ary quadrature amplitude modulation (M-QAM) signal constellation. The source stream may be obtained

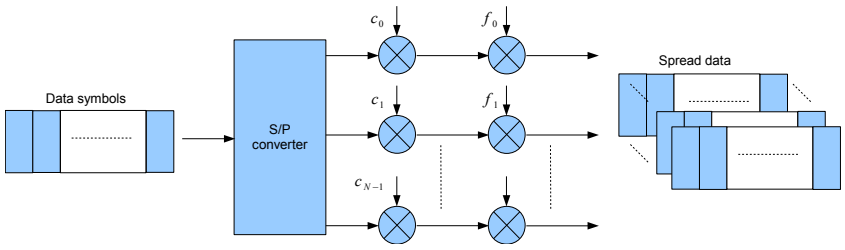

Figure 2.6: Principle of spreading of single user data by MC-CDMA

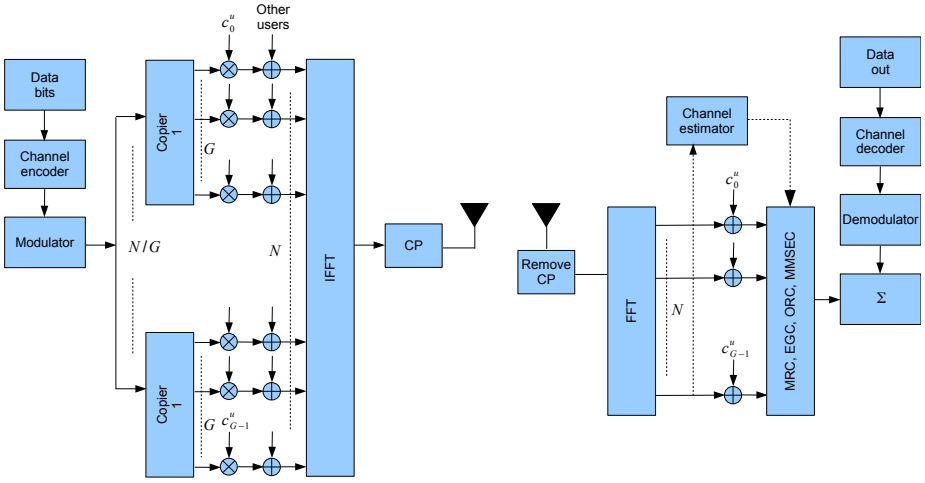

Figure 2.7: MC-CDMA system model(downlink)

after source and channel coding, time-interleaving etc. The processing gain of a MC-CDMA system is defined as $G = N/P$, where P represents the number of symbols that a user may transmit during a signaling interval. The modulated symbols are converted into $P = N/G$ parallel streams, or in other words each symbol is copied according to the spreading factor times and multiplied with the spreading code (Walsh-Hadamard) of the uth user which makes the chip G times higher than the data symbol rate. In the downlink case, the other users are spread by their specific sequences and the resulting spread chips of all U users are added synchronously and modulated by an N point IFFT. Finally, to mitigate the hostile effects of multipath fading, CP is added between each MC-CDMA symbol and the signal is transmitted after up-conversion. Ignoring the CP, the IFFT modulated data can be expressed as

$$s(t) = \sqrt{E_c} \sum_{u=0}^{U_1} \sum_{p=0}^{P-1} \sum_{g=0}^{G-1} b_p^u c_g^u e^{j2\pi(gP+p)t/T} \tag{2.44}$$

where E_c is the energy per OFDM symbol, and $E_c = E_S/N$ where E_S is the energy per symbol before spreading. T is the signaling interval during which P symbols per user are generated. b_p^u and c_g^u are the pth symbol and gth chip of the uth user, respectively. For analytical convenience and simplicity, if $P = 1$ is considered, i.e. only a single data symbol b^u for each user u, then this assumption makes $G = N$. Based on this assumption, the simplified MC-CDMA system block diagram is shown in Figure 2.8, where $\mathbf{F}_N^{\mathrm{H}}$ and $\mathbf{F}_N$ are the IFFT and FFT matrices, respectively. At the receiver, after the removal of CP and subsequent

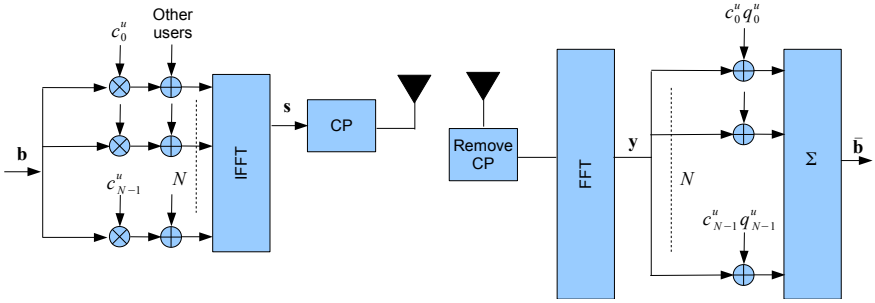

Figure 2.8: Simplified MC-CDMA system model (downlink)

FFT processing, the received signal is subjected to despreading and detection. Ignoring the assumption of $P = 1$ for the time being, the fact that the pth symbol of user u is detected independently from the p' symbols, where $p \neq p'$ for all users. Thus, without loss of generality, the subscript p can be omitted altogether for (2.44) and $G = N$ subcarriers conveying the same symbol can be considered for detection. This validates the assumption of (2.43) and the received signal at the kth subcarrier can be expressed as

$$Y(k) = \sqrt{E_c} \sum_{u=0}^{U-1} b^u c^u(k) H^u(k) + Z(k) \tag{2.45}$$

where $Z(k)$ is the discrete AWGN term and the user index u in the channel transfer function $H^u(k)$ as in (2.29) differentiates between the uplink and downlink scenarios as in the uplink case, the received signal is the sum of the signals of different users passing through different channels, depending on the location of the users. By assuming $G = N$, E_c is the energy per subcarrier or chip. The decision variable $d^{u'}$ of the u'th user's symbol can be expressed as [26]

$$d^{u'} = \sum_{k=0}^{N-1} q(k) c^{u'}(k) Y(k) \tag{2.46}$$

where $q(k)$ is a frequency domain equalization gain factor which varies with the employed single and multiuser diversity combining/detection schemes. Using (2.45) and (2.46), the decision variable $d^{u'}$ can be divided into desired signal DS, I_{MAI} and noise term η, expressed as $d^{u'} = DS + I_{MAI} + \eta$, where the individual terms are given by

$$DS = \sqrt{E_c} b^{u'} \sum_{k=0}^{N-1} H^{u'}(k) q(k) \tag{2.47}$$

$$I_{MAI} = \sqrt{E_c} \sum_{u=0, u \neq u'}^{U-1} b^u b^u \sum_{k=0}^{N-1} c^u(k) c^{u'}(k) H^u(k) q(k) \tag{2.48}$$

$$\eta = \sum_{k=0}^{N-1} c^{u'}(k) Z(k) q(k) \tag{2.49}$$

If N is assumed to be large and random spreading codes and users' bits, the MAI can be modeled as additive zero mean Gaussian by invoking the central limit theorem CLT . Now, since both I_{MAI} and η are independent and Gaussian, the sum of these is also a zero mean Gaussian process with the variance σ^2_{MAI} plus σ^2_η [24]. The instantaneous SNR for MC-CDMA is thus obtained as

$$\gamma = \frac{(DS)^2}{(\sigma^2_{MAI} + \sigma^2_\eta)} \tag{2.50}$$

The gain factor $q(k)$ determines the performance of the MC-CDMA system. These equalization/combining methods are extensively covered in [21, 24, 26]. Next, a brief review of some of the single user detection schemes is presented which fall within the scope of this thesis.

- **Maximum Ratio Combining (MRC)** In general cases, this scheme is the optimum diversity combining technique with respect to BER [69]. In MRC, a stronger signal which is always more reliable than its weaker counterparts, is assigned a higher weight and the diversity branches are weighted by their respective complex conjugate channel coefficients. For MRC, the equalization gain factor of (2.46) can be expressed as

  $$q(k) = H^*(k) \tag{2.51}$$

  MRC provides the best performance for a single user case, since the absence of MAI builds the optimal combining scenario. Thus, for $U = 1$, the BER with MRC is identical to the matched filter (MF) bound which is the lower bound of the bit error probability of any data detector [69]. For this reason, MRC is often used to determine the lower bound on the performance of multi-access systems.

- **Equal Gain Combining (EGC)** In contrast to MRC, this combining scheme attempt to correct the channel induced phase rotations leaving the faded amplitudes uncorrected [24]. It weights all diversity branches i.e. the number of subcarriers for a MC-CDMA system. The equalization gain

factor of (2.46) can be expressed as

$$q(k) = \frac{H^*(k)}{|H(k)|} \tag{2.52}$$

and with that, the enhanced MAI caused by (2.47) can be avoided.

- **Orthogonal Restoring Combining (ORC)** ORC is also known as zero forcing (ZF) or channel inversion equalization. It targets to completely eliminate the MAI by restoring the orthogonality between the spreading codes. For ORC, the equalization gain factor of (2.46) becomes

$$q(k) = \frac{1}{H(k)} \tag{2.53}$$

which corresponds to the inverse of assigned channel coefficients [69]. The associated drawback of ORC is that for small amplitudes of channel coefficients the noise is pronounced and may ultimately force SNR to go to zero on some subcarriers [21].

- **Minimum Mean Square Error (MMSE) Combining** MMSE is the optional equalization method for a fully loaded MC-CDMA system [25]. Equalization according to MMSE criterion minimizes the mean square value of error between the transmitted signal and the output of the equalizer. The mean square error is minimized by using the orthogonality rule which states that the mean square error can be minimized, if the combiner/equalizer coefficients are selected in such a way that the error is orthogonal to the received signal [21]. The equalization coefficient of (2.46) based on MMSE criterion can be expressed as

$$q(k) = \frac{H^*(k)}{|H(k)|^2 + \gamma^{-1}} \tag{2.54}$$

where γ is the SNR per subcarrier which shows that for the computation of MMSE equalization coefficients, an estimate of the actual SNR per subcarrier is required. For $\gamma \to \infty$, the MMSE equalizers equal to the ORC equalizer.

2.8 Summary

This chapter gives the theory and fundamental knowledge to assess the performance of cooperative relay systems presented in this thesis. First, the system performance characteristics are given. The average SNR shows the performance of the system when the effect of fading is to be taken into consideration. The outage probability presents the probability of the output SNR falls under the threshold SNR. For a system with relay diversity, diversity gain depends on the successfully received independent copies of the original transmitted signal. It improves the performance of the system such as the error probability and outage probability.

Transmission over wireless relay channel is affected by noise, interference and fading. Noise originates from the components in the device used, therefore the existence is inevitable. Interference is the result of having multiple coherent signals from adjacent cells, channels or users. This is overcome by using frequency reuse pattern and duplexing modes. Fading can be divided into two categories, namely large-scale and small-scale fading. Shadowing and pathloss are the examples of large scale-fading. The effect of large-scale fading can be counteracted by power control and a proper planning of link budgeting. The focus of this section is on small-scale fading, which is also known as multipath fading. It is caused by reflection, scattering and diffraction of the signal. Multipath fading can be modeled according to statistical characteristics such as Rayleigh, Rician and Nakagami-m.

Using the multipath fading channel model, the performance analysis of wireless relay network can be derived. This gives guideline to assess the performance of rekay diversity schemes presented in the thesis. The analysis can give insights on how to allocate resources optimally.

Finally, the OFDM and MC-CDMA data structure and detections are given. For single user system, OFDM is used and MC-CDMA is used for multiuser cooperative system.

Chapter 3

Distributed Space-Time Block Coding

3.1 Introduction

Space-time block code (STBC) is used to transmit information over a multiple antenna wireless communication system. Consider a wireless communication system with N_{tx} transmit antennas and N_{rx} receive antennas, the goal of STBC is to achieve a maximum diversity of $N_{tx}N_{rx}$. In addition, a good STBC should achieve maximum coding gain, have highest possible throughput and simple decoding at the receiver. The complexity of the STBC should be kept to minimum especially the receiver is a mobile device that has limited power supply.

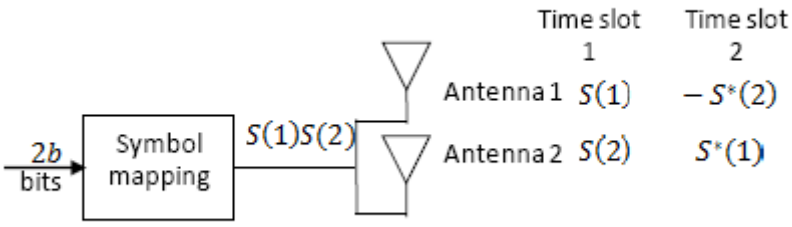

Figure 3.1: Transmitter block diagram for Alamouti code

A simple example of STBC is Alamouti code [2] which is used for a system with $N_{tx} = 2$ and $N_{rx} = 1$. To transmit b bits/symbol, modulation scheme that maps every b bits to one symbol is used from a constellation with 2^b symbols. The constellation can be real or complex such as PAM, PSK, QAM etc. The transmitter block diagram for Alamouti code is shown in Figure 3.1. First, the transmitter picks two symbols from the constellation using a block of $2b$ bits. If $S(1)$ and $S(2)$ are the selected symbols for a block of $2b$ bits, the transmitter sends $S(1)$ from antenna one and $S(2)$ from antenna two simultaneously in the first time slot. Then in the second time slot, the transmitter transmits $-S^*(2)$ and $S^*(1)$ from antenna one and two respectively. Therefore, the transmitted codeword is

$$\mathbf{G}_{Alamouti} = \begin{pmatrix} S(1) & S(2) \\ -S^*(2) & S^*(1) \end{pmatrix} \tag{3.1}$$

This code provides orthogonality between the transmitted symbols over multiple antenna. To check the diversity of the code, the rank of all possible difference matrices need to be calculated. Consider a different pair of symbol $(S'(1), S'(2))$ and the corresponding codeword

$$\mathbf{G}'_{Alamouti} = \begin{pmatrix} S'(1) & S'(2) \\ -S'^*(2) & S'^*(1) \end{pmatrix} \tag{3.2}$$

and the difference matrix $D\left(\mathbf{G}_{Alamouti}, \mathbf{G}'_{Alamouti}\right)$ is given by

$$D\left(\mathbf{G}_{Alamouti}, \mathbf{G}'_{Alamouti}\right) = \begin{pmatrix} S'(1) - S(1) & S'(2) - S(2) \\ S^*(2) - S'^*(2) & S'^*(1) - S^*(1) \end{pmatrix} \tag{3.3}$$

The determinant of the difference matrix $\det D\left(\mathbf{G}_{Alamouti}, \mathbf{G}'_{Alamouti}\right)$ is zero if and only if $S'(1) = S(1)$ and $S'(2) = S(2)$. Therefore $D\left(\mathbf{G}_{Alamouti}, \mathbf{G}'_{Alamouti}\right)$ is always full rank when $\mathbf{G}'_{Alamouti} \neq \mathbf{G}_{Alamouti}$ and the Alamouti code satisfies the determinant criterion. It provides a diversity of two, therefore Alamouti code achieves full diversity.

Let the path gains from transmit antenna one and two to the receive antenna are α_1 and α_2, respectively. The received signals at the decoder at time slot one

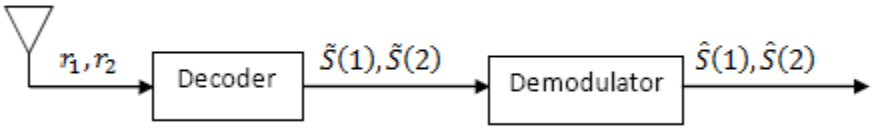

Figure 3.2: Receiver block diagram for Alamouti code

and two, r_1 and r_2 respectively, are given by

$$r_1 = \alpha_1 S(1) + \alpha_2 S(2) + n_1 \tag{3.4}$$

$$r_2 = -\alpha_1 S^*(2) + \alpha_2 S^*(1) + n_2 \tag{3.5}$$

To decode $S(1)$ and $S(2)$, the receiver calculates the following

$$\tilde{S}(1) = r_1 \alpha_1^* + r_2^* \alpha_2 \tilde{S}(2) = r_1 \alpha_2^* - r_2^* \alpha_1 \tag{3.6}$$

and then finds the closest symbols to $\tilde{S}(1)$ and $\tilde{S}(2)$ in the constellation. Figure 3.2 shows the receiver block diagram for Alamouti code.

To design STBC for more than two transmit antenna having similar properties as Alamouti code, the behavior of the code need to be studied. Let a generator matrix G take the structure of Alamouti code as shown below

$$G = \begin{pmatrix} x_1 & x_2 \\ -x_2^* & x_1^* \end{pmatrix} \tag{3.7}$$

the orthogonality of the columns of G is proven by

$$G^H G = \left(|x_1|^2 + |x_2|^2\right) I_2 \tag{3.8}$$

For real numbers, matrices satisfying (3.8) are called orthogonal designs. A complete study of real orthogonal designs was provided by Radon and Hurwitz early in the twentieth century [70].

For a set of $N \times N$ real matrix, a real orthogonal design exists if and only if

$N = 2, 4, 8$. A 2×2 design is given as follows [37]

$$G_2 = \begin{pmatrix} x_1 & x_2 \\ -x_2 & x_1 \end{pmatrix} \tag{3.9}$$

The 4×4 orthogonal design is derived as [37]

$$G_4 = \begin{pmatrix} x_1 & x_2 & x_3 & x_4 \\ -x_2 & x_1 & -x_4 & x_3 \\ -x_3 & x_4 & x_1 & -x_2 \\ -x_4 & -x_3 & x_2 & x_1 \end{pmatrix} \tag{3.10}$$

Similarly, the 8×8 orthogonal design is given by [37]

$$G_8 = \begin{pmatrix} x_1 & x_2 & x_3 & x_4 & x_5 & x_6 & x_7 & x_8 \\ -x_2 & x_1 & -x_4 & x_3 & -x_6 & x_5 & x_8 & -x_7 \\ -x_3 & x_4 & x_1 & -x_2 & x_7 & x_8 & -x_5 & -x_6 \\ -x_4 & -x_3 & x_2 & x_1 & x_8 & -x_7 & x_6 & -x_5 \\ -x_5 & x_6 & -x_7 & -x_8 & x_1 & -x_2 & x_3 & x_4 \\ -x_6 & -x_5 & -x_8 & x_7 & x_2 & x_1 & -x_4 & x_3 \\ -x_7 & -x_8 & x_5 & -x_6 & -x_3 & x_4 & x_1 & x_2 \\ -x_8 & x_7 & x_6 & x_5 & -x_4 & -x_3 & -x_2 & x_1 \end{pmatrix} \tag{3.11}$$

A real STBC can be constructed using the above orthogonal designs. The encoder first select N symbols $S(1), S(2), ..., S(N)$ from a real constellation, for example PAM using Nb input bits. To encode such an input block, the indeterminate variables $x_1, x_2, ..., x_N$ in the orthogonal design are replaced by the N symbols $S(1), S(2), ..., S(N)$ and the (t, n)th element of the resulting matrix is transmitted at time t from antenna n. Note that N different symbols are transmitted simultaneously from N transmit antennas at each time slot t, $t = 1, 2, ..., N$. The resulting real STBC transmits one symbol per time slot. These codes achieve full diversity since N symbols are transmitted in $t = N$ time slot.

For complex orthogonal design, full STBC can only be achieved for $N = 2$ as given in (3.7). However, using generalized complex orthogonal design, half-rate

STBC can be obtained for $N = 3, 4$, as shown below

$$G_4 = \begin{pmatrix} x_1 & x_2 & x_3 & x_4 \\ -x_2 & x_1 & -x_4 & x_3 \\ -x_3 & x_4 & x_1 & -x_2 \\ -x_4 & -x_3 & x_2 & x_1 \\ x_1^* & x_2^* & x_3^* & x_4^* \\ -x_2^* & x_1^* & -x_4^* & x_3^* \\ -x_3^* & x_4^* & x_1^* & -x_2^* \\ -x_4^* & -x_3^* & x_2^* & x_1^* \end{pmatrix} \tag{3.12}$$

$$G_3 = \begin{pmatrix} x_1 & x_2 & x_3 \\ -x_2 & x_1 & -x_4 \\ -x_3 & x_4 & x_1 \\ -x_4 & -x_3 & x_2 \\ x_1^* & x_2^* & x_3^* \\ -x_2^* & x_1^* & -x_4^* \\ -x_3^* & x_4^* & x_1^* \\ -x_4^* & -x_3^* & x_2^* \end{pmatrix} \tag{3.13}$$

In a general wireless relay network, different relays receive different noisy copies of the same information symbols. The relays process these received signals and forward them to the destination. The distributed processing at the different relay nodes thus forms a virtual antenna array, as alluded to before. Therefore, conventional space-time block coding schemes can be applied to relay networks to achieve the cooperative diversity and coding gain.

In this chapter, DSTBC for OFDM system is presented. First, a general DSTBC OFDM system model for broadband channel is given. This followed by the derivation of PEP which provides the information on diversity gain. Next, a specific orthogonal block-code i.e. Alamouti code is used to derive the average SER of the system using MGF. Simulations are done to demonstrate the performance of the system.

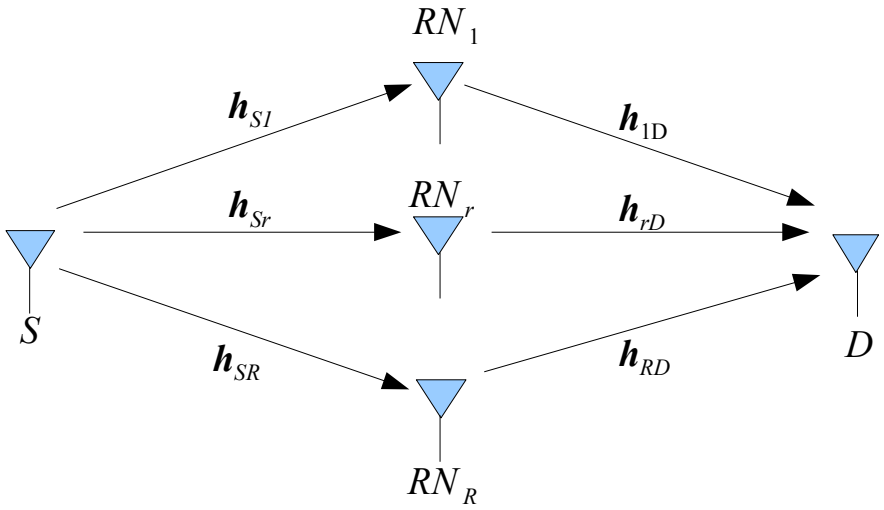

Figure 3.3: Two-hop wireless relay network

3.2 DSTBC OFDM System Model

Consider a relay network consisting a source node, S, a destination node, D and relay nodes $RN_r,\ r = 1, ..., R$ as shown in Figure 3.3. All nodes are equipped with a single antenna. Any linear modulation technique such as M-PSK or M-QAM can be used. The relaying is half duplex and follows AF protocol where in the first transmission phase, the source transmits to the destination node and in the second transmission phase, the relay nodes forward the amplified version of the received signal to the destination node. To simplify the analysis, it is assumed that there is no direct transmission from the source to destination node in both transmission phases.

The channels between communicating terminals are modeled as quasi-static frequency selective Rayleigh fading with uniform delay profile. The channel impulse response for $S \rightarrow RN_r$ and $RN_r \rightarrow D$ links are given by $\mathbf{h}_{Sr} = [h_{Sr}(1), ..., h_{Sr}(L_{Sr})]$ and $\mathbf{h}_{rD} = [h_{rD}(1), ..., h_{rD}(L_{rD})]$ respectively. The entries of random vector h_{Sr} and h_{rD} are independent and identically distributed (i.i.d) zero-mean Gaussian random variables with variances $\Omega_{Sr} = 1/(L_{Sr})$ and $\Omega_{rD} = 1/(L_{rD})$ respectively. The CIR remain constant over a period of one transmission block and vary independently from block to block.

During the first transmission phase, the source transmits OFDM symbol $\mathbf{s} =$

$[s(0), ..., s(N-1)]$, where N is the number of subcarrier, to the relays. Since the FFT operation at relay nodes is canceled by the IFFT operation in the second time slot, it is reasonable to assume that FFT processing takes place only at the destination, not at relay nodes to reduce complexity. After removing the cyclic prefix, the received data block at the rth relay node is given by

$$\mathbf{y}_r = \sqrt{P_S}\mathbf{H}_{Sr}\mathbf{F}_N^H\mathbf{s} + \mathbf{z}_r \tag{3.14}$$

where P_S is the average power per transmitting symbol, $\mathbf{H}_{Sr}$ is a circulant channel matrix with entries $\mathbf{H}_{Sr}(p,q) = \mathbf{h}_{Sr}(p-q)_{\text{mod } N},\ p,q = 1, ..., N$ and $\mathbf{z}_r,\ r = 1, ...R$ denotes the zero mean white Gaussian noise vector with covariance matrix $N_o\mathbf{I}_N$. $\mathbf{F}_N^H$ is the IFFT matrix which is the Hermitian of $N \times N$ FFT matrix, $\mathbf{F}_N$. The relays amplify the received signal with factor A_r and forward the signal to the destination. The received signal at destination node from relay r in the second transmission phase is

$$\mathbf{y}_D = A_r\sqrt{P_S}\mathbf{F}_N\mathbf{H}_{Sr}\mathbf{H}_{rD}\mathbf{F}_N^H\mathbf{s} + A_r\mathbf{H}_{rD}\mathbf{z}_r + \mathbf{z}_D \tag{3.15}$$

where $\mathbf{H}_{rD}$ is a circulant channel matrix with entries $H_{rD}(p,q) = h_{rD}(p-q)_{\text{mod } N},\ p,q = 1, ..., N$. Let $\mathbf{D}_{AB}(k) = \sum_{l=1}^{L_{AB}} \mathbf{h}_{AB}(l)\exp(-j2\pi(l-1)(k-1)/N),\ k = 1, ..., N$, denote the frequency response evaluated at the FFT grid for the $A \to B$ link with channel length L_{AB}. The equation (3.15) can be rewrite as

$$\mathbf{y}_{rD} = \sqrt{P_S}A_r\mathbf{D}_{Sr}\mathbf{D}_{rD}\mathbf{s} + \mathbf{z} \tag{3.16}$$

where the noise vector $\mathbf{z} = \sum_{r=1}^{R} A_r\mathbf{H}_{rD}\mathbf{z}_r + \mathbf{z}_D$ is conditionally zero mean Gaussian distributed with covariance matrix $N_0\Sigma_r$ and $\Sigma_r = A_r^2\mathbf{D}_{rD}\mathbf{D}_{rD}^H + \mathbf{I}_N$. After pre-whitening at the destination, the input signals to the maximum likelihood (ML) detector are given by

$$\mathbf{y} = \text{diag}\left[A_1\sqrt{P_S}\Sigma_1^{-1/2}\mathbf{D}_{S1}\mathbf{D}_{1D}, ..., A_R\sqrt{P_S}\Sigma_1^{-1/2}\mathbf{D}_{SR}\mathbf{D}_{1D}\right]\mathbf{s} + \mathbf{z} \tag{3.17}$$

where the noise vector $\mathbf{z}$ in (3.17) is zero mean white Gaussian with covariance matrix $N_0\mathbf{I}_N$. Next, performance analysis in term of diversity gain of DSTBC is

revisited.

3.3 Pairwise Error Probability

The pairwise error probability (PEP) based performance provides a design criterion to evaluate different DSTBC schemes. Next, this criterion is revisited.

To extract the maximum available diversity from the frequency selective fading, a coded OFDM with linear pre-coder [19] is considered. The precoded data block is expressed as $\mathbf{x} = \Theta\mathbf{s}$ where Θ is the code matrix satisfying the power constraint $\text{tr}\left(\Theta\Theta^H\right) = N$, where N is the total number of subcarriers. Subcarriers are divided into M groups in order to reduce the decoding complexity and and simplify the pre-coder design. Each group contains L equally spaced subcarriers. The pre-coder Θ can be expressed as $\sum_{k=1}^{N} \Psi_k^T \Phi \Psi_k$ [19], where $\Psi_k = \mathbf{I}_N(i_{k,l,:})$ is a $L \times N$ permutation matrix obtained from the rows of identity matrix of size P, i.e. $\{i_{k,l} = (l-1)M + k,\ l = 1, ..., L\}$ and Φ is a matrix of size $L \times L$ that performs precoding within one group.

For a given channel realization and transmitted symbol block $\mathbf{s}$, conditional PEP denotes the probability of deciding in favour of another block $\mathbf{s}'$ and is given by

$$P_e\left(\mathbf{s} \to \mathbf{s}' | \mathbf{h}_{Sr}, \mathbf{h}_{rD}\right) = Q\left(\frac{d(\mathbf{s}, \mathbf{s}')}{2}\right) \tag{3.18}$$

where $d(\mathbf{s}, \mathbf{s}')$ is the Euclidean distance between $\mathbf{s}$ and $\mathbf{s}'$ and $Q(x)$ is the Gaussian-Q function [16]. Let the coded error vector $\mathbf{u} = \Theta(\mathbf{s} - \mathbf{s'})$, therefore

$$d^2(\mathbf{s} \to \mathbf{s}') = \rho \sum_{r=1}^{R} \left\| A_r \Sigma_r^{-1/2} \mathbf{H}_{Sr} \mathbf{H}_{rD} \mathbf{u} \right\|^2 \tag{3.19}$$

where $\rho = P_S/N_0$ denotes the SNR. Notice $\mathbf{D}_{AB}\mathbf{u} = \mathbf{U}\mathbf{h}_{AB}$ where $\mathbf{D}_{AB}$ is a diagonal matrix of size $N \times N$, $\mathbf{U}_{AB} = \text{diag}(\mathbf{u})\mathbf{W}_{AB}$. $\mathbf{W}_{AB}$ denotes a $N \times (L_{AB})$ matrix with element given by $\mathbf{W}_{AB}(k,l) = \exp -j2\pi(k-1)(l-1)/N\ 1 \le k \le N, 1 \le l \le L_{AB}$.

Applying Chernoff bound on (3.18) i.e. $Q(x) \le \frac{1}{2}\exp\left(-\frac{x^2}{2}\right)$, the upper bound

for the average PEP is given by

$$P_e(\mathbf{s} \to \mathbf{s}') \leq \frac{1}{2} \prod_{r=1}^{R} J_r \tag{3.20}$$

where

$$J_r = E_{\mathbf{h}_{Sr}, \mathbf{h}_{rD}} \left\{ \exp\left(\frac{-\rho \left\| \sqrt{P_S} A_r \Sigma^{-1/2} \mathbf{D}_{Sr} \mathbf{D}_{rD} \mathbf{u} \right\|^2}{8} \right) \right\} \tag{3.21}$$

Following steps in Appendix A,

$$\begin{aligned} P_e(\mathbf{s} \to \mathbf{s'}) \quad \leq \quad & C \rho^{-\sum_{r=1}^{R} k_r} (\log\ \rho)^{-\sum_{r=1}^{R} k_r} \\ & + O\left(\rho^{-\sum_{r=1}^{R} k_r} (\log\ \rho)^{\sum_{r=1}^{R} (k_R 1)} \right) \end{aligned} \tag{3.22}$$

where C is defined as

$$C = \frac{(8\pi)^{\sum_{r=1}^{R} k_r} \prod_{r=1}^{R} (L_{Sr})^{k_r}}{2 \det\left(\prod_{r=1}^{R} \omega_r \right) (v P_r)^{\sum_{r=1}^{R} k_r}} \tag{3.23}$$

and $k_r = \min(L_{Sr}, L_{rD})$, $v = 2^{\frac{1}{L}} - 1 \Delta_{min}^2$, Δ_{min} is the minimum Euclidean distance among the constellation points and $\omega_r = \det\left(\mathbf{Q}_r \mathbf{Q}_r^H\right)$. Here, matrix $\mathbf{Q}_r$ contains the $1^{\text{st}}, (M+1)^{\text{th}}, ..., (M+L_{Sr})^{\text{th}}$ row in $\mathbf{W}_{Sr}$.

It is observed in (3.22) that the PEP is not a simple exponential function of the SNR. It involves the term $(\log\ \rho)^{-(\sum_{r=1}^{R} k_r)}$ due to the cascaded nature of channels in the relaying links. This is in line with the observation of the term $(\log\ \rho)^R$ reported in [39] for frequency flat channel. From (3.22), it is also observed that an asymptotical diversity order of $K = \sum_{r=1}^{R} \min(L_{Sr}, L_{rD})$ is available for the coded OFDM with multiple relay system in frequency selective fading environment.

3.4 Distributed Alamouti System Model

Consider a two-hop OFDM relay network consists of a source node S, a destination node D and a set of two relay nodes $RN_r, r = 1, 2$ as shown in Figure 3.4. Every node in the network has a single antenna, which can be used for both

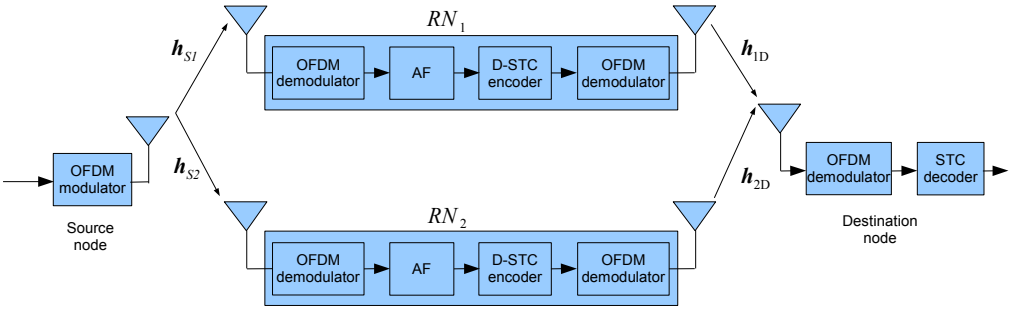

Figure 3.4: Two-hop relay network

transmission and reception. The relay nodes cannot transmit and receive using the same channel resources because the signal received by a relay would be affected by strong interference from the relays own transmitter (self-interference). In order to avoid self-interference and to provide the possibility of diversity reception, half-duplex constraint is set at relay nodes where the relays receive and transmit via different time slot, subchannel or polar. In this thesis, the time division duplexing (TDD) scheme is considered, where two time slots are allocated for transmitting and receiving signals at relays. It is assumed that there is no direct transmission between the source and destination node.

The channel between a transmitting node $\{p\}_{p=S,r}$ and receiving node $\{q\}_{q=r,D}$ is modeled as multipath fading channel with L_{pq} paths as

$$h_{pq}(\tau) = \sum_{l=1}^{L_{pq}} \alpha_{pq,l}\delta(\tau - \tau_{pq,l}) \tag{3.24}$$

where $\tau_{pq,l}$ and $\alpha_{pq,l}$ is the delay and complex amplitude of the lth path respectively. The $\alpha_{pq,l}$ are modeled as zero-mean complex Gaussian random variables with variance $E\{|\alpha_{pq,l}|^2)\} = \Omega_{pq,l}$.The channels are normalized such that $\sum_{l=1}^{L_{pq}} \alpha_{pq,l} = 1$. A cyclic prefix with length $L_{cp} > L_{\max}$ is introduced to convert multipath frequency selective fading channels to flat fading sub-channels on the subcarriers.

At source node, data information symbols are obtained after source and channel coding and/or time-interleaving. The high rate input stream is demultiplexed and transmitted over N low-rate independent frequency subcarriers. This multi-

carrier transmission scheme can be efficiently implemented in practice using the Fast Fourier Transform (FFT). To implement Alamouti coding in OFDM modulation, two blocks of a data sequence of length N, $\mathbf{X}^j = [X^j(0), ..., X^j(N-1)],\ j = 1, 2$ are parsed into N parallel subcarrier and the modulated symbols from the jth block can be expressed as an inverse fast Fourier transform (IFFT)

$$x^j(n) = \frac{1}{\sqrt{N}} \sum_{k=0}^{N-1} X^j(k) e^{-j2\pi nk/N} \tag{3.25}$$

Assuming complete elimination of ISI, the FFT modulated received signal at relay r during the first time slot can be considered separately for each subcarrier given by

$$Y_r^j(k) = \sqrt{P_S} H_{Sr}(k) X^j(k) + Z_r^j(k) \tag{3.26}$$

where P_S is the symbol energy transmitted from the source node, $H_{Sr}(k)$ is the frequency response of the channel between the source and the rth relay on the kth subcarrier and $Z_r^j(k)$ represents the additive white Gaussian noise (AWGN) with the real and imaginary components assumed to be statistically independent Gaussian distributed RVs having zero-mean and variance $N_0/2$ per dimension. The channel frequency response $H_{Sr}(k)$ is assumed to be constant during the transmission of both symbols and is given by

$$H_{Sr}(k) = \sum_{l=1}^{L} \alpha_{Sr,l} e^{-j2\pi(k-1)\Delta_f \tau_l} \tag{3.27}$$

where $\Delta_f = 1/T$ is the subcarrier frequency separation, and T is the OFDM symbol duration. Perfect channel state information is assumed at any receiving node but no channel information at transmitting nodes. Another assumption is that all the noise terms are independent for different receiving node. For distributed Alamouti coding, let the output of the two relays be

$$\begin{bmatrix} X_1^1(k) & X_2^1(k) \\ X_1^2(k) & X_2^2(k) \end{bmatrix} = \begin{bmatrix} A_1 Y_1^1(k) & -A_2 Y_2^{2^*}(k) \\ A_1 Y_1^2(k) & A_2 Y_2^{1^*}(k) \end{bmatrix} \tag{3.28}$$

where $X_r^j(k)$ and A_r are the output and amplification factor of the rth relay

respectively.

The relay nodes will use OFDM modulation for transmission to the destination node. At the destination node, the received signal on the kth subcarrier is given by

$$\begin{bmatrix} Y^1(k) \\ Y^2(k) \end{bmatrix} = \begin{bmatrix} X_1^1(k) & X_2^1(k) \\ X_1^2(k) & X_2^2(k) \end{bmatrix} \begin{bmatrix} H_{1D}(k) \\ H_{2D}(k) \end{bmatrix} + \begin{bmatrix} Z_D^1(k) \\ Z_D^2(k) \end{bmatrix} \tag{3.29}$$

where $H_{rD}(k)$ is the attenuation of the channel between the rth relay and the destination node on the kth subcarrier and $Z_D^j(k)$ is the noise at destination. The $Z_D^j(k)$ is modeled as zero-mean, circularly symmetric complex Gaussian random variables with a variance of $N_0/2$ per dimension. The equation (3.29) can be rewrite as

$$\begin{aligned} \begin{bmatrix} Y^1(k) \\ Y^{2^*}(k) \end{bmatrix} &= \sqrt{P}_S \begin{bmatrix} A_1 H_{S1}(k) H_{1D}(k) & -A_2 H_{S2}^*(k) H_{2D}(k) \\ H_{S2}(k) H_{2D}^*(k) & H_{S2}^*(k) H_{2D}^*(k) \end{bmatrix} \begin{bmatrix} X^1(k) \\ X^2(k) \end{bmatrix} \\ &+ \begin{bmatrix} A_1(H_{1D}(k) Z_1^1(k) - H_{2D}(k) Z_2^{2^*}(k)) \\ A_2(H_{1D}^*(k) Z_1^{2^*}(k) + H_{2D}^*(k) Z_2^1(k)) \end{bmatrix} + \begin{bmatrix} Z_D^1(k) \\ Z_D^{2^*} \end{bmatrix} \end{aligned} \tag{3.30}$$

It can be seen that the coefficient matrix of the original symbol vector is complex orthogonal and the covariance of the last two noise terms is $(A_r^2 |H_{rD}(k)|^2 + 1) N_0$. Therefore the optimal detection of the original symbols can be carried out on each individual components of the following sufficient statistics

$$\begin{bmatrix} r^1(k) \\ r^2(k) \end{bmatrix} = \begin{bmatrix} A_1 H_{S1}(k) H_{1D}(k) & -A_2 H_{S2}^*(k) H_{2D}(k) \\ H_{S2}(k) H_{2D}^*(k) & H_{S2}^*(k) H_{2D}^*(k) \end{bmatrix}^H \begin{bmatrix} y^1(k) \\ y^2(k) \end{bmatrix} \tag{3.31}$$

and the probability of detection error is governed by the SNR of this statistics. The instantaneous SNR of (3.31) can be shown to be

$$\gamma = \rho \frac{\sum_{r=1}^{2} A_r^2 |H_{Sr}(k)|^2 |H_{rD}(k)|^2}{\sum_{r=1}^{2} A_r^2 |H_{rD}(k)|^2 + 1} \tag{3.32}$$

where $\rho = \frac{P_S}{N_0}$ is the average SNR of the signal received by each relay. Next, the average symbol error probability of distributed Alamouti system is derived using MGF-based approach.

3.5 Average Symbol Error Probability

In this section, the average symbol error probability is derived for distributed Alamouti coding in Rayleigh fading channel. As shown in (3.32), it is really hard to derive the error function as the noise variances depends on different channel coefficients. Therefore, a tight lower bound is derived by assuming equal noise power for each relay such that $(A_1^2|H_{1D}(k)|^2+1)N_0 = (A_2^2|H_{2D}(k)|^2+1)N_0$ [4]. The upper bound for the instantaneous SNR can be written as

$$\gamma < \gamma^u = \rho \sum_{r=1}^{2} \frac{A_r|H_{Sr}(k)|^2|H_{rD}(k)|^2}{A_r^2|H_{rD}(k)|^2+1} \tag{3.33}$$

For CSI-assisted relaying, the amplification factor is chosen to be $A_r^2 = \frac{P_R}{P_S|H_{Sr}(k)|^2+N_0}$ and (3.33) can be written as a function of the instantaneous SNR of each hop given by

$$\gamma^u = \sum_{r=1}^{2} \frac{\gamma_{Sr}\gamma_{rD}}{\gamma_{Sr}+\gamma_{rD}+1} \tag{3.34}$$

With fading realization defined as in (3.24) the SNR per hop are defined as

$$\gamma_{Sr} = \frac{P_S|H_{Sr}(k)|^2}{N_0} \qquad \gamma_{rD} = \frac{P_R|H_{rD}(k)|^2}{N_0} \tag{3.35}$$

which are independent and exponentially distributed with means

$$\bar{\gamma}_{Sr} = \frac{P_S\Omega_{Sr}}{N_0} \qquad \bar{\gamma}_{rD} = \frac{P_R\Omega_{rS}}{N_0} \tag{3.36}$$

respectively.

The MGF-based approach [81] is used to get the error performance. The MGF of $\gamma_r^u,\ r=1,2$ is given by [4]

$$\begin{aligned}\mathcal{M}_{\gamma_r^u}(\mu) \;=\; & \frac{\bar{\gamma}_{sr}\bar{\gamma}_{\delta r}-4\bar{\gamma}_{pr}}{\bar{\gamma}_{\rho r}^2} - \frac{\mu\bar{\gamma}_{pr}(\bar{\gamma}_{\rho r}+2\bar{\gamma}_{pr})}{\bar{\gamma}_{\rho r}^3} e^{\frac{\bar{\gamma}_{\delta r}-\bar{\gamma}_{\rho r}}{2\bar{\gamma}_{pr}}} E_1\left(\frac{\bar{\gamma}_{\delta r}-\bar{\gamma}_{\rho r}}{2\bar{\gamma}_{pr}}\right) \\ & - \frac{\mu\bar{\gamma}_{pr}(\bar{\gamma}_{\rho r}-2\bar{\gamma}_{pr})}{\bar{\gamma}_{\rho r}^3} e^{\frac{\bar{\gamma}_{\delta r}+\bar{\gamma}_{\rho r}}{2\bar{\gamma}_{pr}}} E_1\left(\frac{\bar{\gamma}_{\delta r}-\bar{\gamma}_{\rho r}}{2\bar{\gamma}_{pr}}\right)\end{aligned} \tag{3.37}$$

where $\bar{\gamma}_{\rho r} = \sqrt{\bar{\gamma}_{\delta r}^2 - 4\bar{\gamma}_{pr}}$, $\bar{\gamma}_{\delta r} = \bar{\gamma}_{sr} - \bar{\gamma}_{pr}\mu$, $\bar{\gamma}_{Sr} = \bar{\gamma}_{Sr} + \bar{\gamma}_{rD}$ and $\bar{\gamma}_{pr} = \bar{\gamma}_{Sr}\bar{\gamma}_{rD}$ for

$r = 1, 2$. The proof of (3.37) is given in Appendix B.

Therefore, the closed-form lower bound ASER of the AF DSTBC OFDM system employing M-PSK modulation is given by

$$P_e^l = \frac{1}{\pi}\int_0^{\pi/2}\prod_{r=1}^{2}\mathcal{M}_{\gamma_r^u}\left(\frac{g_{\text{MPSK}}}{\sin^2\theta}\right)d\theta + \frac{1}{\pi}\int_{\pi/2}^{\frac{(M-1)\pi}{M}}\prod_{r=1}^{2}\mathcal{M}_{\gamma_r^u}\left(\frac{g_{\text{MPSK}}}{\sin^2\theta}\right)d\theta \qquad (3.38)$$

where $g_{\text{MPSK}} = \sin^2(\pi/M)$.

3.6 Simulation Results

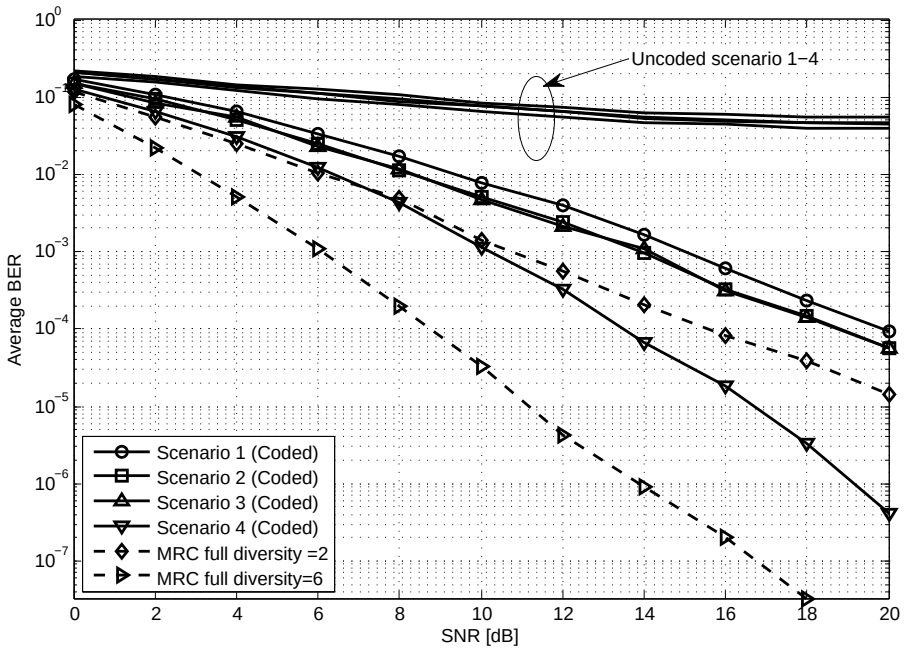

Figure 3.5: BER performance of DSTBC OFDM with two relay nodes

Monte Carlo simulation results are presented to demonstrate the error rate performance of the precoded cooperative OFDM system under consideration. The modulation scheme is chosen to be BPSK. In order to perform the grouping technique [52], the number of subcarrier is chosen to be $N = 64$, depending on the value of $L = \max(L_{Sr}, L_{rD})$. The performance of DSTBC system with two and three relay nodes are investigated under various scenarios as below:

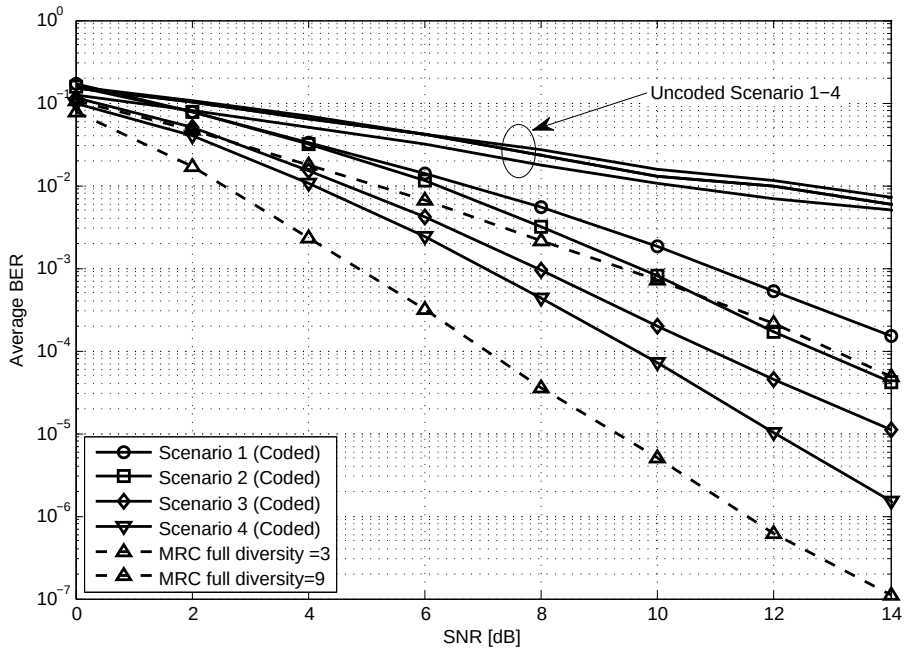

Figure 3.6: BER performance of DSTBC OFDM with three relay nodes

- **Scenario 1:** $L_{Sr} = 1$, $L_{rD} = 1$
- **Scenario 2:** $L_{Sr} = 1$, $L_{rD} = 3$
- **Scenario 3:** $L_{Sr} = 3$, $L_{rD} = 1$
- **Scenario 4:** $L_{Sr} = 3$, $L_{rD} = 3$

As clearly seen from Figure 3.5 and Figure 3.6, the system without channel coding the system failed to give a reasonable performance nor providing optimum spatial diversity gain. Using channel coding, DSTBC OFDM system is able to extract underlying rich multipath diversity. For two relay systems, it is observed that an identical diversity order is achieved for scenario 1, 2 and 3. As predicted by the diversity gain analysis, the maximum diversity gain is given by $\sum_{r=1}^{N_R} \min(L_{Sr}, L_{rD})$, which in this case equivalent to 2. The diversity gain increase for scenario 4, where the channel length for both source-to-relay and relay-to-destination are equal to 3. The maximum diversity order available for this scenario is 6. However, the cascaded nature of Rayleigh channels in relaying

links allows only partial diversity to be observed in the practical SNR range under consideration. This can be observed better through a comparison with the performance of maximum ratio combining (MRC) with 2 and 6 co-located antennas, which is also plotted in Figure 3.5. For the three-relay systems, the maximum diversity order as calculated for scenario 1-3 and 4 are 3 and 9 respectively. The performance of 3 and 9 co-located antennas are also included in Figure 3.6 for comparison purposes. In term of the error performance, the relay system experience a performance degradation compared to the point-to-point system. In a specific relay node configuration, the system with more selective channel has better performance than the ones with less selective.

The performance of DSTBC is compared to the conventional STBC with different number of antennas and relay nodes. For $N_R = N_T = 2$, Alamouti code has been used and half-rate orthogonal code is employed for $N_T = N_R = 3, 4$. It can be seen that in Figure 3.7 and 3.8, the DSTBC performance is worse than the conventional STBC. This is expected as the result of cascaded relay channel. As the number of relay node increases the performance becomes better. However, DSTBC with $N_R = 2, 3$ experience rate loss due to the orthogonal coding. This can be overcome by using higher order of constellation symbols for modulation.

3.7 Summary

This chapter presents DSTBC for OFDM system with AF relaying over Rayleigh fading channel. First, the construction of orthogonal design for STBC is given. For real orthogonal design, full-rate and full-diversity STBC can be achieved for two, three and four transmit antenna. However, for complex orthogonal design, full-rate and full-diversity STBC is only available for two transmit antenna system, while the three and four transmit antenna can only achieve full-diversity with half data rate.

A generalized DSTBC system model for any number of relay nodes is given. In this system, STBC is constructed distributively at relay nodes based on the received signal and retransmitted the scaled version to the destination. The PEP for the system is derived to evaluate the diversity gain.

Then, the focus is on the system with orthogonal STBC. For example, or-

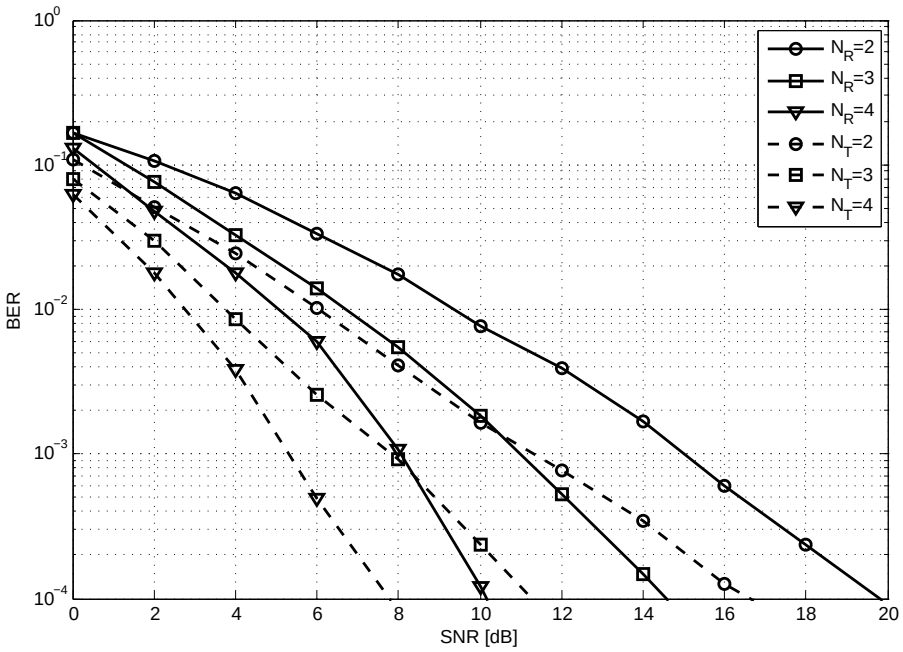

Figure 3.7: BER performance of DSTBC OFDM with $R = 2, 3, 4$ with channel fading tap $L_{Sr} = L_{rD} = 1$

thogonal STBC for two relay nodes i.e. Alamouti code is used for the system model. The instantaneous SNR of the system is derived and the derivation can be extended easily to systems with other full-diversity orthogonal STBC. Using the MGF-based approach, the lower bound for average SER is derived.

Finally, simulations results are presented to demonstrate the error performance of the DSTBC system. DSTBC gives better error performance compared to STBC in transmit diversity system. The diversity gain can be extracted by using coded OFDM. It is also proved that with the increase of diversity order (number of relay nodes), the error performance becomes better.

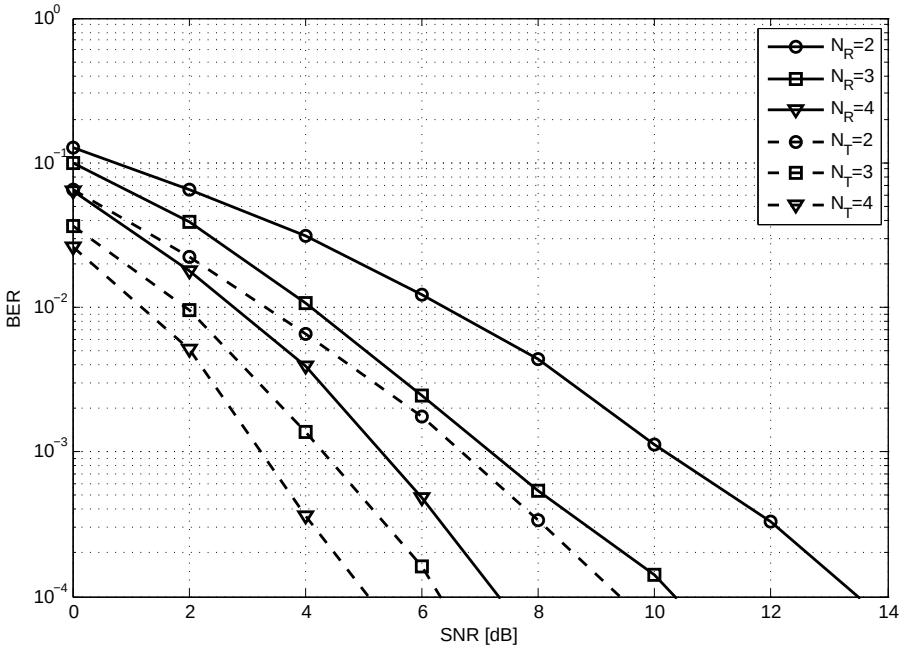

Figure 3.8: BER performance of DSTBC OFDM with $R = 2, 3, 4$ with channel fading tap $L_{Sr} = L_{rD} = 3$

Chapter 4

Relay Cyclic Delay Diversity

4.1 Introduction

CDD is first proposed for MIMO system is originally from DD, which was proposed by Wittneben in [97]. DD processes the FEC or channel coded information bearing symbols from multiple antenna simultaneously, but with a successive delay of one symbol interval. The effect of this technique is to change a narrow band purely frequency flat fading channel into a frequency selective fading channel. Essentially, with DD, the receiver sees an equivalent SISO channel with an enhanced channel delay spread and can be considered as a specific case of STC. Simulation results further demonstrated that a sequence estimator at the receiver can be achieved at order diversity of the number of transmit antenna [87]. However the associated drawback of DD is reduced by bandwidth efficiency as the time delay are strongly restricted by guard period. This prohibits the straightforward implementation of DD for OFDM-based system because of ISI and specific time delay values.

CDD provides an elegant solution to realize DD for OFDM without exceeding the guard interval [17]. This is achieved by introducing cyclic delay within each OFDM symbol, instead of time delays, thereby keeping the length of OFDM symbol as well as the CP the same. The difference between DD and CDD is illustrated in Figure 4.1, where two consecutive OFDM symbols are shown along with their CP as guard intervals. To avoid the ISI, the length of CP is chosen

to be greater than the expected delay spread τ_{max} of the channel. For clarity, a sine wave represents the signal on the first subcarrier and this reference signal is transmitted without any delay. In the case of DD, although the signal is a simple copy of the reference signal but delayed by δ_d. Due to this delay, the OFDM symbols of DD signal partly overlap the CP of the reference signal at about δ_d and results in ISI. To avoid ISI, either the CP has to be increased or delay δ_d to be reduced. In both cases, spectral efficiency or the performance has to be sacrificed. Conversely, CDD ensures no overlapping of the cyclically delayed OFDM symbols with the reference signal. From Figure 4.1, it can be observed that the phase of CDD signal is equal to DD signal. This makes the performance of CDD equal to DD provided there is no ISI in case of DD. The OFDM symbols of CDD signal can easily be generated from the reference signal by applying a cyclic shift δ_{cyc} to the reference OFDM symbols and subsequent insertion of CP.

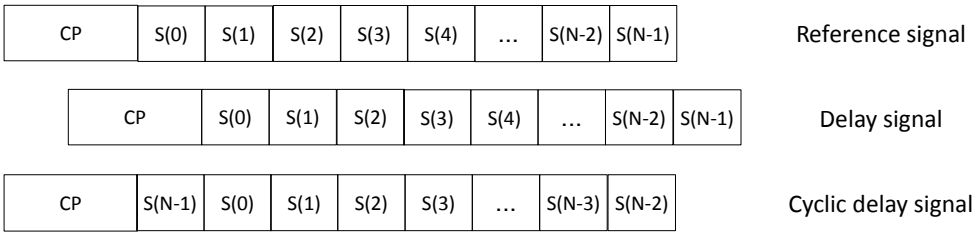

Figure 4.1: Principle of DD and CDD

In this chapter, the system model of RCDD is presented. The transformation of spatial diversity into frequency diversity is shown by using the equivalent frequency domain model i.e. phase diversity. The relationship between the channel delay spread and cyclic delay values for different relay nodes is established. Then the performance of RCDD is analyzed. For uncoded system, it is shown that the error rates of RCDD system is equal to a a single two-hop relay channel because of the fact that RCDD converts the relay channel into a SISO channel. However, when employed with channel codes, the enhanced selectivity introduced by RCDD greatly minimizing the error rates.

4.2 RCDD OFDM System Model

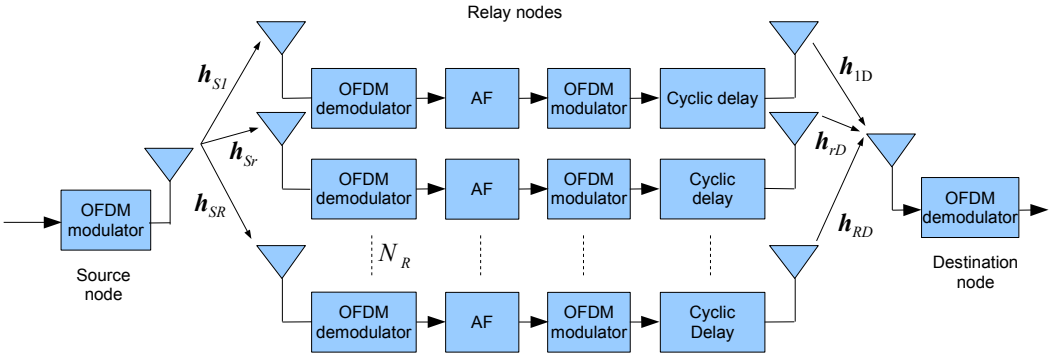

Figure 4.2: Two-hop relay system

We consider a two-hop wireless relay network that consists of a source node, S, a destination node, D, and relay nodes RN_r, $r = 1, 2, ..., R$, as shown in Figure 4.2. Each nodes has a single antenna. We assume perfect channel state information at all receivers and the transmitter only knows the statistic of fading but not the current realization.

The transmission to and from relay terminals occurs in two orthogonal subchannels. In the first subchannel, the source terminal broadcasts its coded symbol to the relay terminals. For AF relaying, amplification factor, A_r is multiplied to the received signal to compensate the degradation from the first hop transmission. Cyclic delay is then applied to introduce diversity channel in the second-hop transmission. The destination node receives signals from the relay nodes in the second subchannel. We assume that there is no direct transmission from source node to the destination node.

The channel impulse response between two terminal $\{p\}_{p=S,r}$ and $\{q\}_{q=r,D}$ is modeled as multipath fading channel with L_{pq} paths as

$$h_{pq}(\tau) = \sum_{l=1}^{L_{pq}} h_{pq}(l)\delta(\tau - \tau_{pq}(l)) \tag{4.1}$$

where τ_l and $h_{pq}(l)$ is the delay and complex amplitude of the lth path respectively. The $h_{pq}(l)$ are modeled as zero-mean complex Gaussian random variables with

variance $E\{|h_{pq}(l)|^2\} = \Omega_{pq}(l)$, where we assume symmetry between relay nodes to simplify the analysis. The channels are normalized such that $\sum_{l=1}^{L} h_{pq}(l) = 1$. A cyclic prefix with length $L_{cp} > L_{pq}$ is introduced to convert multipath frequency selective fading channels to flat fading sub-channels on the subcarriers.

At source node, data information symbols is convolutional coded and the high rate input stream is demultiplexed and transmitted over N low-rate independent frequency subcarriers. This multicarrier transmission scheme can be efficiently implemented in practice using the Fast Fourier Transform (FFT). High rate data sequence of length N, $\mathbf{S} = [S(0), ..., S(N-1)]$ are parsed into N parallel subcarrier and the modulated symbol OFDM can be expressed as an inverse fast Fourier transform (IFFT)

$$s(n) = \frac{1}{\sqrt{N}} \sum_{k=0}^{N-1} S(k) e^{-j2\pi nk/N};\ n = 0, 1, ..., N-1 \tag{4.2}$$

Assuming complete elimination of ISI, the FFT modulated received signal at relay r during the first time slot can be considered separately for each subcarrier given by

$$Y_r(k) = \sqrt{P_S} H_{Sr}(k) S(k) + Z(k) \tag{4.3}$$

where P_S is the transmitted energy per symbol at source node, $H_{Sr}(k)$ is the frequency response of the channel between the source and the rth relay on the kth subcarrier and $Z_r(k)$ represents the AWGN) with the real and imaginary components assumed to be statistically independent Gaussian distributed RVs having zero-mean and variance $N_0/2$ per dimension. The channel frequency response $H_{Sr}(k)$ is assumed to be constant during the transmission of the OFDM symbol and is given by

$$H_{Sr}(k) = \sum_{l=1}^{L_{Sr}} h_{Sr}(l) e^{-j2\pi kl/N} \tag{4.4}$$

where L_{Sr} is the length of taps in the first hop channel. We assume perfect channel state information at any receiving node but no channel information at transmitting nodes. All the noise terms are assumed to be independent for different receiving node.

Figure 4.3 shows the relay structure for the proposed relay diversity scheme.

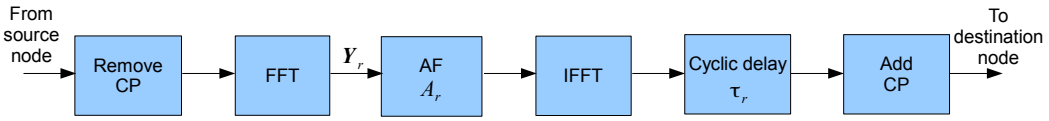

Figure 4.3: RCDD relay structure

For AF transmission, the amplification factor, A_r is multiplied to the received signal to compensate the degradation from the first hop transmission.

After the IFFT operation for the second hop transmission, the amplified signal is given by

$$x_r(n) = \frac{1}{\sqrt{N}} \sum_{k=0}^{N-1} A_r Y_r(k) e^{-j2\pi nk/N} \tag{4.5}$$

The signal $x_r(n)$ is then cyclically delayed by a relay specific delay of length τ_r. Due to the insertion of these delay, (4.5) becomes

$$\underbrace{x_r\left([n-\delta_r]_N\right)}_{\text{cyclically delayed signal}} = \frac{1}{\sqrt{N}} \sum_{k=0}^{N-1} A_r(k) \underbrace{e^{j2\pi k\tau_r/N} Y_r(k)}_{\text{Phase delayed signal}} e^{j2\pi kn/N} \tag{4.6}$$

where $[a]_b$ denotes a modulo b which is the remainder of a divided by b. From the above expression, it can be observed that a cyclic delay of δ_r in time domain is equivalent to a multiplication of phase factor $P_r(k) = e^{-j2\pi\tau_r k/N}$ in the frequency domain, where the phase is linearly increasing with the subcarrier index. This equivalence is the property of DFT which confirms that CDD can also be implemented in the frequency domain as phase shift at relay node. For CDD in multiple transmit antenna, phase shift is unattractive as it requires multiple IFFT operation at the source node. In relay system, either cyclic delay in time-domain or phase shift in frequency domain can be used.

For the transmission in the second time slot, CP of length $L_{cp} \geq L_{Sr} + L_{rD}$, where L_{rD} is the channel tap of the second hop channel, is added to the transmitted symbol. Assuming complete elimination of ISI, the FFT modulated received signal at destination node can be represented as

$$Y(k) = \sum_{r=1}^{R} A_r H_{Sr}(k) H_{rD}(k) P_r(k) X(k) + Z(k) \tag{4.7}$$

where $H_{rD}(k)$ is the channel response denoted between relay r and the destination given by

$$H_{rD}(k) = \sum_{l=1}^{L_{rD}} h_{rD}(l) e^{-j2\pi kl/N} \tag{4.8}$$

The total noise at the destination node is given by

$$Z(k) = \sum_{r=1}^{R} A_r H_{rD}(k) P_r(k) Z_r(k) + Z_D(k) \tag{4.9}$$

which has zero mean and variance

$$\sigma_z^2 = \left(\sum_{r=1}^{R} A_r^2 H_{rD}^2(k) + 1 \right) N_0 \tag{4.10}$$

4.3 Construction of the Delay Matrix

In RCDD OFDM system, the spatial diversity of the relay nodes is converted into frequency diversity. This is achieved by appropriately selecting the cyclic delay τ_r for relay r. The chosen delay values are such that the $L_r = L_{Sr} + L_{rD}$ of all end-to-end relay channel becomes consecutive in their delay lags. By doing so, the overall system can be represented by a 2-hop single relay system with an enhanced delay spread of RL_r taps. To show this, (4.7) is expressed in vector matrix form as

$$\mathbf{Y} = \sum_{r=1}^{R} A_r \mathbf{H}_{Sr} \mathbf{H}_{rD} \mathbf{P}_r \mathbf{X} + \mathbf{Z} \tag{4.11}$$

which is length N column vector corresponding to one OFDM symbol. Here, $\mathbf{Z}$ is total noise vector at the destination and $\mathbf{P}_r$ is the cyclic shift matrix that will be discussed later. The channel matrices from the first and second hop transmission are given by $\mathbf{H}_{Sr} = \text{diag}[H_{Sr}(0), ..., H_{Sr}(N-1)]$ and $\mathbf{H}_{rD} = \text{diag}[H_{rD}(0), ..., H_{rD}(N-1)]$ respectively.

The end-to-end channel matrix can be split into impulse response and DFT part as

$$\mathbf{H}_r = \sum_{l_{Sr}=0}^{L_{Sr}-1} \sum_{l_{rD}=0}^{L_{rD}-1} h_{Sr}(l_{Sr}) h_{rD}(l_{rD}) \mathbf{W}_{l_r = l_{Sr} + l_{rD}} \tag{4.12}$$

where

$$\mathbf{W}_{l_r} = \text{diag}\left[1, e^{-j2\pi l_r/N}, ..., e^{-j2\pi l_r(N-1)/N}\right] \tag{4.13}$$

From (4.12), it can be noted that different end-to-end relay channels may have different channel multipaths, but they possess the same delay lags in the FFT domain as seen in $\mathbf{W}_{l_r}$. In order to shift the L_r multipaths of each end-to-end channel corresponding to relay r in such a way that all channel multipaths become consecutive in their delay lags the matrices $\mathbf{P}_r$ is chosen to be

$$\mathbf{P}_r = \text{diag}[1, \mathrm{e}^{\mathrm{j}\tau_\mathrm{r}}, ..., \mathrm{e}^{\mathrm{j}\tau_\mathrm{r}(\mathrm{N}-1)}] \tag{4.14}$$

with

$$\tau_r = -2\pi(r-1)L_r/N \tag{4.15}$$

which makes

$$\mathbf{W}_{l_r}\mathbf{P}_r = \mathbf{W}_{l_r+(r-1)L_r} \tag{4.16}$$

for $l_{Sr} \in [0, L_{Sr}-1]$, $l_{rD} \in [0, L_{rD}-1]$. Hence, the equivalent end-to-end channel vector becomes

$$\mathbf{h} = \left[(\mathbf{h}_1)^T, ..., (\mathbf{h}_R)^T\right]^T \tag{4.17}$$

Now, since $\mathbf{h}_r$ has length RL_r, it can be viewed as coming from a single two-hop frequency selective channel. Based on (4.16), the diagonal matrix $\mathbf{H}$ can be expressed in terms of longer equivalent channels as

$$\begin{aligned} \mathbf{H} &= \sum_{r=1}^{R} \mathbf{H}_{Sr}\mathbf{H}_{rD}\mathbf{P}_r \\ &= \sum_{l_{Sr}=0}^{R(L_{Sr}-1)} \sum_{l_{rD}=0}^{R(L_{rD}-1)} h_{Sr}(l_{Sr})h_{rD}(l_{rD})\mathbf{W}_{l_r} \end{aligned} \tag{4.18}$$

Thus the phase shift matrix $\mathbf{P}_r$ shifts the delay lags of the rth relay channels from $[0, L_{Sr}-1]$ and $[0, L_{rD}-1]$ to $[(r-1)L_{Sr}, r(L_{Sr}-1)]$ and $[(r-1)L_{rD}, r(L_{rD}-1)]$ respectively.

Based on the analysis in the frequency domain above, the delay matrix which

is the time domain of (4.14) can be written as

$$\mathbf{p}_r = \begin{bmatrix} 0 & \mathbf{I}_{L_r(r-1)} \\ \mathbf{I}_{R-(r-1)L_r} & 0 \end{bmatrix} \tag{4.19}$$

4.4 Performance Analysis-Diversity Gain

We consider a coded OFDM relay system with convolutional code to extract the maximum diversity gain. In case of a convolutional code, the maximum diversity level which can be exploited by the decoder is determined by the free distance d_{free} of the code [7]. Therefore, the full spatial diversity can only be picked up if $d_{free} \geq N_R$.

Let $\mathbf{s}$ denote the information block of length N. The precoded data block is expressed as $\mathbf{x} = \Theta\mathbf{s}$ where Θ is the code matrix. For a given channel realization and transmitted symbol block $\mathbf{s}$, conditional PEP denotes the probability of deciding in favour of another block $\mathbf{s}'$ and is given by

$$P_e\left(\mathbf{s} \to \mathbf{s}' | \mathbf{h}_{Sr}, \mathbf{h}_{rD}\right) = Q\left(\frac{d(\mathbf{s}, \mathbf{s}')}{2}\right) \tag{4.20}$$

where $d(\mathbf{s}, \mathbf{s}')$ is the Euclidean distance between $\mathbf{s}$ and $\mathbf{s}'$ and $Q(x)$ is the Gaussian-Q function [16]. Let the coded error vector $\mathbf{u} = \Theta(\mathbf{s} - \mathbf{s'})$, therefore we have

$$d(\mathbf{s} \to \mathbf{s}) = \rho \sum_{r=1}^{R} \left\| A_r \Sigma_r^{-1/2} \mathbf{H}_{Sr} \mathbf{H}_{rD} \mathbf{u} \right\|^2 \tag{4.21}$$

where $\rho = P_s/N_0$ and $\Sigma_r = A_2 \mathbf{H}_{rD} \mathbf{H}_{rD}^H + \mathbf{I}_N$. The channel matrices can be rewritten as

$$\mathbf{H}_{pq} = \mathbf{h}_{pq} \mathbf{W}_{l_{pq}} \tag{4.22}$$

where $\mathbf{h}_{pq}$ is the channel vector between node p and q and the respective exponential factor is $\mathbf{W}_{l_{pq}}(k, l) = \exp(-j2\pi(k+1)(l+1)/P),\ 0 \leq k \leq N-1,\ 0 \leq l \leq L_{pq-1}$. Applying Chernoff bound of $Q(x) \leq \frac{1}{2}\exp\left(-\frac{x^2}{2}\right)$ on (4.20), the upper

bound for the average PEP is given by

$$P_e(\mathbf{s} \to \mathbf{s}') \leq \frac{1}{2} E_{h_{Sr}, h_{rD}} \left\{ \prod_{r=1}^{R} \exp\left(\frac{-\rho \left\| A_r \Sigma^{-1/2} \mathbf{H}_{Sr} \mathbf{H}_{rD} \mathbf{u} \right\|^2}{8} \right) \right\}$$
$$\leq E_{\mathbf{h}_{rD}} \left\{ \det\left(\mathbf{I} + \frac{\rho \ A_r^2}{8(L_{Sr} \mathbf{W}_{Sr}^H \left(\mathbf{I} + A_r^2 \mathbf{H}_{rD} \mathbf{H}_{rD}^2 \right)^- 1) \mathbf{H}_{rD} \mathbf{H}_{rD}^H \mathrm{diag}(\|\mathbf{u}\|^2) \mathbf{W}_{Sr}} \right)^{-1} \right\} \tag{4.23}$$

Since the component in $\mathbf{h}_{rD}$ are i.i.d. Gaussian with variance $1/L_{rD}$, we have $\mathbf{H}_{rD}$ with zero-mean and unit variance. Taking the expectation with respect to $\mathbf{h}_{rD}$, we found the upper bound of PEP to be

$$P_e(\mathbf{s} \to \mathbf{s'}) \leq \beta(\rho)^{-(\sum_{r=1}^{R} k_r)} (\log \rho)^{-(\sum_{r=1}^{R} k_r)} \tag{4.24}$$

where $k_r = \min(L_{Sr} + L_{rD})$ and

$$\beta = \frac{(8\pi)^{\sum_{r=1}^{R} k_r} \prod_{r=1}^{R} L_{Sr}^{k_r}}{2 \det \mathbf{U}} \tag{4.25}$$

It is observed in (4.24) that the PEP is not a simple exponential function of the SNR. It involves the term $(\log \rho)^{-(\sum_{r=1}^{R} k_r)}$ due to the cascaded nature of channels in the relaying links. This is in line with the observation of the term $(\log \rho)^R$ reported in [39] for frequency flat channel. From (4.24), we also observed that an asymptotical diversity order of $K = \sum_{r=1}^{R} \min(L_{Sr}, L_{rD})$ is available for the coded OFDM with multiple relay system.

4.5 Simulation Results

In this section, we present Monte-Carlo simulation results to demonstrate the error rate performance of RCDD in OFDM system. We use half-rate convolutional code with constraint length 7 which is long enough for our system to achieve maximum diversity from the multipath channel. The coded symbols are BPSK modulated and passed through $N = 64$-point IFFT for OFDM process.

First, we investigate the performance of RCDD system with two and three

relay nodes under various scenarios as below:

- **Scenario 1:** $L_{Sr} = 1$, $L_{rD} = 1$
- **Scenario 2:** $L_{Sr} = 1$, $L_{rD} = 3$
- **Scenario 3:** $L_{Sr} = 3$, $L_{rD} = 1$
- **Scenario 4:** $L_{Sr} = 3$, $L_{rD} = 3$

As clearly seen from Figure 4.4 and Figure 4.5, the system without channel coding the system failed to give a reasonable performance nor providing optimum spatial diversity gain. Using channel coding, RCDD OFDM system is able to extract underlying rich multipath diversity. For two relay systems, it is observed that an identical diversity order is achieved for scenario 1, 2 and 3. As predicted by the diversity gain analysis, the maximum diversity gain is given by $\sum_{r=1}^{N_R} \min(L_{Sr}, L_{rD})$, which in this case equivalent to 2. The diversity gain increase for scenario 4, where the channel length for both source-to-relay and relay-to-destination are equal to 3. The maximum diversity order available for this scenario is 6. However, the cascaded nature of Rayleigh channels in relaying links allows only partial diversity to be observed in the practical SNR range under consideration. This can be observed better through a comparison with the performance of MRC with 2 and 6 co-located antennas, which is also plotted in Figure 4.4. For the three-relay systems, the maximum diversity order as calculated for scenario 1-3 and 4 are 3 and 9 respectively. The performance of 3 and 9 co-located antennas are also included in Figure 4.5 for comparison purposes. In term of the error performance, the relay system experience a performance degradation compared to the point-to-point system. In a specific relay node configuration, the system with more selective channel has better performance than the ones with less selective.

Next we compare the performance of RCDD to the conventional CDD with different number of antennas and relay nodes. We can see that in Figure 4.6 and Figure 4.7, the RCDD performance is worse than the conventional CDD. This is expected as the result of cascaded relay channel. As the number of relay node increases the performance becomes better. Unlike STBC, CDD and RCDD

system provide full rate transmission regardless the number transmit antenna and relay nodes respectively.

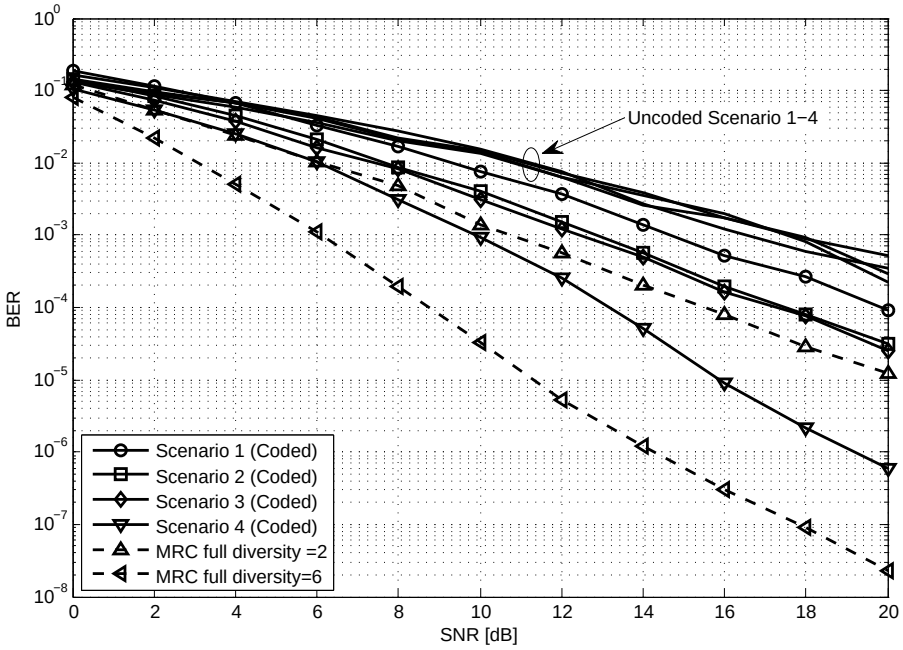

Figure 4.4: BER performance of RCDD OFDM with two relay nodes

4.6 Summary

In this chapter, the principles of RCDD OFDM systems were reviewed. The transformation of relay diversity into frequency was explained with the help of phase diversity.

The construction of delay matrix is given. The delay value is derived such that the end-to-end relay channel becomes consecutive in their delay lags. The PEP for RCDD is derived to obtained the diversity gain. For relaying channel, it is shown that the PEP is not a simple exponential function of the SNR but also contains a constant due to the cascaded nature of the channel.

The performance of channel coded and uncoded RCDD OFDM were evaluated for AF relaying over Rayleigh fading channel. The simulation results show that the uncoded error rates of RCDD OFDM remain unchanged to a single

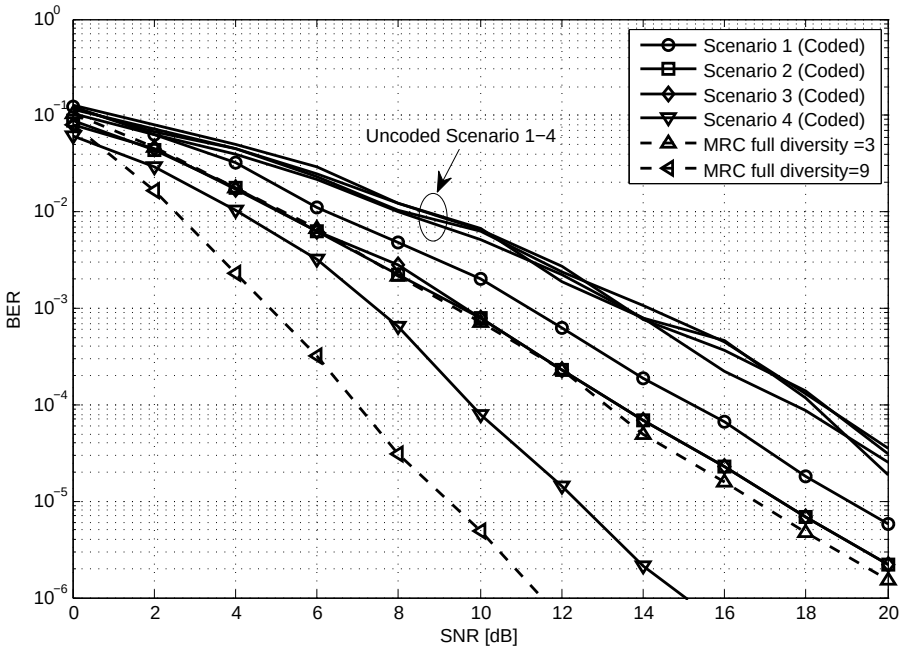

Figure 4.5: BER performance of RCDD OFDM with three relay nodes

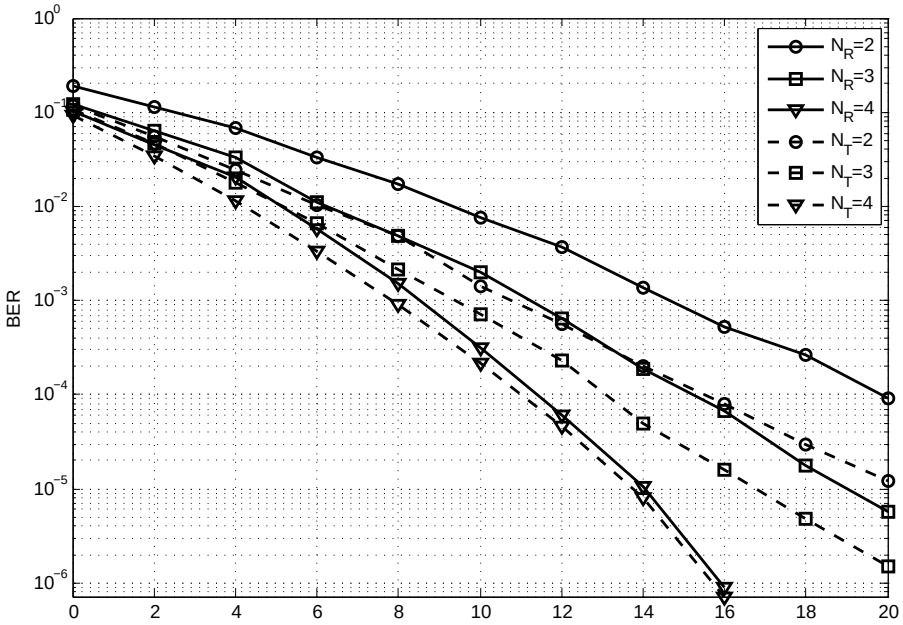

Figure 4.6: BER performance of RCDD OFDM with $N_R = 2, 3, 4$ with channel fading tap $L_{Sr} = L_{rD} = 1$

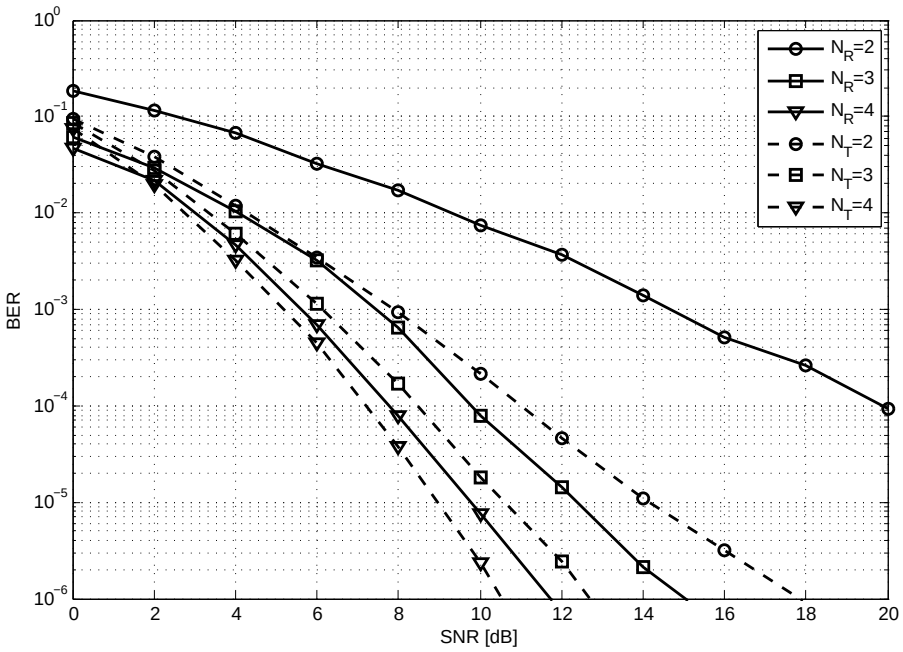

Figure 4.7: BER performance of RCDD OFDM with $N_R = 2, 3, 4$ with channel fading tap $L_{Sr} = L_{rD} = 3$

relay OFDM system because of the fact that RCDD converts the relay spatial diversity into frequency. However, the channel coded results showed that the enhanced selectivity introduced by RCDD greatly helps in improving the system performance.

Chapter 5

Error Probabilities of DSTBC and RCDD MC-CDMA

5.1 Introduction

MC-CDMA is one of the most promising candidates for future broadband mobile communication networks standards. It mitigates the degradation due to severe multipaths with the help of OFDM and addresses the two adverse effects associated with OFDM simplicity which are the inability to extract multipath diversity that presents inherently in broadband wireless channel and to guarantee symbol detection when channel nulls occur on parallel subchannels. To overcome these issues, MC-CDMA uses spread and coded signals over parallel subcarriers, thereby making full advantage of frequency diversity and guaranteeing better symbol detection. Combined with STC schemes, MC-CDMA has the potential of fulfilling the promises offered by future applications and services.

As presented in Chapter 3, distributed orthogonal block codes has been considered as the best choice for relay diversity in narrowband environments but their use is broadband channels is questionable due to their inability to to pick up mulitpath diversity. However when used in conjunction with an MC-CDMA system, they achieve not only spatial diversity but also variable multipath diversity depending upon the employed spreading. In comparison, CDD is an attractive approach towards achieving spatial and multipath diversity. The inherent

simplicity and comformability with current standards makes RCDD even more desirable for MC-CDMA system.

It is well-known that the attainable frequency diversity in MC-CDMA system is severely hindered by PAP fluctuations which restricts the usage of large spreading factors. Also in low delay spread channel environments, the adjacent subcarriers are subjected to correlated fading resulting in relatively high coherence bandwidth and consequently, combining adjacent subcarrier signals do not achieve the expected performance when transmitting over low dispersion fading channels. In light of above, CDD may be the simplest solution in low delay spread environments which provides excellent frequency diversity even with relatively small spreading factors. The combination of induced frequency selectivity from CDD branches and inherent frequency domain spreading of an MC-CDMA system helps in improving the system's performance independent of FEC or channel codes which are otherwise compulsory in a simple OFDM system. CDD can be considered as STC with no additional complexity at the receiver where the receiver remains the same as in the case of a single two-hop relay. Above all, it can be used for any number of relay nodes without any loss in spectral efficiency and can be applied directly to existing standards.

To date, few studies have considered relay diversity scheme to improve the performance of MC-CDMA system. Mostly, these studies have focused on the application of STBC. In this section, DSTBC and RCDD schemes are introduced for MC-CDMA system. By using this basic signal structure of the subject system which was presented in section 2.7, the instantaneous SNRs of these two relay diversity methods are calculated with the MRC detection technique which are used for the SER analysis in the next section.

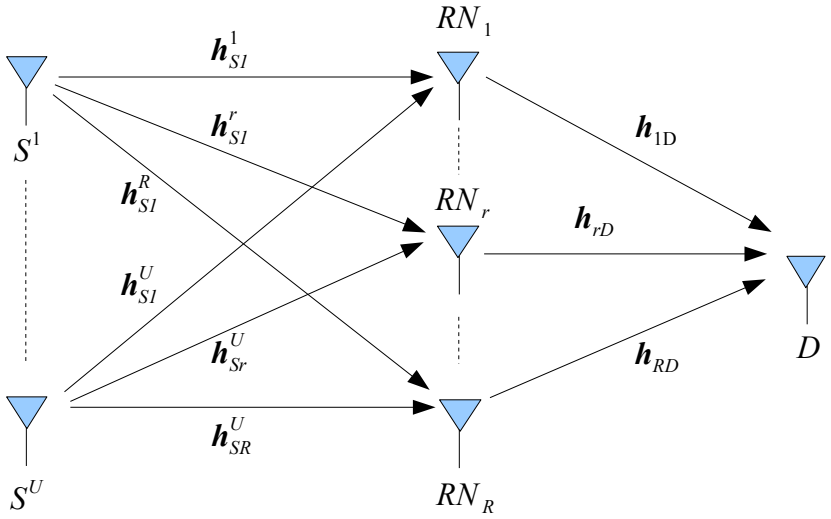

Figure 5.1: Distributed framework for cooperative MC-CDMA

5.2 RCDD and DSTBC MC-CDMA System Modeling

5.2.1 RCDD MC-CDMA

A cooperative MC-CDMA system consists of U users denoted by $S^u,\ u = 1, ..., U$, a destination node, D and R relay nodes denoted by $RN_r,\ r = 1, ..., R$ as shown in Figure 5.1. The number of users supported by the system is $U, u = 1, ..., U$ and restricted by $U \leq G$, where G is the spreading factor. The relay nodes operate in half-duplex mode where they receive signals from source nodes in the first time slot and retransmit to the destination node in the second time slot. The relay nodes employ DF protocol where they decode the received and combined symbols and then re-encode and spread the user data using their original spreading code from the first transmission. The signal from each relay is cyclically-delayed to produce an artificial multipath effect seen by the destination node. It is obvious that the first transmission hop is a multiple access case of MC-CDMA and the second hop is a downlink MC-CDMA.

The equiprobable source data stream of the uth user is modulated and mapped as symbol selected from the M-ary phase shift keying (M-PSK) or M-ary quadrature amplitude modulation (M-QAM) signal constellation. The source stream

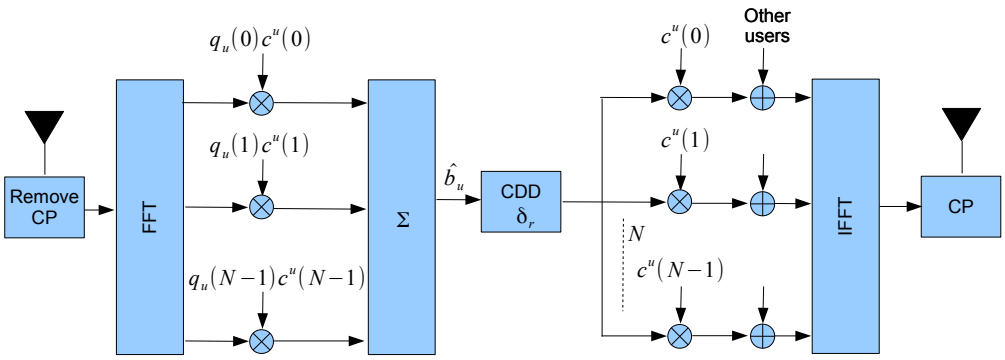

Figure 5.2: RCDD MC-CDMA relay structure

may be obtained after source, channel coding and/or time-interleaving. The processing gain of an MC-CDMA system is defined as $G = N/P$, where P represents the number of symbols that a user may transmit during a signaling interval and N is the number of subcarrier. The modulated symbols are converted into $P = N/G$ parallel streams, or in other words each symbol is copied according to the spreading factor and multiplied with Walsh-Hadamard spreading code of the uth user which makes the chip G times higher than the data symbol rate. Finally, to mitigate the effects of multipath fading, CP is added between each MC-CDMA symbol and the signal is transmitted after up-conversion. Ignoring the CP, the IFFT modulated data can be expressed as

$$s_u(t) = \sqrt{E_c} \sum_{p=0}^{P-1} \sum_{g=0}^{G-1} b_p^u c_g^u e^{j2\pi(gP+p)t/T} \tag{5.1}$$

E_c is the energy per OFDM symbol, and $E_c = E_S/N$ where E_S is the energy per symbol before spreading. T is the signaling interval during which P symbols per user are generated. b_p^u and c_g^u are the pth symbol and gth chip of the uth user, respectively. For analytical convenience and simplicity, only a single data symbol i.e. $P = 1$ is considered and therefore b^u for each user and $G = N$.

At relay node r, after the removal of CP and subsequent FFT processing, the received signals are subjected to despreading and detection. Ignoring the assumption of $P = 1$ for the time being, the fact that the pth symbol of user u is detected independently from the p' symbols, where $p \neq p'$ for all users. Thus,

without loss of generality, the subscript p can be omitted altogether for (5.1) and the $G = N$ subcarriers conveying the same symbol can be considered for detection. The received signal at the kth subcarrier can be expressed as

$$Y_r(k) = \sqrt{P_S} \sum_{u=0}^{U-1} b^u c^u(k) H_{Sr}^u(k) + Z_r(k) \tag{5.2}$$

where P_S is the transmitted power from all users and $Z_r(k)$ is the discrete AWGN term at relay r, modeled as a zero-mean complex Gaussian random variable with variance N_0. The channel frequency response from source user u to relay node r is given by $H_{Sr}^u(k) = \sum_{l=0}^{L_{Sr}-1} h_{Sr,l} \exp(-j2\pi kl/N)$ where tap amplitude $h_{Sr,l}$ is modeled as Gaussian random variable with zero mean and variance $\sigma_{Sr,l}^2$. The channel are normalized such that $\sum_{l=0}^{L_{Sr}-1} h_{Sr,l} = 1$. The estimated symbol at relay node r is given by

$$\hat{b}_r^u = \text{sgn}\left(\sum_{k=0}^{N-1} Y_r(k) q(k) \right) \tag{5.3}$$

where $q(k)$ is the frequency domain equalization gain factor which is dependent on the employed diversity combining schemes, as discussed earlier in Section 2.7. In the second time slot, we consider MC-CDMA downlink transmission where the estimated users' data are spread by their original spreading code from the first transmission. For DF protocol, if the relay node is able to decode the received signal correctly, then it forwards the decoded signal with power P_R to the destination. Otherwise, the relay does not send the signal and remains idle. Let δ_r be the cyclic delay for relay r. After adding CP, the relay nodes transmit simultaneously to the destination. Assuming there is no ISI, the received signal is given by

$$Y_D(k) = \sqrt{\tilde{P}_r} \sum_{r=1}^{R} b_r^u c_r^u(k) H_{rD}(k) + Z_D(k) \tag{5.4}$$

where $\tilde{P}_r = P_r$ if the relay node decodes the received signal correctly and $\tilde{P}_R = 0$ otherwise. The noise at destination, $Z_D(k)$ is the discrete AWGN term at relay r, modeled as a zero-mean complex Gaussian random variable with variance N_0. The channel frequency response from relay node r to destination node is

given by $H_{rD}(k) = \sqrt{\frac{1}{N}} \sum_{l=0}^{L_{rD}-1} h_{rD,l} \exp(-j2\pi kl/N)$ where tap amplitude $h_{rD,l}$ is modeled as Gaussian random variable with zero mean and variance $\sigma^2_{rD,l}$. Due to the effect of cyclic delay, the channel frequency response from relay r becomes

$$H_{rD}(k) = \sum_{l=\delta_r}^{L_{rD}-1+\delta_r} h_{rD,l} e^{-j2\pi kl/N} \tag{5.5}$$

We choose the length of cyclic delay for relay r to be $\delta_r = (r-1)L_{rD}$ so that the channel taps from all relay nodes become consecutive in their delay lags, as investigated in Section 4.3. Therefore, the received signal can be rewritten as

$$Y_D(k) = \sqrt{\tilde{P}_R} b^u c^u(k) H_{\delta,rD}(k) + Z_D(k) \tag{5.6}$$

where

$$H_{\delta,rD}(k) = \sum_{l=0}^{RL_{rD}-1} h_{rD,l} e^{-j2\pi kl/N} \tag{5.7}$$

We assume an ideal DF cooperation protocol [85] where the relay is able to detect whether the transmitted symbol is decoded correctly or not, which is also referred as a selective relaying In practice, we may apply an SNR threshold at the relay. If the received SNR at the relay is higher than the threshold, then the symbol has a high probability to be decoded correctly. Based on the analysis above, it is shown that the RCDD MC-CDMA collapse to a single relay system with a highly selective channel in the second hop transmission. We assume the total transmit power is $P_T = P_S + P_R$.

The decision variable $d^{u'}$ of the u'th user's symbol at destination node can be expressed as [26]

$$d^{u'} = \sum_{k=0}^{N-1} q(k) c^{u'}(k) Y_D(k) \tag{5.8}$$

where $q(k)$ is a frequency domain equalization gain factor which varies with the employed single and multiuser diversity combining/detection schemes. In this analysis, we employ MRC detection as described in Section 2.7. Let $q(k) = H^*_{\delta,rD}(k)$ and substitute together with (5.2) in (5.8), the decision variable $d^{u'}$ is

given by

$$\begin{aligned} d^{u'} &= \sum_{k=0}^{N-1} H^*_{\delta,rD}(k) c^{u'}(k) Y_D(k) \\ &= \sqrt{\tilde{P}_R} \sum_{k=0}^{N-1} |H_{\delta,rD}(k)|^2 + \sqrt{\tilde{P}_R} \sum_{u=1,u\neq u'}^{U} b^u \sum_{k=0}^{N-1} c^u c^{u'} |H_{\delta,rD}(k)|^2 \\ &\quad + \sum_{k=0}^{N-1} c^{u'}(k) Z_r(k) H^*_{\delta,rD}(k) \\ &= DS + I_{MAI} + \eta \end{aligned} \tag{5.9}$$

where I_{MAI} and η are the MAI and noise component respectively. For a system with large N, the chip of the spreading codes and the input data symbol are random, I_{MAI} can be well approximated by zero mean Gaussian with variance [24]

$$\sigma^2_{I_{MAI}} = \tilde{P}_R (U-1) \sum_{k=0}^{N-1} |H_{\delta,rD}(k)|^2 \tag{5.10}$$

Utilizing the central limit theorem, η is also approximated by zero mean Gaussian with variance

$$\sigma^2_{\eta} = N_0 \sum_{k=0}^{N-1} |H_{\delta,rD}(k)|^2 \tag{5.11}$$

The instantaneous SINR at destination is then obtained as

$$\begin{aligned} \gamma &= \frac{DS^2}{\sigma^2_{I_{MAI}} + \sigma^2_{\eta}} \\ &= \frac{\tilde{P}_R \sum_{k=0}^{N-1} |H_{\delta,rD}(k)|^2}{\tilde{P}_R (U-1) + N_0} \end{aligned} \tag{5.12}$$

5.2.2 DSTBC MC-CDMA

The application of DSTBC for CDMA has been presented in [102] for two users to cooperate by help transmitting each other's using Alamouti code. In [68], Urothota present multiuser cooperation for more than two users in MC-CDMA system. The relay node structure for decode and forward MC-CDMA relaying is shown in Figure 5.3. Continuing from the model for RCDD, the received

estimated data symbols at relay node in (5.3) are encoded by distributed STC defined by a $T_b \times R$ column orthogonal matrix $\mathcal{G}$. These ST encoded symbol are then passed to the spreading section, where each symbol is copied G times and multiplied with its original spreading code from the first transmission.

For analytical convenience, consider $P = 1$, i.e. all U users employ the full N MC-CDMA subcarriers. The received signal at destination node can be expressed as

$$\begin{bmatrix} Y_D^1(k) \\ \vdots \\ Y_D^{T_b}(k) \end{bmatrix} = \sqrt{\tilde{P}_R} \sum_{u=0}^{U-1} \sum_{k=1}^{N} c^u(k) \mathcal{G} \begin{bmatrix} H_{rD}(k) \\ \vdots \\ H_{rD}(k) \end{bmatrix} + \begin{bmatrix} z_D^1(k) \\ \vdots \\ z_D^{T_b}(k) \end{bmatrix} \tag{5.13}$$

Assuming the channel response remains constant for T_b time slot and perfect CSI is available at the receiver, then using the decoding method of [86], the recovered MC-CDMA symbols can be written as

$$\begin{bmatrix} V^1 \\ \vdots \\ V^F \end{bmatrix} = \sqrt{\tilde{P}_R} \sum_{u=0}^{U-1} \sum_{k=1}^{N} c^u(k) \hat{\mathbf{H}}(k) \begin{bmatrix} b^u \\ \vdots \\ b^U \end{bmatrix} \begin{bmatrix} Z^1(k) \\ \vdots \\ Z^F(k) \end{bmatrix} \tag{5.14}$$

where

$$\begin{aligned} \hat{\mathbf{H}}(k) &= \begin{bmatrix} \sum_{r=1}^{R} |H_{rD}(k)|^2 & \dots & 0 \\ \vdots & \ddots & \vdots \\ 0 & \dots & \sum_{r=1}^{R} |H_{rD}(k)|^2 \end{bmatrix} \\ &= \sum_{r=1}^{R} |H_r(k)|^2 \cdot \mathrm{diag}[1] \end{aligned} \tag{5.15}$$

The exact expression of modified noise terms $\left[Z^1(k), ..., Z^F(k)\right]^T$ varies from symbol to symbol and depends as well on the number of relay nodes.

5.3 Performance Analysis for DSTBC and RCDD MC-CDMA

Based on the analysis of the previous section, it is concluded that the relay MC-CDMA system employing RCDD is equivalent to a single relay channel system with enhanced delay spread, whereas the DSTBC MC-CDMA system also collapse to an equivalent single relay model. In this section, the SER of the subject systems are presented.

For M-PSK modulation system, the conditional SER can be written as [81]

$$P_{\mathrm{PSK}}(E|\gamma) = \frac{1}{\pi}\int_0^{(M-1)\pi/M} \exp\left(-\frac{g_{\mathrm{PSK}}\gamma}{\sin^2\theta}\right) d\theta \tag{5.16}$$

where $g_{\mathrm{PSK}} = \sin^2(\pi/M)$.

For the transmission from the source to relay nodes in the first time slot, the probability of incorrect decoding at relay r is $P(E|\gamma_r)$ and the probability of correct decoding is $1 - P(E|\gamma_r)$. Consider two scenarios of $\tilde{P}_r = P_r$ and $P_r = 0$, the conditional SER is given as

$$\begin{aligned} P_{\mathrm{PSK}}(E|\gamma) &= P_{\mathrm{PSK}}(E|\gamma_D)|_{\tilde{P}_r=0} P_{\mathrm{PSK}}(E|\gamma_r) \\ &\quad + P_{\mathrm{PSK}}(E|\gamma_D)|_{\tilde{P}_r=P_r} \left[1 - P_{\mathrm{PSK}}(E|\gamma_r)\right] \\ &= \frac{1}{\pi}\int_0^{(M-1)\pi/M} \exp\left(-\frac{g_{\mathrm{PSK}}\gamma_r}{\sin^2\theta}\right) d\theta \\ &\quad + \frac{1}{\pi}\int_0^{(M-1)\pi/M} \exp\left(-\frac{g_{\mathrm{PSK}}\gamma_D}{\sin^2\theta}\right) d\theta \\ &\quad \times \left[1 - \frac{1}{\pi}\int_0^{(M-1)\pi/M} \exp\left(-\frac{g_{\mathrm{PSK}}\gamma_r}{\sin^2\theta}\right) d\theta\right] \end{aligned} \tag{5.17}$$

Averaging the conditional SER (5.17) over Rayleigh fading channels $H_{Sr}(k)$ and $H_{rD}(k)$, the SER of DF relay system with M-PSK modulation is as follows:

$$P_{\mathrm{PSK}} = F_1\left(1 + \frac{g_{\mathrm{PSK}}\bar{\gamma}_R}{\sin^2\theta}\right) \tag{5.18}$$

$$+F_1\left(\frac{1 + g_{\mathrm{PSK}}\bar{\gamma}_D}{\sin^2\theta}\right)\left[1 - F_1\left(1 + \frac{g_{\mathrm{PSK}}\bar{\gamma}_R}{\sin^2\theta}\right)\right] \tag{5.19}$$

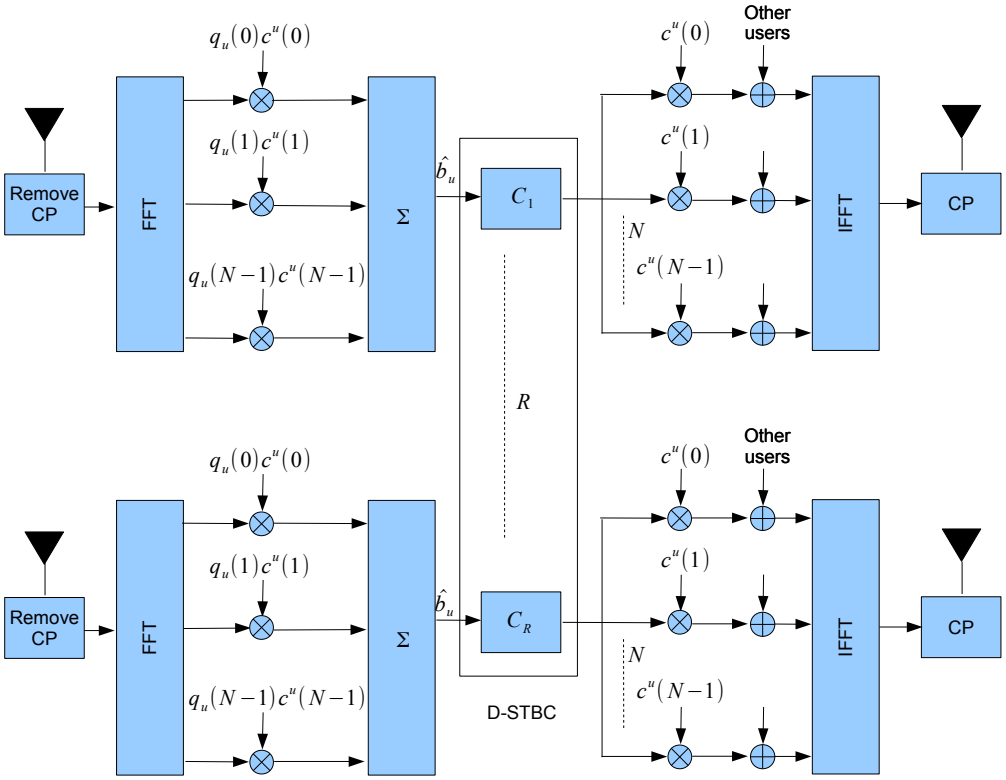

Figure 5.3: DSTBC MC-CDMA relay structure

where $F_1(x(\theta)) = \frac{1}{\pi}\int_0^{(M-1)\pi/M} \frac{1}{x(\theta)} d\theta$, in which $x(\theta)$ denotes a function with variable θ.

5.4 Performance Comparison - DSTBC and RCDD MC-CDMA

In the previous sections, the system modeling along with performance analysis of RCDD and DSTBC MC-CDMA systems were presented. However the analysis were limited to MRC which is only optimum for a single user case. Moreover, the numerical and and simulation results were investigated only for an uncoded system. As channel coding is an integral part of all system's standard, therefore for the true performance prediction of a certain scheme, the incorporation of such methods becomes necessary, and especially for RCDD which relies mainly

System Parameter		
System Bandwidth	B	101.5 MHz
FFT/IFFT points	$\mathbf{F}_N/\mathbf{F}_N^H$	1024
Number of Subcarriers	N	768
Subcarrier spacing	$f_s = B/N$	131.836 KHz
MC-CDMA Symbol Duration	$T_{mc} = 1/f_s$	7.585 μsec
Cyclic Prefix	L_g	0.6444 μsec
Total MC-CDMA Symbol Duration	$T_{mc} + L_g$	8.2294 μsec
Sampling Time	$T_{mc}/\mathbf{F}_N^H$	7.402$n$sec
Spreading Codes		Walsh-Hadamard
Spreading Length	G	16
Active Users	U	1,16
Detection Method		MRC, $U = 1$
		MMSEC, $U = 16$
Channel Encoding		Convolutional code $(r_{cc} = 1/2, (133, 171)_8)$
Channel Decoding		Soft Viterbi
Channel Estimation		Perfect
Channel Model with		18-taps Rayleigh
Delay Spread	τ_{max}	0.63 μs
Doppler Spread	$f_{D_{max}}$	20 Hz
Relay Nodes	N_{rx}	1

Table 5.1: Parameter settings for simulation results

on channel coding to extract the maximum diversity from the induced selectivity of the CDD branches. Also the results were presented with the basic MC-CDMA system configuration by assuming $N = G$ which mean each user occupying the whole system bandwidth.

In Figure 5.4, the SER of a RCDD MC-CDMA system has been shown with $N = 16$, $R = 2, 4$ and $L = 3$. It can be observed that as the number of relay CDD are increased from 2 to 4, the improvement in performance is significant. The simulations also confirm the numerical results. For the performance evaluation of DSTBC MC-CDMA system, a full rate transmission matrix $\mathcal{G}_2$ is used for $R = 2$, while for $R = 3, 4$ relays, half rate matrices $\mathcal{G}_3$ and $\mathcal{G}_4$ of [86] have been chosen. The SER evaluation has been done by normalizing the subchannel to unity. In Figure 5.5, the numerical SER are plotted for $R = 2, 3, 4$ with channel

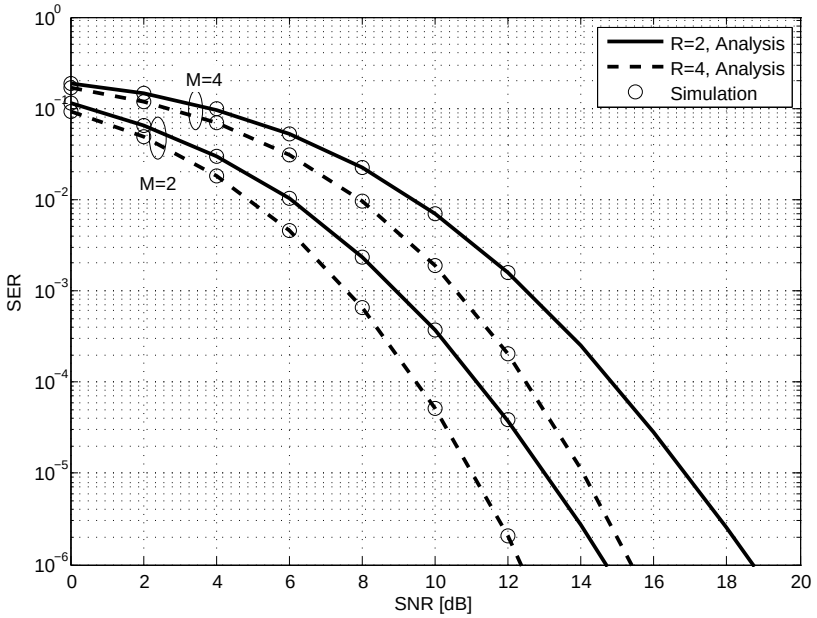

Figure 5.4: Performance of RCDD MC-CDMA with $R = 2, 3$, $N = 16$ and $L = 3$. Analytical results are generated by (5.3)

order $L = 2$. The simulation results show excellent agreement with the numerical curves, thereby validating the closed-form SER expression.

In Figure 5.6, both RCDD and DSTBC diversity techniques are plotted with $R = 3$. As the diversity order is similar, if equal number of multipath are realized, therefore the clarity or error curves RCDD has been simulated with channel orders of $L = 1, 3$ while DSTBC employs $L = 4$. As expected, DSTBC performs better than CDD because higher channel order and consequently, the diversity gain.

5.5 Summary

This chapter presents the DSTBC and RCDD for MC-CDMA system. First, a brief overview on cooperative MC-CDMA is given. Next, the system model of DSTBC and RCDD in MC-CDMA is presented based on the distributed framework for cooperative MC-CDMA. The instantaneous SNR for both systems is obtained where MRC detection is used at the destination.

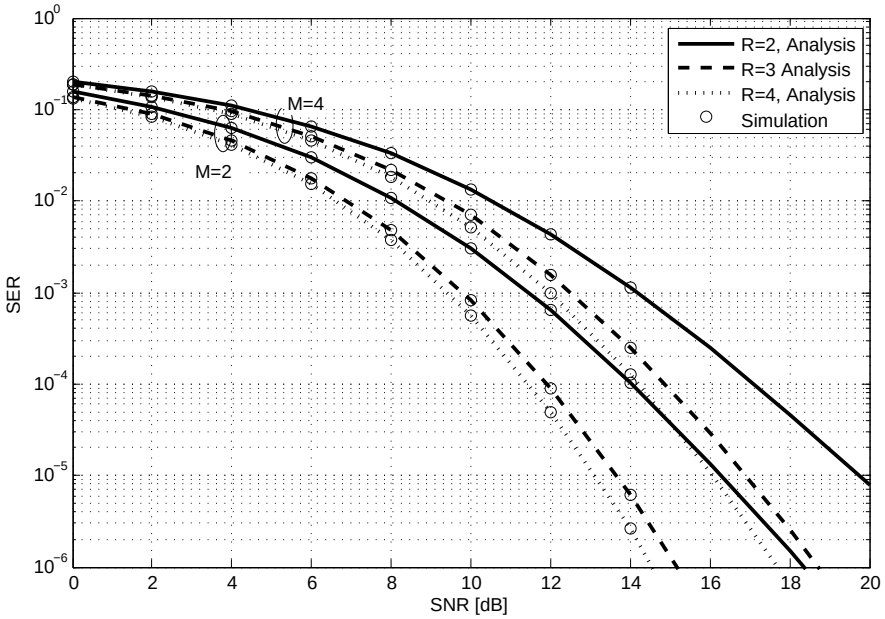

Figure 5.5: Performance of DSTBC MC-CDMA system with $R = 2, 3, 4$, N=16 and $L = 2$. Analytical results are generated by using (5.3)

The contribution of the chapter is the derivation of closed-form expression of the symbol error probabilities of RCDD and DSTBC MC-CDMA system. It has been shown that both uncoded systems can achieve RL diversity order, however compared to RCDD, the DSTBC system suffers from rate loss for more than two relays and also complexity at the destination end. RCDD provides significant performance improvement in both low and and high delay spread channels. The enhanced frequency selectivity induced by the RCDD relays provides additional coding gain when used with channel codes and even outperform DSTBC.

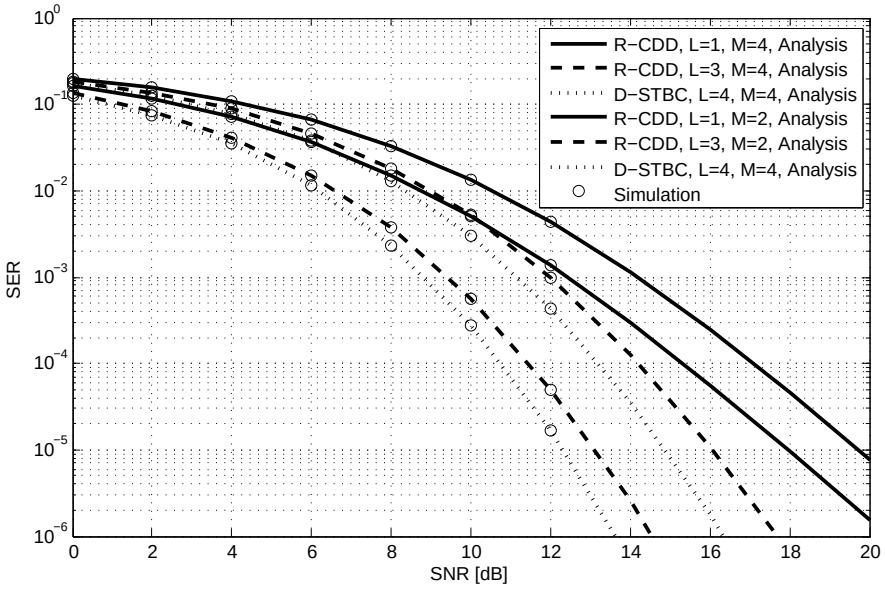

Figure 5.6: Performance comparison of DSTBC and RCDD MC-CDMA with $R = 3$. Analytical results are generated by (5.3)

Chapter 6

Hybrid Relay Diversity

6.1 Introduction

In this chapter, a cyclically delayed DSTBC or hybrid relay diversity (HRD) is presented for OFDM system. This relay diversity addresses the issue of achieving maximum spatial and multipath diversity from the broadband channel environments. Hybridizing RCDD with distributed orthogonal block coding may be the least complex relay structure as the cyclic delay converts spatial diversity into frequency by artificially increasing the channel delay spread and importantly without increasing the complexity at the destination.

Relay diversity techniques of RCDD and DSTC has been thoroughly investigated for OFDM and MC-CDMA in the previous chapters. The performance analysis combined with numerical and simulation results were presented for the individual incorporation of this relay diversity schemes. It was concluded that CDD is extremely simple to implement and becomes real competitive with block codes, however in certain scenarios such as fully loaded MC-CDMA system, the DSTBC always perform better than RCDD. Similarly, for a simple OFDM system, the coded results revealed that RCDD cannot compete with the distributed Alamouti scheme. RCDD can outperform block codes for the same spectral efficiency but for that additional relay nodes are required. In parallel, the realization of block codes for more than two relay nodes becomes impractical because of the complexity at destination node and loss of spectral efficiency.

Based on the above observations, a novel hybrid relay diversity (HRD), is presented in this chapter. It provides a simple solution to realize an excellent performance, low complexity and highly spectral efficient OFDM relay system.The basic idea is to extract the spatial diversity with orthogonal STBC, whereby the presence of cyclic delay helps in achieving the maximum frequency diversity from the broadband channel. To achieve this goal, an arbitrary number of relay nodes are employed and by trading the order of cyclic delay, a low delay spread broadband channel is converted into a highly selective one. Similarly, for large enough delay spread, low order of cyclic delay could be employed to achieve the same performance. Hence, it is an interplay between spatial and frequency diversity. The amount of spatial diversity purely depends on the employed STC technique. Cyclic delay converts the spatial diversity of the cyclic delayed branches into frequency which is picked by the FEC or other channel coding techniques.

6.2 HRD for Relay OFDM

We consider a two-hop OFDM wireless relay network with N subcarriers, that consists of a source node, S, a destination node, D, and relay nodes RN_r, $r = 1, ..., R$, as shown in Figure 4.2. Each nodes has a single antenna. We assume perfect channel state information at all receivers and the transmitter only knows the statistic of fading but not the current realization. The relay system is half-duplex where transmission to and from relay terminals occurs in two orthogonal subchannels. In the first subchannel, the source terminal broadcasts its coded symbol to the relay terminals. For AF relaying, amplification factor, A_r is multiplied to the received signal to compensate the degradation from the first hop transmission. A novel hybrid delay diversity coding is applied to introduce diversity channel in the second-hop transmission. The destination node receives signals from the relay nodes in the second subchannel. We assume that there is no direct transmission from source node to the destination node.

For simplicity, equal number of Q cyclic delay process for each P coding is assumed and with that the relay indices (p, q) can be mapped to relay node index r by

$$r(p, q) = (p - 1)Q + q \text{ for } 1 \leq p, q \leq P, Q \tag{6.1}$$

The channel coded information sequence $\hat{\mathbf{b}} = [\hat{b}_1, \hat{b}_2, ..., \hat{b}_F]^T$ of length F is generated by the discrete time convolution of source bit column vector $\hat{\mathbf{a}} = [\hat{a}_1, \hat{a}_2, ..., \hat{a}_{N_c}]^T$, $\hat{a}_i \in \{-1, +1\}$ of length N_c with the impulse response of the encoder. A convolutional encoder is considered here, however any other channel coding technique can be applied. N_c bits are fed to encoder to generate F channel encoded bits [69]. The symbol mapper produce vector $\mathbf{b} = [s_1, s_2, ..., s_{\bar{F}}]^T$ of size FM by mapping each $\log_2 M$ bits of $\hat{\mathbf{s}}$, where $\bar{F} = F/\log_2 M$. The modulated symbols are then processed by the $N \times N$ IFFT matrix to yield

$$\mathbf{x} = \mathbf{F}_N^H \mathbf{s} \tag{6.2}$$

To incorporate the block fading channel model [9], the coded frame length F has been divided into V independent fading blocks, each packed with $\bar{U}$ symbols. Channel coherence time, coherence bandwidth and OFDM symbol duration are presented by T_c, B_c and T_s respectively. Let $T_c = JT_s$ then $\bar{U} = JN$ and $F = V\bar{U} = VJN$, where J is an integer. The channel order or the selectivity is defined as $L + B/B_c$, where B represents the total signal bandwidth. We introduce the block fading indices, $1 \leq v \leq V$ and $1 \leq j \leq J$ into the channel frequency response expression of $H_i(k)$ so that

$$H_i(v, j, k) = \sum_{l=0}^{L_i - 1} h_i(v, l) e^{-j2\pi kl/N} \tag{6.3}$$

where $H_i(v, j, k)$ represents the channel frequency response of link i, $i = Sr, rD$ at kth subcarrier, jth OFDM symbol and within the vth time block. The channel impulse responses are assumed invariant over all J OFDM symbols as the channel impulse responses are the same within the vth time block. The taps $h_i(v, l) = \alpha_i(v, l)e^{j\theta_l}$ are uncorrelated with phase θ_l uniformly distributed over $[0, 2\pi]$ for all $i = Sr, rD$; $r = 1, ..., R$. Finally, with the introduction of block fading indices, the transmitted symbol matrix can be expressed as

$$\mathbf{X} = [\underbrace{\mathbf{x}_{1,1}, ..., \mathbf{x}_{1,J}}_{J}, \underbrace{\mathbf{x}_{2,1}, ..., \mathbf{x}_{2,J}}_{J}, ..., \underbrace{\mathbf{x}_{V,1}, ..., \mathbf{x}_{V,J}}_{J}]^T \tag{6.4}$$

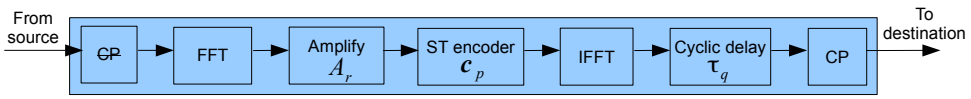

Figure 6.1: Hybrid relay structure

where $\mathbf{x}_{v,j} = [x_{v,j}(0), ..., x_{v,j}(N-1)]^T$. After the insertion of CP with length $L_{cp} \geq L_{Sr}$, the signal is transmitted to R relay nodes.

6.2.1 Relay Node Processing

At relay node, after removal of CP and subsequent processing by the $N \times N$ FFT matrix $\mathbf{F}_N$, the signal received at the rth relay node can be expressed as

$$\mathbf{y}_r(v,j) = \mathbf{H}_{Sr}\mathbf{x}_{v,j} + \mathbf{z}_r \tag{6.5}$$

where $\mathbf{z}_r$ is the i.i.d AWGN vector with length N and the diagonal channel matrix is given by $\mathbf{H}_{Sr} = \text{diag}[H_{Sr}(v,j,0), ..., H_{Sr}(v,j,N-1)]$ with each component $H_{Sr}(v,j,k)$ according to (6.3). The received vector are fed to ST encoder which produces vectors $\mathbf{c}_r^p = [c_r^p(0), c_r^p(1), ..., c_r^p(N-1)]^T$, where p is the index of STBC encoder at relay node r. Each vector $\mathbf{c}^p$ is processed by the $N \times N$ IFFT matrix to yield

$$\mathbf{s}_r^p = \mathbf{F}_N^H \mathbf{c}^p \tag{6.6}$$

After the insertion of CP with length $L_{cp} \geq R(L_{Sr} + L_{rD})$, the signal transmitted from rth relay is given by

$$\mathbf{x}_r = A_r \mathbf{p}^q \mathbf{s}^p \tag{6.7}$$

where the cyclic delay matrix is chosen to be

$$\mathbf{p}_q = \begin{bmatrix} 0 & \mathbf{I}_{L_r(q-1)} \\ \mathbf{I}_{N-L_r(q-1)} & 0 \end{bmatrix} \tag{6.8}$$

which is exactly the same as (4.19) except for the relay index. Then the relay nodes transmit the signal simultaneously to the destination.

6.2.2 Destination Node Processing

At the destination, after the removal of CP and subsequent processing by $N \times N$ FFT matrix $\mathbf{F}_N$, the received signal can be expressed as

$$\mathbf{y}(v,j) = \sum_{p=1}^{P} \sum_{q=1}^{Q} A_{r(p,q)} \mathbf{H}_{Sr(p,q)} \mathbf{H}_{r(p,q)D} \mathbf{x}_r(v,j) + \mathbf{Z}_D \tag{6.9}$$

where $\mathbf{Z}_D$ is the i.i.d. AWGN vector with length N and the diagonal channel matrix $\mathbf{H}_{rD} = \text{diag}[H_{rD}(v,j,0), ..., H_{rD}(v,j,N-1)]$ with each component $H_{rD}(v,j,k)$ is as in (6.3). Following analysis in Section 4.3, it can be shown that for HRD scheme, the spatial diversity of the RCDD relay for each STBC coded is converted into frequency diversity and the receiver sees the signal coming from P relay nodes, regardless the fact that a total of R relay nodes are being used for transmission. Hence by selecting the CDD matrices $\mathbf{P}_q$ as per (4.14), the received signal of (6.9) simplifies to

$$\mathbf{y}(v,j) = \sum_{p=1}^{P} \mathbf{H}_{rD'}^{p} \mathbf{x}_r^p + \mathbf{z}_D \tag{6.10}$$

where $\mathbf{H}_{rD}^{p} = \text{diag}[H_{rD}^{p}(0), ..., H_{rD}^{p}(N-1)]$ is the modified diagonal channel matrix. Also, the frequency response of (6.3) changes to $H_{rD}(v,j,k) = \sum_{l=0}^{QL-1}$ is the modified diagonal channel matrix. The HRD scheme can thus be summarized as i) a simple SF/ST coded system which provides Pth order spatial diversity and QL order channel selectivity, ii) zero cyclic delays on the first CDD branches,$(q = 1)$ corresponding to each p, lead to the original ST/SF encoded symbol being transmitted., iii) for $P = 1$, the HRD scheme collapse to a simple CDD relay with no ST/SF coding and iv) for the realization of combined spatial and frequency diversity $R \geq 3$.

6.3 Simulation Results

In this section, simulation results are presented to test the performance of HRD OFDM system. All results are produced for BER versus SNR per bits (E_b/N_o).

A total bandwidth of 20 MHz with $N = 64$ subcarriers (IFFT/FFT points) and a mandatory guard interval of 16 samples are chosen. A half rate convolutional encoder ($r_{cc} = 1/2, (133, 171)_8$) and soft Viterbi decoder is used for channel decoding. Perfect channel estimation and MRC detection scheme is used for the error performance evaluation.

The channel delay spread plays an important role in the performance of HRD scheme. In order to appreciate the importance of multipath diversity, HRD is simulated with $R = 3, 4, 6$ relays in the presence of multipath channel with different channel orders of of $L = 1, 3$. The relay nodes configuration $R = 3$ used here to employ $P = 2$ and one additional CDD with any of the pth relay. The frame size is now $F = 2048$ bits representing a total of $V = 16$ independent fading blocks with QPSK modulation. The improvement in performance by increasing the number of either tap or the CDD relay is obvious in Figure 6.2.

Next, the error curves for HRD scheme employing only STC block encoded relays i.e. $R = P = 3, 4$ are plotted in comparison with the hybrid of ST block encoded and CDD relays ($P = 2, Q = 1, 2$) employing $R = 3, 4$ relay nodes. A coded frame length of $F = 2048$ is considered. An 18-tap Rayleigh channel model is chosen. As shown in Figure 6.3, in highly selective channel, the performance of HRD and DSTC is comparable although with $R = 4$, there is a small performance gain for HRD at high SNR. Note that although the performance of DSTBC is comparable to HRD, it suffers rate loss due coding and more complexity at the receiver end. Finally, the performance comparison for HRD against stand alone RCDD is given in Figure 6.4. In this case HRD outperform the RCDD. Therefore, HRD provides alternative solution for the realization of maximum of spatial and multipath diversity for more than relay nodes.

6.4 Summary

In this chapter, a new combination of orthogonal block code and CDD was introduced for OFDM system. The system has been investigated in AF relay protocol in broadband channel. The hybrid relay diversity scheme combines the simplicity and standard conformability of CDD with STBC. In order to achieve maximum spatial and frequency diversity, the novel combination of full rate block codes

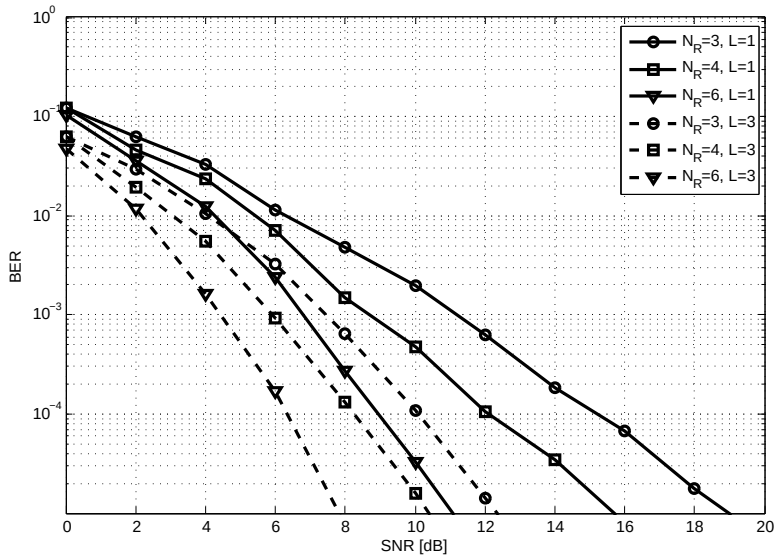

Figure 6.2: BER performance of HRD scheme for R=3,4,6 relay nodes $P = 2$ ST encoded and $Q = 1, 2, 3$ CDD branches for channel orders $L = 1, 3$

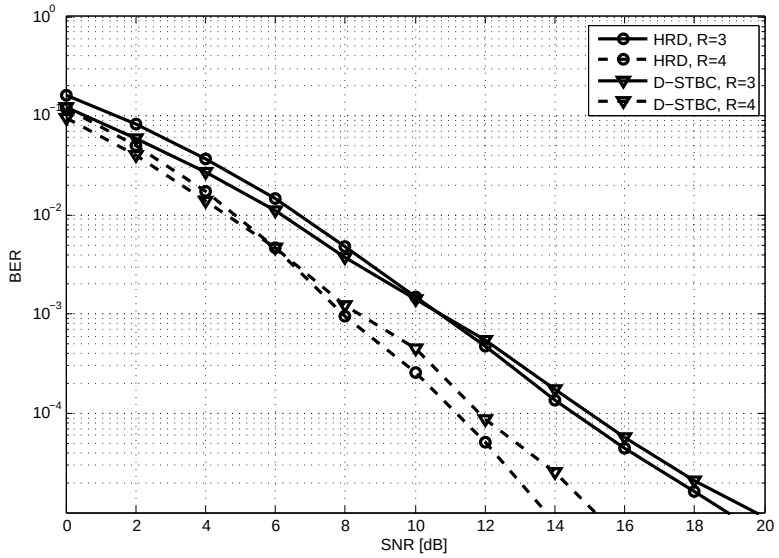

Figure 6.3: BER performance of HRD OFDM and DSTBC with $R = 4$, $p = 2$ and $q = 2$

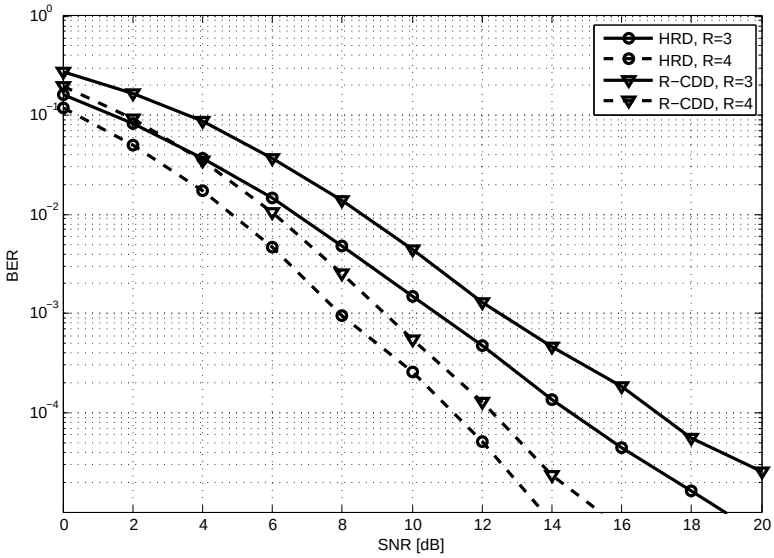

Figure 6.4: BER performance of HRD OFDM and RCDD with $R = 4$, $p = 2$ and $q = 2$

with variable CDD process provides a simple solution for more than two relay nodes.

The simulation results show the performance of HRD with various configurations. The results also proved that HRD gives better error performance compared to DSTBC and RCDD while maintaining the diversity order and signal data rate.

Chapter 7

Concluding Remarks

In this thesis, distributed orthogonal block code and relay CDD were explored for OFDM and MC-CDMA systems. These schemes are amongst the most attractive relay diversity schemes because of their excellent performance. The performance of these relay diversity techniques has been been investigated with frequency selective Rayleigh fading channel model. In addition, a hybrid combination of CDD and orthogonal block code was presented which provides an attractive solution to improve the system performance while maintaining affordable complexity at the destination terminal.

7.1 Thesis summary

The contribution of this thesis are based on the works presented in Chapter 3, 4, 5 and 6. These are thoroughly explained in Chapter 1 and summarized as below.

7.1.1 Chapter 1

An overview of the research is given. Cooperative communications is proposed to overcome the limitations of MIMO systems to having multiple (more than two) antenna embedded on user devices. Multiple antenna need to transmit signals in a way that they do not interfere each other while maintaining the spectral efficiency to provide diversity. Relay diversity techniques of DSTC and RCDD are proposed.

7.1.2 Chapter 2

Fundamentals needed to understand and appreciate the thesis. Wireless communication channels subject ot degradation due to time variant multipath propagation. Channels are modeled statistically using Rayleigh, Nakagami-m and Rician. OFDM is chosen in broadband due to its ability to combat multipath fading using cyclic prefix and simple equalization at receiver. MC-CDMA is an OFDM-based multiple access scheme. Relaying can be in parallel (two-hop) or series (multihop). Parallel gives diversity and multiplexing gain and series gives pathloss gain. Relays operate in time-duplex which receive and transmit in different time slots or subchannel. Relay protocol can be AF or DF. The protocol is chosen based on the channel condition; if the channel is good, choose DF, if channel is bad, choose AF so there will be no error propagation. Performance measures are diversity, multiplexing and multipath gain, average SNR and error probability.

7.1.3 Chapter 3

DSTBC system over multipath fading channel can achieve diversity gain of LR where $L = \min(L_{Sr}, L_{rD})$ for $r = 1, ..R$, where R is the number of relay. However, with increase number of relay, it is not possible to have full-rate transmission due to the design of the orthogonal code. DSTBC cannot compete with MIMO STBC in terms of error, although can achieve similar diversity gain.

7.1.4 Chapter 4

RCDD is a simple diversity technique that can be implemented with any number of relay nodes without the need of complicated receiver structure. RCDD can achieve diversity gain of LR which is similar to DSTBC. RCDD wins over DSTBC in terms of simplicity and data rate although DSTBC has better error performance. The implementation of delay can be done in time-domain (time delay) or frequency-domain (phase shift.)

7.1.5 Chapter 5

In this chapter, the performance of RCDD and distributed orthogonal block code coded are investigated for MC-CDMA system. The relaying employs decode-and-forward protocol and the closed form exact SER for M-PSK signals were derived. Performance comparison between between DSTBC and RCCD are presented with simulations. The average SER of the system is derived using MGF-based approach.

7.1.6 Chapter 6

A novel hybrid relay diversity technique which combines cyclic delay and orthogonal block code was presented. This new architecture cyclically delayed orthogonal coded symbol to increase the diversity of the channel. The simulation results showed that the HRD scheme outperform its constituents by a significant margin. This technique provides design flexibility to devise the best suited relay configuration strategy for any desired performance according to the wireless channel environments.

7.2 Future Research Directions

Although the concept of relaying has been around for decades, there are still many open problems for this channel. For example, in general the capacity of the relay channel is unknown even for the case of Gaussian channels. As a result, most of the research efforts have focused on finding efficient protocols that lead to lower bound on the capacity [49].

In order to further enrich the future works, the author of this thesis suggests the following possible research direction:

- Finally, the HRD scheme presented in the thesis provides an alternative architecture to realize the combination of spatial and multipath diversity. Standalone RCDD and distributed orthogonal block code is well known, however, when used as a hybrid technique, these two relay diversity techniques compliment each other by providing flexible solutions for a system

with more than two relay nodes. In the literature, various combinations of STC with other techniques exist, such as selection diversity and beamforming.

Appendix A: Proof of Equation (3.22)

From (3.21), taking the expectation with respect to $\mathbf{h}_{Sr}$, we obtain J_r [19]

$$J_r = E_{\mathbf{h}_{rD}}\Bigg\{ \det\Bigg(\mathbf{I} + \frac{\rho P_S A_r^2}{8L_{Sr}}\mathbf{W}_{Sr}^H\left(\mathbf{I} + A_r^2\mathbf{D}_{rD}\mathbf{D}_{rD}^H\right)^{-1} \times \mathbf{D}_{rD}\mathbf{D}_{rD}^H \mathrm{diag}(\|\mathbf{u}\|^2)\mathbf{W}_{Sr}\Bigg)^{-1}\Bigg\} \quad (1)$$

For a given error vector $\mathbf{e} = \mathbf{s} - \mathbf{s}' \neq= 0$, errors occur in at least one group. The precoded error vector in a group has all non-zero entries if the error vector in that group is non-zero [52]. Suppose the mth group is one of the erroneous groups, i.e. $\mathbf{s}_m \neq \mathbf{s}'_m$, $1 \leq m \leq M$. Then we have $\mathbf{u}_m(q) \neq 0,\ \forall q \in \{1, 2, ..., L\}$. Noting $L = \max(L_{Sr}, L_{rD})$ and introducing a matrix $\mathbf{P}$ which contains the first L_{Sr} rows in Ψ_m, we rewrite (1) as

$$J_r = E_{\mathbf{h}rD}\left\{\det\left(\mathbf{I} + \frac{\rho P_S A_r^2}{8L_{Sr}}\mathbf{W}_{Sr}^H\mathbf{P}^T\mathbf{P}\mathbf{G}_r\mathbf{P}^T\mathbf{P}\mathbf{W}_{Sr}\right)^{-1}\right\} \quad (2)$$

when $\mathbf{G}_r = \left(\mathbf{I} + A_r^2\mathbf{D}_{rD}\mathbf{D}_{rD}^H\mathrm{diag}\left(\|u\|^2\right)\right)$. Since the matrix inside the determinant bracket of (2) is positive definite, an upper bound for J_r can be written as

[19]

$$J_r \leq \frac{L_{Sr}^{2L_{Sr}}}{\omega} E_{\mathbf{h}_{rD}} \left\{ \prod_{l=1}^{L_{Sr}} \frac{1}{1+\rho\alpha_r |\mathbf{u}(i_{m,l})|^2} \times \left(1 + \frac{\frac{\rho\alpha_r |\mathbf{u}(i)|^2}{A_r^2+\rho\alpha_r |\mathbf{u}(i_{m,l})|^2 A_r^2}}{|\mathbf{D}_{rD}(i_{k,l})|^2 + \frac{1}{A_r^2+\rho\alpha_r |\mathbf{u}(i_{k,l})|^2 A_r^2}} \right) \right\} \tag{3}$$

where $\alpha_r = L_{Sr} P_S/8$ and $i_{k,l} = (l-1)N + k,\ l = 1, ..., L_{Sr}$. Since the components in $\mathbf{h}_{rD}$ are i.i.d. Gaussian with variance $1/L_{rD}$, we have $\mathbf{D}_{rD}(i_{k,l})\ \mathcal{CN}(0,1)$. taking the expectation with respect to $\mathbf{h}_{rD}$, we obtain the following two cases at high SNR:

- **Case 1** ($L_{Sr} \leq L_{rD}$):

$$J_{r,\text{case 1}} \leq a_{r,\text{case 1}} \left(\rho^{-1} \log \rho\right)^{L-Sr} + O\left(\rho^{L_{Sr}(\log\ \rho)^{L_{Sr}-1}}\right) \tag{4}$$

  where $a_{r,\text{case1}} = \frac{\left(8\pi L_{Sr}^{L_{Sr}}\right)^{L_{Sr}}}{\omega (vP_R)^{L_{Sr}}}$. Here we have used the fact $|\mathbf{u}(i_{k,l})|^2 \geq v$ [52].

- **Case 2** ($L_{Sr} > L_{rD}$)

$$J - r \leq \frac{(8\pi L_{Sr})^{k_r}}{\omega\,(vP_R)^{k_r}} \left(\rho^{-1} \log\ \rho\right)^{k_r} + \left(\rho^{-k_r} (\log \rho)^{k_r - 1}\right) \tag{5}$$

Replacing (5) in (3.21), we obtain (3.22).

Appendix B: Proof of Equation (3.37)

In order to prove (3.37), we need to find the MGF of $\Gamma(X,Y) := XY/(X+Y+1)$, where X and Y are two independent and exponentially distributed random variables with mean $\bar{X}$ and $\bar{Y}$. The cumulative distribution function (CDF) of $\Gamma(X.YX)$ to be

$$F_{\Gamma}(\gamma) = 1 - \frac{2\sqrt{\gamma^2+\gamma}}{\sqrt{p}} e^{-\gamma\frac{\sigma}{p}} K_1\left(\frac{2\sqrt{\gamma^2+\gamma}}{\sqrt{p}}\right) \tag{6}$$

for $\gamma > 0$, where $\sigma := \bar{X} + \bar{Y}$, $p := X\bar{Y}$ and $K_v(\cdot)$ denotes the modified Bessel function of the second kind and order v.

We take the derivative with respect to σ in (6) to obtain the probability density function (PDF) of $\Gamma(X,Y)$ and we use [1] for the derivative of $K_1(\gamma)$ in order to establish the following PDF for $\Gamma(X,Y)$

$$\begin{aligned} f_{\Gamma}(\gamma) &= \sqrt{4\gamma+2} p e^{-\gamma\frac{\sigma}{p}} K_0\left(\frac{2}{\sqrt{p}}\sqrt{\gamma^2+\gamma}\right) \\ &\quad + \frac{2\sigma\sqrt{\gamma^2+\gamma}}{p\sqrt{p}} e^{-\gamma\sqrt{\sigma p}} K_1\left(\frac{2}{\sqrt{p}}\sqrt{\gamma^2+\gamma}\right), \ \gamma > 0 \end{aligned} \tag{7}$$

We use the definition of the moment generating function along with (7) to

write

$$\mathcal{M}_\Gamma(\mu) = \frac{2}{p}\int_0^\infty \left[(2\gamma+1)e^{-\gamma\frac{\sigma-p\mu}{p}}K_0\left(\frac{2\sqrt{\gamma^2+\gamma}}{\sqrt{p}}\right)\right.$$
$$\left. + \frac{\sigma}{\sqrt{p}}\sqrt{\gamma^2+\gamma}e^{-\gamma\frac{\sigma-p\mu}{p}}K_1\left(\frac{2}{\sqrt{p}}\sqrt{\gamma^2+\gamma}\right)\right]d\gamma \quad (8)$$

Using the change of variable $\gamma \to \gamma - 1/2$ and after some manipulations we obtain:

$$\mathcal{M}_\Gamma(\mu) = \frac{2}{p}e^{\frac{\alpha}{2}}\left[2\mathcal{I}_0(\mu) + \frac{\sigma}{\sqrt{p}}\mathcal{I}_1(\mu)\right] \quad (9)$$

where

$$\mathcal{I}_0(\mu) := \int_{1/2}^\infty \gamma e^{-\alpha\gamma}K_0\left(\beta\sqrt{\gamma^2-(1/2)^2}\right)d\gamma \quad (10)$$

and

$$\mathcal{I}_1(\mu) := \int_{1/2}^\infty \sqrt{\gamma^2-(1/2)^2}e^{-\alpha\gamma}K_1\left(\beta\sqrt{\gamma^2-(1/2)^2}\right)d\gamma \quad (11)$$

where $\alpha := (\sigma - p\mu)/p$, $\beta := 2/\sqrt{p}$.

In order to simplify the integrand in (10), we write $\mathcal{I}_0(\mu)$ as

$$\mathcal{I}_0 = \frac{-\partial}{\partial\alpha}\left\{\frac{-1}{2\sqrt{\alpha^2-\beta^2}}\left[e^{-\frac{\sqrt{\alpha^2-\beta^2}}{2}}E_1\left(\frac{\alpha-\sqrt{\alpha^2-\beta^2}}{2}\right)\right.\right.$$
$$\left.\left. - e^{\frac{\sqrt{\alpha^2-\beta^2}}{2}}E_1\left(\frac{\alpha+\sqrt{\alpha^2-\beta^2}}{2}\right)\right]\right\} \quad (12)$$

and after differentiating with respect to α, and then letting $\alpha = (\sigma - p\mu)/p$ we find

$$\mathcal{I}_0(\mu) = \frac{pe^{-\frac{\delta}{2p}}}{4\rho^3}\left[\delta(\delta+2p)e^{\frac{\delta-\rho}{2p}}e^{\frac{\delta-\rho}{2p}}E_1\left(\frac{\delta-\rho}{2p}\right) + \delta(\delta-2p)e^{\frac{\delta+\rho}{2p}}E_1\left(\frac{\delta+\rho}{2p}\right) - 4\rho p\right] \quad (13)$$

for $\mathcal{R}]\{\mu\} < \sigma/p + 2/\sqrt{p}$, where $\rho := \sqrt{\delta^2-4p}$ and $\delta := \sigma - p\mu$. Similar to (12),

we write $\mathcal{I}_1\mu$ in (5) as

$$\mathcal{I}_1(\mu) = \frac{-\partial}{\partial\beta}\left[\int_{1/2}^{\infty} e^{-\alpha\gamma} K_0\left(\beta\sqrt{\gamma^2-(1/2)^2}\right) d\gamma\right] \tag{14}$$

We note that the above integral is the same as the integral in (12). Consequently, we use [22] again to find the integral in (14) and after differentiating with respect to β, and letting $\beta = 2/\sqrt{p}$ we obtain

$$\mathcal{I}_1(\mu) = \frac{p\sqrt{p}e^{-\frac{\delta}{2p}}}{2\rho^3}\left[-(\delta+2p)e^{\frac{\delta-\rho}{2p}} E_1\left(\frac{\delta-\rho}{2p}\right) - (\delta-2p)e^{\frac{\delta+p}{2p}} E-1\left(\frac{\delta+\rho}{2p}\right) + \rho\delta\right] \tag{15}$$

for $\mathcal{R}]\{\mu\} < \sigma/p + 2/\sqrt{p}$. Now, if we substitute (3.21) and (15) into (1), we obtain the MGF of $\Gamma(X,Y)$, and consequently after replacing X with $\gamma_{1,r}$ and Y with $\gamma_{2,r}$ we obtain (3.37).

List of Publication

- N. Abdul Razak, F. Said, and A. Aghvami, "*Performance of Relay Cyclic Delay Diversity in Multicarrier System*", IEEE 20th International Symposium on Personal, Indoor and Mobile Radio Communications, pages 2025-2029, September 2009
- N. Abdul Razak, F. Said, "*Hybrid Relay Diversity for OFDM system*", IEEE 13th International Conference on Communications Systems, November 2012
- N. Abdul Razak, F. Said, "*R-CDD and D-STBC in Cooperative MC-CDMA*", submitted to Communications Journal

Bibliography

[1] M. Abramowitz and I. A. Stegun. *Handbook of mathematical functions with formulas, graphs, and mathematical tables*, **i**. Dover publications, 1964. 125

[2] S. M. Alamouti. A simple transmit diversity technique for wireless communication. *IEEE Journal on Selected Areas Communications*, **16**:1451–1458, 1998. 27, 67

[3] P. Anghel and M. Kaveh. Exact symbol error probability of a cooperative network in a Rayleigh-fading environment. *IEEE Transactions on Wireless Communications*, **3**:1416–1421, 2004. 51

[4] P. Anghel, G. Leus, and M. Kaveh. Distributed space-time coding for cooperative networks. In *Proc. of Intl. Conf. on Acoustics, Speech and Signal Proc.*, pages 273–276. University of British Columbia, 2003. 78

[5] P. Anghel, G. Leus, and M. Kaveh. Multi-user space-time coding in cooperative networks. *ICASSP*, pages 273–276, 2003. 27, 51

[6] S. Barbarossa, L. Pescosolido, D. Ludovici, L. Barbetta, and G. Scutari. Cooperative wireless networks based on distributed space-time coding. *International Workshop on Wireless Ad-Hoc Networks*, pages 30–34, 2004. 27, 52

[7] G. Bauch and J. S. Malik. Orthogonal frequency division multiple access with cyclic delay diversity. *ITG Workshop on Smart Antennas*, pages 17–24, 2004. 91

[8] P. A. Bello. Characterization of Randomly Time-variant Linear Channels. *IEEE Transaction on Wireless Communications*, **11**:360–393, 1963. 38, 40

[9] E. Biglieri, J. Proakis, and S. Shamai. Fading channels: Information-theoretic and communications aspects. *Information Theory, IEEE Transactions on*, **44**[6]:2619–2692, 2006. 113

[10] A. Bletsas, A. Khisti, D. P. Reed, and A. Lippman. A simple cooperative method based on network path selection. *IEEE Journal on Selected Areas in Communications*, **24**[3]:659–672, 2006. 21

[11] A. Bletsas, H. Shin, and M. Win. Outage-optimal cooperative communications with regenerative relays. *Conference on Information Sciences and Systems*, 2006. 23

[12] M. Bossert, A. Huebner, F. Schuehlein, H. Haas, and E. Costa. On cyclic delay diversity in OFDM based transmission schemes. In *OFDM workshop*, pages 1–5, 2002. 29

[13] J. Boyer, D. Falconer, and H. Yanikomeroglu. Multihop diversity in wireless relaying channels. *IEEE Transactions Communications*, **52**:1820–1930, 2004. 24, 51

[14] Y. Chen and Q. Zhao. Maximizing the lifetime of sensor network using local information on channel state and residual energy. *Proceedings of the Conference on Information Science and Systems (CISS)*, 2005. 23

[15] T. Cover and A. E. Gamal. Capacity theorems for the relay channel. *IEEE Transactions on Information Theory*, **25**[5]:572–584, 1979. 19

[16] J. W. Craig. A new, simple and exact result for calculating the probability of error for two dimensional signal constellation. *Proc. IEEE Milit. Commun. Conf.*, pages 571–575, 1991. 73, 91

[17] A. Dammann and S. Kaiser. Standard conformable antenna diversity techniques for OFDM and its application to the DVB-T system. In

IEEE Global Telecommunications Conference, number Dd, pages 3100–3105. IEEE, 2001. 84

[18] V. DaSilva and E. S. Sousa. Performance of orthogonal CDMA codes for quasi-synchronous communication systems. In *Personal Communications: Gateway to the 21st Century. Conference Record., 2nd International Conference on Universal Personal Communications*, **2**, pages 995–999. IEEE, 1993. 58

[19] Y. Ding and M. Uysal. Amplify-and-forward cooperative OFDM with multiple-relays: performance analysis and relay selection methods. *IEEE Transactions on Wireless Communications*, **8**[10]:4963–4968, October 2009. 73, 123, 124

[20] M. Dohler and Y. Li. *Cooperative communications: hardware, channel & PHY*, **6**. Wiley, 2010. 36

[21] K. Fazel and S. Kaiser. *Multi-carrier and spread spectrum systems*. Wiley, 2003. 42, 53, 54, 56, 57, 58, 63, 64

[22] I. S. Gradshtein, I. M. Ryzhik, A. Jeffrey, and D. Zwillinger. *Table of integrals, series and products*. 2007. 127

[23] I. Hammerstroem, M. Kuhn, and A. Wittneben. Impact of relay gain allocation on the performance of cooperative diversity networks. In *IEEE Vehicular Technology Conference*, 2004. 23

[24] L. Hanzo, M. Munster, B. J. Choi, and T. Keller. *OFDM and MC-CDMA for broadband multi-user communications, WLANs and broadcasting*. J Wiley, 2004. 58, 63, 103

[25] S. Hara and R. Prasad. Overview of multicarrier CDMA. *IEEE Communications Magazine*, **35**[12]:126–133, 1997. 58, 64

[26] S. Hara and R. Prasad. Design and performance of multicarrier CDMA system in frequency-selective Rayleigh fading channels. *IEEE Transactions on Vehicular Technology*, **48**[5]:1584–1595, 1999. 62, 63, 102

[27] M. O. Hasna and M. S. Alouini. Outage probability of multihop transmission over Nakagami fading channels. *IEEE Communcations Letters*, **7**[1]:216–218, 2003. 51

[28] M.O. Hasna and M. S. Alouini. End-to-end performance of transmission systems with relays over rayleigh-fading channels. *IEEE Transactions on Wireless Communications*, **2**[6]:1126–1131, November 2003. 51

[29] M.O. Hasna and M. S. Alouini. Harmonic mean and end-to-end performance of transmission systems with relays. *IEEE Transactions on Communications*, **52**[1]:130–135, January 2004. 51

[30] P. Herhold, E. Zimmermann, and G. Fettweis. On the performance of cooperative amplify-and-forward relay networks. In *International ITG Conference on Source and Channel Coding (SCC)*, page 451. VDE-Verlag, 2004. 18

[31] Y. W. Hong and A. Scaglione. Energy-efficient broadcasting with cooperative transmissions in wireless sensor networks. *IEEE Transactions Communications*, **5**[10]:2844–2855, 2006. 17, 25

[32] W. Huang, Y. Hong, and C. J. Kuo. Lifetime maximization for amplify-and-forward cooperative networks. *Proc. IEEE Wireless Communications and Networking Conference (WCNC)*, 2007. 23

[33] O. Hyunseok. Novel transmit diversity techniques for broadcast services in cellular networks. In *IEEE Vehicular Technology Conference*, pages 896–900, 2005. 29

[34] A. Ibrahim, Z. Han, and K. J. R. Liu. Distributed energy-efficient cooperative routing in wireless networks. *IEEE Transaction on Wireless Communications*, **7**[11]:757–759, 2008. 25

[35] IEEE. IEEE Standard 802.16-2004. *Part 16: Air interface for broadband wireless access systems*, 2004. 34

[36] Salama Ikki and Mohamed H. Ahmed. Performance analysis of cooperative diversity wireless networks over Nakagami-m fading channel. *IEEE Communcations Letters*, **11**[4]:334–336, April 2007. 52

[37] H. Jafarkhani. *Space-time coding theory and practice*. Cambridge University Press, 2005. 51, 69

[38] Y. Jing and B. Hassibi. Cooperative diversity in wireless relay net- works with multiple-antenna nodes. *IEEE Int. Symp. Inform. Theory*, 2005. 28

[39] Y. Jing and B. Hassibi. Distributed space-time coding in wireless relay networks. *IEEE Transactions on Wireless Communications*, **5**[12]:3524–3536, 2006. 27, 28, 74, 92

[40] Y. Jing and H. Jafarkhani. Using orthogonal and quasi-orthogonal designs in wireless relay networks. *IEEE Transactions on Information Theory*, **53**[11]:4106–4118, November 2007. 27, 28

[41] Y. Jing and H. Jafarkhani. Distributed differential space-time coding for wireless relay networks. *IEEE Trans. of Communications*, **56**[7]:1092–1100, 2008. 28

[42] G. J. Foschini Jr. and M. J. Gans. On limits of wireless communication in a fading environment when using multiple antennas. *Wireless Personal Commun.*, 1998. 26

[43] Z. Kang, K. Yao, and F. Lorenzelli. Nakagami-m fading modeling in the frequency domain for OFDM system performance analysis. *IEEE Communcations Letters*, **7**[10]:484–486, 2003. 48

[44] G. K. Karagiannidis. Moment based approach to the performance analysis of equal gain diversity in Nakagami-m fading. *IEEE Transactions Communications*, **52**[5]:685–690, 2004. 51

[45] G. K. Karagiannidis. Performance bounds of multihop wireless communications with blind relays over generalized fading channels. *Wireless Communications, IEEE Transactions on*, **5**[3]:498–503, 2006. 51

[46] G. K. Karagiannidis, T. Tsiftsis, and R. K. Mallik. Bounds for multihop relayed communications in Nakagami-m fading. *IEEE Transactions Communications*, **54**[1]:18–22, 2006. 51

[47] A. Khandani, J. Abounadi, E. Modiano, and L. Zheng. Cooperative routing in static wireless networks. *IEEE Transactions Communications*, **55**[11]:2185–2192, 2007. 25

[48] J. N. Laneman, D Tse, and G. Wornell. Cooperative diversity in wireless networks: Efficient protocols and outage behavior. *IEEE Transactions on Information Theory*, **12**:3062–3079, 2004. 18, 20

[49] J. N. Laneman and G. Wornell. Distributed space-time block coded protocols for exploiting cooperative diversity in wireless networks. *IEEE Transactions on Information Theory*, **49**:2415–2425, 2003. 17, 19, 20, 23, 27, 121

[50] J. N. Laneman, G. Wornell, and D Tse. An efficient protocol for realizing cooperative diversity in wireless networks. In *ISIT*, page 294, 2001. 20, 21

[51] F. Li, K. Wu, and A. Lippman. Energy-efficient cooperative routing in multihop wireless ad-hoc networks. *IEEE International Performance, Computing, and Communications Conference*, pages 215–222, 2006. 25

[52] Z. Liu and G. Giannakis. Linear constellation precoding for OFDM with maximum multipath diversity and coding gains. *IEEE Transactions on Communications*, **51**[3]:416–427, March 2003. 79, 123, 124

[53] J. Luo, L. Blum, L. Cimini, L. Greenstein, and A. Haimovich. Decode-and-forward cooperative diversity with power allocation in wireless networks. *IEEE Global Telecommunications Conference*, pages 3048–3052, 2005. 23

[54] B. Maham and A. Hjø rungnes. Orthogonal code design for MIMO amplify-and-forward cooperative networks. *IEEE Information Theory Workshop*, 2007. 28

[55] B. Maham and A. Hjø rungnes. Minimum power allocation in SER constrained amplify-and-forward cooperation. *Proc. IEEE Vehicular Technology Conference (VTC 2008-Spring)*, pages 2431–2435, 2008. 23

[56] B. Maham and A. Hjø rungnes. Power Allocation Strategies for Distributed Space-Time Codes in Amplify-and-Forward Mode. *EURASIP Journal on Advances in Signal Processing*, 2009. 21

[57] B. Maham, A. Hjø rungnes, and B. S. Rajan. Quasi-orthogonal design and performance analysis of amplify-and-forward relay networks with multiple-antennas. *IEEE Wireless Communications and Net- working Conference (WCNC)*, 2010. 28

[58] B. Maham and A. Hjorungnes. Power allocation strategies for distributed space-time codes in amplify-and-forward mode. *EURASIP Journal on Advances in Signal Processing*, 2009. 23, 24

[59] B. Maham, A. Hjorungnes, and G. Abreu. Distributed GABBA space-time codes in amplify-and-forward relay networks. *IEEE Transactions on Wireless Communications*, **8**[4]:2036–2045, 2009. 27, 28

[60] B. Maham, R. Narasimhan, and A. Hjorungnes. Energy-efficient space-time coded cooperative routing in multihop wireless networks. *IEEE Global Telecommunications Conference*, 2009. 25

[61] I. Maric and R. D. Yates. Bandwidth and power allocation for cooperative strategies in gaussian relay networks. In *Proc. Asilomar Conf. Signals, Systems, and Computers*, 2004. 22

[62] I. Maric and R. D. Yates. Forwarding strategies for Gaussian parallel-relay networks. *Proceedings of the Conference on Infocrmation Sciences and Systems (CISS)*, 2004. 23

[63] R.U. Nabar, H. Bolcskei, and F. W. Kneubuhler. Fading relay channels: Performance limits and space-time signal design. *IEEE Journal on Selected Areas in Communications*, **22**[6]:1099–1109, 2004. 20

[64] M. Nakagami. The m-distribution - A general formula of intensity distribution of rapid fading. In W. G. Hoffman, editor, *Statistical Methods in Radio Wave Propagation*. Ed. Oxford, U.K., 1960. 44, 45, 46, 48

[65] R. V. Nee, G. Awater, M. Morikura, H. Takanashi, M. Webster, and K. W. Halford. New highrate wireless LAN standards. *IEEE Communications Magazine*, pages 82–88, 1999. 34

[66] a. Nosratinia, T.E. Hunter, and a. Hedayat. Cooperative communication in wireless networks. *IEEE Communications Magazine*, **42**[10]:74–80, October 2004. 17

[67] F. Oggier and B. Hassibi. An algebraic coding scheme for wireless relay networks with multiple-antenna nodes. *IEEE Trans. of Signal Pro- cessing*, **56**[7]:2957–2966, 2008. 28

[68] S. Oruthota and N. Rajatheva. Cooperative diversity based multicarrier CDMA system with decode and forward relays in Rayleigh fading channels. In *Wireless Personal Communications*. Springer, September 2010. 103

[69] J. G. Proakis. *Digital communications* . McGraw-Hill, New York, 1983. 37, 39, 55, 56, 63, 64, 113

[70] J. Radon. Lineare scharen orthogonaler matritzen. *Abhandlungen aus dem matematischen Seminar der Hamburgischen Universitat*, **1**[2]:1–14, 1922. 27, 68

[71] G. Rajan and B. Rajan. Leveraging coherent distributed space-time codes for noncoherent communication in relay networks via training. *IEEE Trans. Wireless Commun.*, **8**[2]:683–686, 2009. 28

[72] G. S. Rajan and B. S. Rajan. Distributed space-time codes for cooperative networks with partial CSI. *IEEE Wireless Communications and Networking Conference*, pages 902–906, 2007. 27, 28

[73] K. T. Rajan and B. S. Rajan. Partially-coherent distributed space-time codes with differential encoder and decoder. *IEEE Journal on Selected Areas Communications*, **25**[2]:426–433, 2007. 28

[74] A. Ribeiro, X. Cai, and G. Giannakis. Symbol error probabilities for general cooperative links. **4**[3]:1264–1273, 2005. 26, 51, 52

[75] A. K. Sadek, W. Su, and K.J.R. Liu. Multinode cooperative communications in wireless networks. *IEEE Transactions on Signal Processing*, **55**[1]:341–355, 2007. 26

[76] S. R. Saunders. *Antenna and Propagation for Wireless Communications System*. John Wiley & Sons, New York, 2000. 37, 38, 39, 41, 42

[77] K. Seddik, A. Sadek, A. Ibrahim, and K. Liu. Design criteria and performance analysis for distributed space-time coding. *IEEE Trans. on Vehicular Technology*, **57**:2280–2292, 2008. 20

[78] A Sendonaris, ASE Erkip, and B Aazhang. User cooperation diversity. Part I. System description. *IEEE Transactions on Communications*, **51**[11]:1927–1938, 2003. 17

[79] A. Sendonaris, E. Erkip, and B. Aazhang. User cooperation diversity. Part II. Implementation aspects and performance analysis. *IEEE Transactions on Communications*, **51**[11]:1939–1948, 2003. 17

[80] C. E. Shannon. A mathematical theory of communication. *Bell Systems Technology Journal*, **27**:379–423, 1948. 34

[81] M. K. Simon and M. S. Alouini. Digital communication over fading channels. 2005. 44, 45, 78, 105

[82] B. Sirkeci-Mergen and A. Scaglione. Randomized space-time coding for distributed cooperative communication. *IEEE International Conference on Communications*, 2006. 27

[83] S. B. Slimane and A Osseiran. Relay communication with delay diversity for future communication systems. **06**[2]:321–325, September 2006. 29

[84] W. Su, A. K. Sadek, and K. J. R. Liu. SER performance analysis and optimum power allocation for decode-and-forward cooperation protocol in wireless networks. *IEEE Wireless Communications and Networking Conference*, pages 984–989, 2005. 52

[85] W. Su, A. K. Sadek, and K. J. Ray Liu. Cooperative Communication Protocols in Wireless Networks: Performance Analysis and Optimum Power Allocation. *Wireless Personal Communications*, **44**[2]:181–217, 2007. 102

[86] V. Tarokh, H. Jafarkhani, and A. R. Calderbank. Space-time block codes from orthogonal designs. *IEEE Transactions on Information Theory*, **45**[5]:1456–1467, July 1999. 27, 30, 104, 107

[87] V. Tarokh, N. Seshadri, and A. R. Calderbank. Space-time codes for high data rate wireless communication: performance criterion and code construction. *IEEE Transactions on Information Theory*, **44**[2]:744–765, March 1998. 84

[88] V. Tarokh, N. Seshadri, and A. R. Calderbank. Spacetime codes for high data rate wireless communication: Performance analysis and code construction. *IEEE Trans. Inform. Theory*, **44**:744–765, 1998. 26

[89] E. Telatar and Others. Capacity of multi-antenna Gaussian channels. *European transactions on telecommunications*, **10**[6]:585–596, 1999. 26

[90] K. Tourki, M. S. Alouini, and L. Deneire. Blind cooperative diversity using distributed space-time coding in block fading channels. In *IEEE International Conference on Communications*, 2008. 21

[91] M. Uysal and O. Canpolat. On the distributed space-time signal design for a large number of relay terminals. *Proc. IEEE Wireless Communications and Networking Conference (WCNC)*, **2**:990–994, 2005. 20

[92] E. van der Meulen. Three-terminal communication channel. *Advance Applied Probability*, **3**:120–154, 1971. 19

[93] L. Vanderdorpe. Multitone direct sequence CDMA system in an indoor wireless environment. In *IEEE Symposium in Communication and Vehicular Technology*, 1993. 58

[94] T. Wang, Y. Yao, and G. B. Giannakis. Non-coherent distributed space-time processing for multiuser cooperative transmissions, vol. 5, no. 12, pp. 33393343, Dec. 2006. *IEEE Trans. Wireless Commun.*, **5**[12]:3339–3343, 2006. 20

[95] S. Weinstein and P. Ebert. Data transmission by frequency-division multiplexing using the discrete Fourier transform. *IEEE Transactions on Communications*, **19**[5]:628–634, October 1971. 55

[96] K. Witrisal, Y. H. Kim, R. Prasad, and L. P. Ligthart. Antenna diversity for OFDM using cyclic delays. In *Proceedings of the 8th Symposium on Communication and Vehicular Technology*, pages 13–17, 2001. 29

[97] A Wittneben. A new bandwidth efficient transmit antenna modulation diversity scheme for linear digital modulation. In *Communications, 1993. ICC 93. Geneva. Technical Program, Conference Record, IEEE International Conference on*, **3**, pages 1630–1634. IEEE, 2002. 28, 84

[98] KK Wong, RD Murch, and KB Letaief. Performance enhancement of multiuser MIMO wireless communication systems. *IEEE Transactions on Communications*, **50**[12]:1960–1970, 2002. 18

[99] L. Yang and L. Hanzo. Multicarrier DS-CDMA:A multiple access scheme for ubiquitous broadband wireless communications. *IEEE Communications Magazine*, **35**:116–124, 2003. 59

[100] N. Yee, J. P. M. G. Linnartz, and G. Fettweis. Multi-carrier CDMA in indoor wireless radio networks. *IEICE Transactions on Communications*, **77**:900–904, 1994. 58

[101] Z. Yi and I. Kim. Joint optimization of relay precoders and decoders with partial channel side information in cooperative networks. *IEEE Journal on Selected Areas in Communications*, **25**:447–458, 2007. 24

[102] X. Zhao, B. Zheng, C. Chen, and J. Cui. The BER performance analysis of a cooperative diversity scheme. In *International Conference on Communications, Circuits and Systems Proceedings*, **2**, pages 870–874. IEEE, 2007. 103

[103] Y. Zhao, R. Adve, and T. J. Lim. Improving Amplify-and-Forward Relay Networks: Optimal Power Allocation versus Selection. *2006 IEEE International Symposium on Information Theory*, pages 1234–1238, July 2006. 23